1965

The structures of the ethyl grignard reagent in diethyl ether and a troponoid photo-oxidation product

Lloyd Joseph Guggenberger
Iowa State University

66-3874

GUGGENBERGER, Lloyd Joseph, 1939-

THE STRUCTURES OF THE ETHYL GRIGNARD REAGENT IN DIETHYL ETHER AND A TROPONOID PHOTO-OXIDATION PRODUCT.

Iowa State University of Science and Technology
Ph.D., 1965
Chemistry, physical

University Microfilms, Inc., Ann Arbor, Michigan

THE STRUCTURES OF THE ETHYL GRIGNARD REAGENT IN DIETHYL ETHER AND A TROPONOID PHOTO-OXIDATION PRODUCT

by

Lloyd Joseph Guggenberger

A Dissertation Submitted to the
Graduate Faculty in Partial Fulfillment of
The Requirements for the Degree of
DOCTOR OF PHILOSOPHY

Major Subject: Physical Chemistry

Approved:

Signature was redacted for privacy.
In Charge of Major Work

Signature was redacted for privacy.
Head of Major Department

Signature was redacted for privacy.
Dean of Graduate College

Iowa State University
Of Science and Technology
Ames, Iowa

1965

TABLE OF CONTENTS

INTRODUCTION

The organomagnesium halides produced by the reaction of organic halide and metallic magnesium in a suitable solvent, such as diethyl ether, have been called Grignard reagents after their discoverer, Victor Grignard (1). Although the Grignard reagent is now more than half a century old, the exact constitution and molecular structure of this reagent are still being very actively investigated. The Grignard reagents are generally considered to be the most important of all organometallic compounds.

The structural history of the Grignard reagent includes a very large number of journal publications. This history is somewhat unusual in that it has not been one of continual convergence on a single structure; various structures have been favored in different periods. Just a few years ago it seemed that a good deal of the early confusion and sometimes conflicting observations might be the result of contaminated reagents. It is very difficult to avoid contamination completely with such a reactive reagent. A survey of the recent literature indicates that very scrupulous exclusion of contaminants, especially oxygen and moisture, does lead to better reproducibility, but the basic structural problem remains. The great volume of data accumulated in recent years suggests that the problem is even more complicated than imagined, say ten years ago.

The first part of this thesis involves a discussion of the nature and structure of the Grignard reagent. In particular the results of an

X-ray diffraction analysis of the ethyl Grignard reagent in diethyl ether will be described and discussed.

In the second part of this thesis a discussion of the structure of the troponoid photo-oxidation product, $C_{16}H_{11}O_3C\ell$, will be presented. The systematic name for $C_{16}H_{11}O_3C\ell$ is 1-(p-chlorophenoxy)-2-oxa-4,5-benzo-bicyclo-[4.1.0]-hept-4-ene-3-one. This compound is a result of the photochemical oxidation of 2-(p-chlorophenoxy)-4,5-benztropone (2). Some emphasis will be placed on the method of solution since the more conventional "heavy atom" and Fourier synthesis approaches are not readily applicable in this case.

STRUCTURE OF THE ETHYL GRIGNARD REAGENT

Literature Review

Several reviews have been written on the Grignard structure problem; the reader is referred to Kharasch and Reinmuth (3), and Rochow, Hurd, and Lewis (4) for a list of references to these as well as much of the earlier work done in this area. Salinger (5) has presented a more recent review and Yoffe' and Nesmeyanov (6) have published an impressive compilation of Grignard reactions. Since the early work is so well documented only a few of the more important of these investigations will be cited here. The stress here will be on the more recent work in this area.

In this thesis the RMgX notation will generally be used to represent the solvated Grignard reagent even though the solvent molecules may not always be explicitly expressed. This notation is consistent with the results of this investigation. The R might be an alkyl or aryl group and the X either Cl, Br, or I. Grignard reagents containing F cannot be prepared under normal conditions. The unsolvated RMgX reagents are dismissed immediately since they are infusible solids, insoluble in hydrocarbons, and most probably polymeric (4).

In the years preceding 1929 several structures were proposed for the Grignard reagent (3); some of these are still considered possibilities while others no longer make "chemical sense." Early pertinent observations were that Grignard solutions became viscous on concentration and that one molecule of ether was retained with great tenacity, even under reduced pressures (7). There was also ebullioscopic molecular weight evidence to

indicate various degrees of association with respect to the RMgX species (8).

In 1929 the Schlenks (9) observed that a magnesium halide-dioxane complex was precipitated from ethereal solutions of the Grignard reagent on the addition of dioxane. The Schlenks concluded that the Grignard reagent must exist in a state of equilibrium which could be represented as

$$2RMgX \rightleftarrows R_2Mg + MgX_2. \qquad (A)$$

They excluded the equilibrium

$$R_2Mg \cdot MgX_2 \rightleftarrows R_2Mg + MgX_2 \qquad (B)$$

on the basis of equilibrium-concentration studies. However, investigations by Noller and White (10) and later by Kullmann (11) showed that the method of dioxane precipitation was not reliable as a means of establishing the state of equilibrium of Grignard solutions.

In 1956 Wotiz, Hollingsworth, and Dessy (12) observed that equimolar mixtures of Et_2Mg and $MgBr_2$ in ether gave a solution having the same relative rate of reaction and kinetics with 1-hexyne as did the Grignard prepared in the normal manner. This suggests an equilibrium such as Equilibrium B. To test their hypothesis Dessy *et al.* (13) mixed equimolar amounts of Et_2Mg and $MgBr_2$ where the $MgBr_2$ was labelled with radioactive Mg^{28}. The dioxane precipitation method was used to separate Et_2Mg and $MgBr_2$ after equilibration. Almost all of the radioactivity was found in the $MgBr_2$-dioxane precipitate; this indicates the absence of a RMgX species

since equilibration with such a species would lead to complete statistical exchange of Mg^{28}. They concluded that the equilibrium must be with a dimeric species of the type $Et_2Mg \cdot MgBr_2$ and that this formula would be a better representation of the ethyl Grignard reagent.

Dessy and Handler (14) also found evidence for two types of magnesium atoms in an electrolysis investigation of a mixture of R_2Mg and $Mg^{28}Br_2$. Here it was found that the magnesium plating out at the cathode originated in the R_2Mg while the magnesium migrating to the anode compartment originated in the $MgBr_2$. Dessy (15) also found a break in the plot of dielectric constant versus concentration for $MgBr_2/Et_2Mg$ ratios. This break was at a one to one ratio and the dielectric constant here was the same as that observed for EtMgBr prepared in the conventional manner. Generally, the work of Dessy et al. stimulated research on the Grignard structure problem. A variety of independent experiments were undertaken, but many of these involved preconceived assumptions as to the structure of the Grignard reagent.

French investigators, Hayes (16), Hamelin (17), and Kirrmann (18), have been very actively interested in the structure of the Grignard reagent. They have examined the Grignards by the crystallization of Grignard solutions, vapor pressure measurements, and infrared spectra analysis. In their studies they never isolated a definite compound from Grignard solutions except $MgBr_2$, R_2Mg, and solvent. Their conclusion was that the Grignard reagent was a composite of $MgBr_2$, R_2Mg, and solvent, but that this composite was not a simple one. Some of the results (18) of their solid state investigations of EtMgBr in different solvents are shown

in Table 1. THF here, as well as elsewhere in this thesis, represents tetrahydrofuran. The values in Table 1 show that the structure of the Grignard reagent is quite dependent on the nature of the solvent employed.

Table 1. The solvation of EtMgBr

Solvent	Solubility $n = \frac{EtMgBr}{solvent}$	Solvation of solid No. moles solvent/Mg
Anisole	0.03	2.26
$(iPr)_2O$	0.14	1.23
Bu_2O	0.92	0.57
Et_2O	0.71	1.23
THF	0.12	4.90

The situation up until 1963 was this. The RMgX species and the Schlenk equilibrium generally accepted for some twenty years were almost completely discarded. The favored description for the Grignard reagent now involved the $R_2Mg \cdot MgX_2$ species and Equilibrium B (page 4). It was generally assumed that the $R_2Mg \cdot MgX_2$ structure might be represented best by either the unsymmetrical dimer C or the symmetrical dimer D.

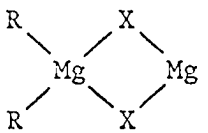

(C)

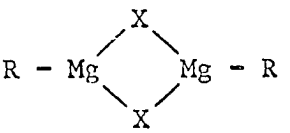

(D)

In 1963 Ashby and Becker (19) observed that the Grignard reagent was monomeric in THF over a wide range of concentrations, and that the fractional crystallization of EtMgCl in THF produced $EtMg_2Cl_3$ and Et_2Mg in quantitative yield. From this they concluded that there was alkyl exchange in THF and the predominant species in THF is RMgX. Their ebullioscopic molecular weight evidence for EtMgCl in diethyl ether indicated a dimeric structure.

A significant breakthrough was made by Vreugdenhil and Blomberg (20) when they observed monomeric molecular weights for EtMgBr and Et_2Mg in diethyl ether solutions at .001 - .01 molar concentrations. Since earlier work by Slough and Ubbelohde (21) pointed out the necessity of excluding contaminants, they made use of high vacuum techniques to insure the exclusion of contaminants. They found that the association number for EtMgBr and Et_2Mg was 1.00 and did not change after 72 hours even in the presence of $MgBr_2$. This observation is inconsistent with the equilibrium

$$Et_2Mg \cdot MgBr_2 \rightleftharpoons Et_2Mg + MgBr_2.$$

For pure $MgBr_2$ they observed association numbers in the range of 1.09 - 1.17 indicating polymeric forms for this species. These measurements were extended to THF (22) where the results were the same except that here the association number for $MgBr_2$ is also 1.00.

Ashby and Smith (23) have also performed some ebullioscopic molecular weight measurements on some Grignard solutions in diethyl ether. They found that the extent of association for the bromides and iodides increased uniformly with concentration, going from the monomeric species

at low concentrations (0.05 M) to dimeric species at higher concentrations (0.5 - 1.0 M). Usual laboratory Grignard preparations are 1 or 2 molar. The chlorides were found to be essentially dimeric at all concentrations.

Dessy et al., realizing that the fundamental justification for the $R_2Mg \cdot MgX_2$ structure was the exchange work, redid the Mg^{28} exchange studies (24). They now found both no exchange and statistical exchange. The only possible correlation seems to be that the no-exchange results occurred when a specific Mg source was used. It is rationalized that some trace impurities may inhibit the exchange. Dessy's observation on the Grignard structure problem is that it is "an apparently insolvable and irreconcilable dichotomy."

Cowan et al. (25) carried out a slightly different kind of exchange experiment in Et_2O using high-purity magnesium-25. They mixed EtMgBr with $Mg^{25}Br_2$ and after 1.5 hr. precipitated the $MgBr_2$ from the solution with dioxane. In this way they avoided the question as to whether a mixture of Et_2Mg and $MgBr_2$ is equivalent to the conventional Grignard reagent. They found that statistical equilibrium was achieved among the various magnesiums present, thus supporting the original Schlenk equilibrium.

Salinger and Mosher (26) have made an infrared spectral study of Grignard solutions in THF and in diethyl ether. They found that the spectra of the Grignard solutions prepared in THF and the spectra of the corresponding dialkylmagnesium solutions in THF are noticeably different and can be interpreted in terms of the Schlenk equilibrium

$$2RMgX \rightleftharpoons R_2Mg + MgX_2.$$

With the exception of C_6H_5MgI, they found that the Grignard reagents studied in diethyl ether gave spectra very similar to those of the corresponding dialkylmagnesium compounds; hence, no conclusions could be drawn in this solvent.

As in the infrared, the proton magnetic resonance spectra of the Grignard reagents are very similar to those of the corresponding dialkylmagnesium compounds (27). This is unusual since the halogen would be expected to have an influence on the chemical shifts of the methylene protons. Ashby and Smith (23) have postulated that this represents an inability of n.m.r. to distinguish between two structures. No satisfactory explanation has been given for the similarity of the two spectra. There is some evidence that in concentrated solutions there is some difference between the proton spectra of R_2Mg·ether and RMgX·ether (28).

Complete three-dimensional X-ray diffraction studies have been made on the ethyl (29) and phenyl (30) Grignard reagents in diethyl ether. These structures consist of ethyl(phenyl) magnesium bromide dietherate monomers with the ethyl(phenyl) group, a bromine atom, and two ether molecules forming a somewhat distorted tetrahedron about a single magnesium atom. This is direct and unambiguous evidence for the existence of monomeric dietherates in the solid state.

Schröder (31) has investigated the solid state $MgBr_2$·THF and C_6H_5MgBr·THF systems. This investigation includes some X-ray diffraction evidence to show that the correct molecular formulas are $MgBr_2$·4THF and

$C_6H_5MgBr \cdot 2THF$. The number of solvent molecules coordinated per magnesium can be rationalized somewhat in terms of the inductive and steric requirements of the magnesium derivative, and the electronic nature of the bonding atom and steric requirements of the solvent. In general the more basic solvents would be expected to coordinate more solvent molecules per magnesium. Thus, there is $MgBr_2 \cdot 4THF$, but only mono-, di-, and trietherates have been reported for $MgBr_2 \cdot$ether (32) in the solid state. There is $C_6H_5MgBr \cdot 2THF$, but also $C_6H_5MgBr \cdot 2Et_2O$ (30); this makes the value of 4.9 in Table 1 for the THF solvation of EtMgBr somewhat questionable. Ethylmagnesium bromide coordinates only one triethylamine (33) and it is a stronger base than both THF and Et_2O in some respects. Most probably steric factors prevent a higher degree of solvation in this case. In fact, more solid state studies on the organomagnesium systems will probably show that the steric requirements are structure determining, at least as far as solvent coordination is concerned. In this regard it is worth noting that the structure of $(CH_3)_2Mg$ has been done (34) and found to be polymeric with the $[(CH_3)_2Be]_n$ structure.

No mention has been made on the possibility of ionic structures in solution. The electrical conductivity of Grignard solutions suggest that these should be considered. Recent electrical measurements have been made by Dessy and Jones (35) and Vreugdenhil and Blomberg (36). The work of Vreugdenhil and Blomberg is probably the more reliable. At higher concentrations in Et_2O they found no significant differences between the conductivity of an EtMgBr solution and the conductivity of a mixture of Et_2Mg and $MgBr_2$. It is generally assumed that ionic species

play only a minor role in describing Grignard solutions. See Kharasch and Reinmuth (3) for a discussion of the electrolytic properties of Grignard solutions and possible ionic structures.

It is evident that ideas regarding the nature of the Grignard reagent have changed since 1963. It is now popular with some authors (23, 24) to describe this reagent in diethyl ether by the equilibrium

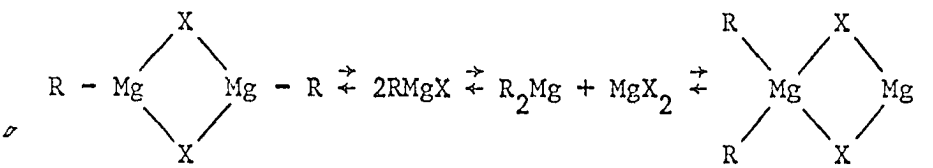

where the equilibrium is supposedly a function of the R group, the halogen, the solvent, and the concentration. In THF the Schlenk equilibrium (Equilibrium A, page 4) is considered to be an adequate representation of EtMgBr.

The significance of the results of this investigation, as well as the implications with respect to the above equilibrium, will be discussed in the discussion section.

Purpose

When this investigation was begun it was generally believed that the Grignard reagent was associated and probably dimeric in the liquid and solid states. Stucky and Rundle (30) were just finishing up their studies which showed that the phenyl Grignard reagent in the solid state was actually the monomeric $C_6H_5MgBr \cdot 2Et_2O$.

The purpose of the investigation of the ethyl Grignard reagent in diethyl ether was to extend Stucky and Rundle's work to include an alkyl Grignard reagent. The ethyl Grignard, EtMgBr·ether, was chosen because it has been the one most studied by other investigators. The primary objective in undertaking this study was to characterize the molecular configuration of the ethyl Grignard reagent in diethyl ether. It was hoped that the phenyl and ethyl Grignard structures would solve the problem of the solid state etherates.

A specific aspect of the molecular configuration of interest was the bonding about the ether oxygens. The question is whether the oxygens use sp^2 or sp^3 hybrid orbitals. The data on $C_6H_5MgBr \cdot 2Et_2O$ (37) were not good enough to get reasonable ether carbon positions so that it was not possible to unambiguously characterize the bonding about the ether oxygens.

Preparation and Purification

The apparatus for the preparation of the ethyl Grignard reagent consisted of a 500 cc. three-necked, round-bottom reaction flask, fitted with a magnetic stirrer, condenser, cylindrical dropping funnel, and transfer tube extending well into the reaction flask. The function of the transfer tube was to transfer the final product through a fritted glass filter into the receiving vessel shown in Figure 1. The reaction and receiving assemblies were fitted with stopcocks and mineral oil valves in such a way that the entire apparatus could be evacuated and filled with argon. All joints were of the ground glass variety; a minimum amount of stopcock grease was used since it is soluble in ether.

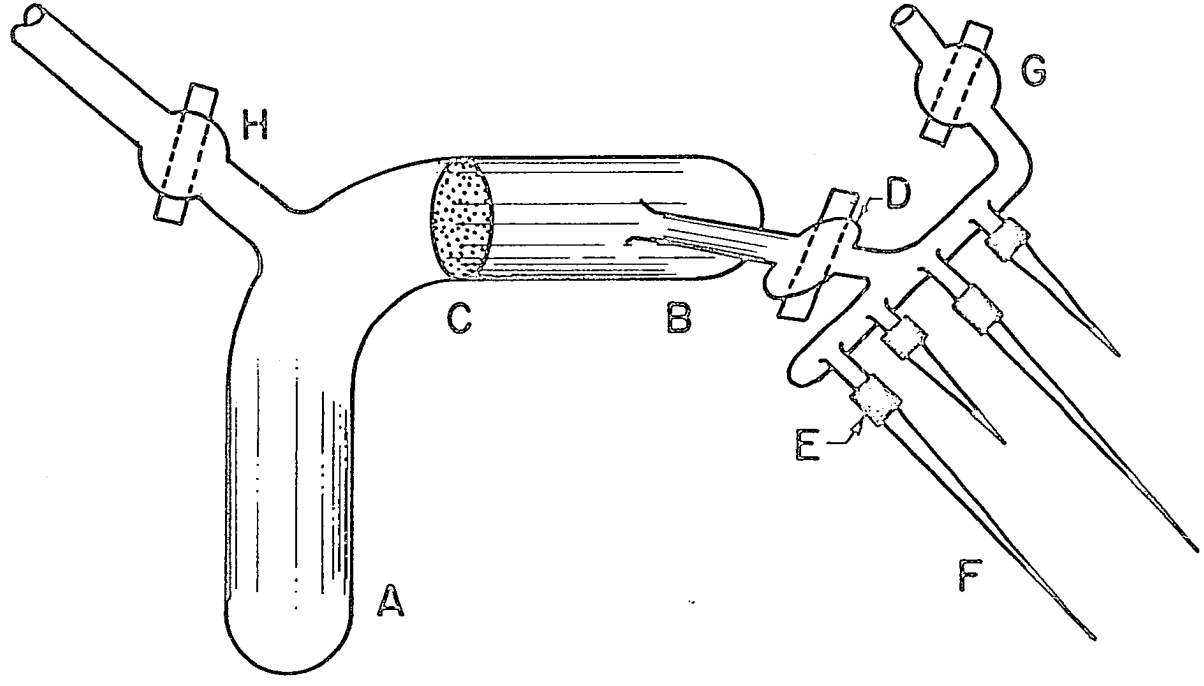

Figure 1. Apparatus for the purification of $EtMgBr \cdot 2Et_2O$

All preparations were made about 1 molar. Specifically, 12 g. of magnesium was added to the reaction vessel and the system was then evacuated and flushed with argon to assure the absence of moisture and an inert atmosphere. The necessity of excluding moisture and oxygen has been pointed out by Slough and Ubbelohde (21). A solution of 25.4 cc. ethyl bromide in 300 cc. diethyl ether was then added dropwise. Sometimes a more concentrated solution of ethyl bromide was added initially to get the reaction started. The reaction proceeds readily and is very exothermic. A Graham condenser worked quite well in preventing the loss of ether during the reaction. At the end of the reaction the solution was refluxed for 15 minutes. Fisher's magnesium turnings and Baker's ethyl bromide and canned anhydrous ether were used. The argon was dried by passing it through P_2O_5 drying towers.

About 50 cc. of product was transferred under an inert atmosphere into side A of the receiving vessel shown in Figure 1; the solution was already filtered once through a fritted glass filter in the transfer process. This receiving vessel was partially evacuated, closed at H, and disconnected from the rest of the transfer assembly. At this point the solution was a gray to black in color. The solution was poured through the fritted glass disc at C (medium porosity) to side B where it was cooled by liquid nitrogen or a Dry Ice-acetone bath until crystals formed. The mother liquor was decanted over to A and then pure solvent was returned to the crystals by distillation. The crystals were redissolved and the purification cycle was reiterated. The extent of purification was varied; pure product was colorless.

The pure ethyl Grignard was poured through a stopcock D into the .3 mm. Lindemann glass capillaries. The capillaries were cut and sealed with a torch; they were cut into sections about 1 cm. in length with each section containing about 1 mm. of Grignard. The capillaries were sealed at E with surgical rubber tubing. The stopcock at G was to allow for the evacuation of four new capillaries. The whole process of purification, isolation of the right amount of material of the right consistency, and obtaining a good seal is a matter of skill acquired by long practice.

Low Temperature Apparatus and Crystal Growth

The main features of the low temperature apparatus are shown in Figure 2. The lettered items are as follows:

A. Heater and bimetallic safety switch in 12 liter Dewar.

B. Metal tube containing a positive nitrogen pressure.

C. Vacuum jacketed spout.

D. Valve and joint to disconnect transfer tube.

E. Vacuum jacketed transfer tube.

F. Liquid nitrogen reservoir--50 liters.

G. Gauge and valve to regulate pressure on the reservoir.

H. Solenoid valve.

I. Variac to regulate heater.

J. Honeywell Pressuretrol switch--activates solenoid valve.

K. Tork time switch.

L. Thermocouple--measures temperature at tip of spout.

M. Goniometer containing crystal.

Figure 2. Diagram of low temperature apparatus

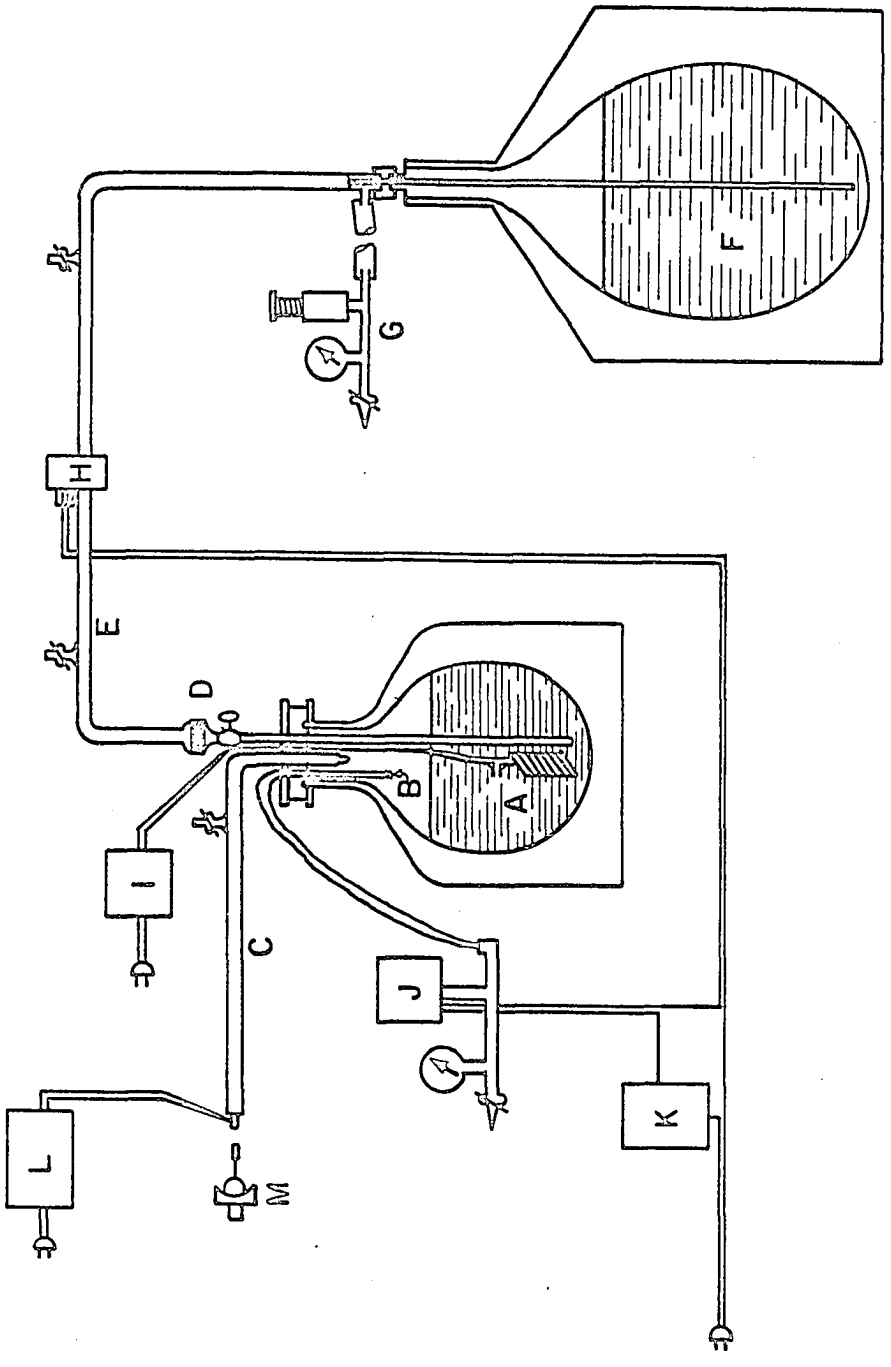
A
B
C
D
E
F
G
H
I
J
K
L
M

When the liquid nitrogen level in the small Dewar is high there is no pressure in tube B and the solenoid valve H is closed. When the liquid level goes down the pressure builds up in B activating the switch J so that the valve H opens. When H opens the positive pressure in the large Dewar forces liquid nitrogen into the small Dewar until H closes. The filled pressure and cut-in pressure can be adjusted at J. The timer K was used independently or in conjunction with the switch J. The transfer tube can be disconnected at D to allow for the filling of the 50 liter Dewar. The spout and transfer tube are made of copper. The variac was actually two variacs connected in series.

Because of supercooling it was usually necessary to get the capillary very cold before crystallization was induced. The initial crystalline mass was allowed to melt slowly until several nuclei remained. These nuclei were then alternately grown and melted until a single nuclei remained. This single nuclei was slowly cooled until the entire mother liquor had crystallized giving one perfect single crystal. Small temperature gradients were sometimes obtained by touching the capillary with a wire which had been at room temperature.

The entire crystal growing process was observed continually through a Bausch and Lomb Stereo-Zoom (30X magnification) microscope equipped with a long focal length objective. A small light was placed directly under the crystal. Crossed polaroids were found to be very helpful in orienting the crystal prior to taking X-ray photographs. Since the crystals are monoclinic the crossed polaroids are helpful in locating the b axis and the a-c plane.

Lattice Constants and Space Group

The lattice constants were measured directly from the three zero level intensity photographs. The 6.00 cm. crystal to film distance was confirmed by taking pictures of a standard NaCl crystal. The observed lattice constants and their estimated standard deviations are

$$a = 13.18 \pm 0.03 \text{ Å}$$

$$b = 10.27 \pm 0.03 \text{ Å}$$

$$c = 11.42 \pm 0.03 \text{ Å}$$

$$\beta = 103.3 \pm 0.3°.$$

These lattice parameters were used in the structure refinement.

The Laue symmetry observed was P2/m so that the crystal system is monoclinic. The following extinctions were observed:

$\{h0\ell\}$ $\ell = 2n + 1$

$\{0k0\}$ $k = 2n + 1$

On the basis of these extinctions the space group was uniquely determined to be $P2_1/c$. The equivalent positions for the space group $P2_1/c$ are given in Table 2.

A crude density measurement gave a density of 1.13 g./cm.^{3}. This measurement was obtained by weighing a certain volume of sample contained in a commercial n.m.r. tube of uniform thickness. This density indicates that there are four molecules per unit cell. The calculated density on the basis of four molecules per unit cell is 1.24 g./cm.^{3}. The linear

Table 2. Equivalent positions of $P2_1/c$

No. of positions	Point symmetry	Equivalent positions
4	1	x,y,z;
		$\bar{x},\bar{y},\bar{z}$;
		$\bar{x},1/2+y,1/2-z$;
		$x,1/2-y,1/2+z$

absorption coefficient with Mo radiation, based on the preceding density and the molecular formula $EtMgBr \cdot 2Et_2O$, is 29.1 $cm.^{-1}$.

Collection and Correction of Data

The following intensity data were collected on the precession camera on two different crystals: {0kℓ}, {1kℓ}, and {2kℓ} on crystal number 1; {h0ℓ}, {h1ℓ}, {h2ℓ}, {hk0}, {hk1}, and {hk2} on crystal number 2. The precession angle was 25° for crystal number 1 and 30° for crystal number 2. The reason for using two crystals was that crystal number 1 was oriented in such a way that the other zones could not be aligned. The data were taken at about -70° C. At this temperature the condensation of moisture on the capillary containing the crystal is a big problem. Several different types of tips were used on the cold gas spout to minimize the moisture problem, but the only method which proved successful was to enclose the entire camera in a polyethylene tent.

The crystals used were cylindrical in shape with a diameter of about .3 mm. In growing crystals an effort was always made to keep the length

of the cylinder about the same as the diameter. Keeping the crystal as symmetrical as possible minimizes any error due to X-ray absorption. The μR for these cylindrical crystals is about 0.45.

The exposure times were taken according to ar^n with a = 1 min., r = 2, and n = 0,1,....,8. Since the intensities were to be judged by comparison with a standard series of spots, an extra layer of data was taken to make up the standard series, namely the {1kℓ} layer. There was too much streaking in the zero layers to use any of these spots for the standard series. The times for the standard series were taken according to ar^n with a = 1.5 min., r = 1.5, and n = 0,1,....,11. In preparing a standard series it is desirable to have the blackness of the spot exposed for ar^n minutes just distinguishably greater than the blackness of the spot exposed for ar^{n-1} minutes.

The intensity data were judged twice by the author. The structure factors from the first judging were used to solve the structure. The second judging was done a year later and these structure factors were used in the refinement. A total of 979 reflections were judged the first time. On those photographs showing $C_{2\ell}$ (mm) symmetry two quadrants were judged and then averaged. The number of times a reflection was judged on a given layer depended on its intensity, but most reflections were judged at least twice. The intensities from photographs of the same layer were scaled together by the time factor or by the average ratio of the corresponding intensities on successive photographs, depending on how many spots were judged.

A program was written to correct the observed intensities for the Lorentz factor, L(hkl), and the polarization factor, p(hkl). They are related according to

$$I(hk\ell) = KL(hk\ell)p(hk\ell)\left|F(hk\ell)\right|^2$$

where I(hkℓ) is the intensity, F(hkℓ) is the structure factor, and K is a scale factor.

The 9 layers were scaled together by considering the structure factors from the same reflections as they appeared on different layers. For example, the scale factor between layers 1 and 2 can be obtained by

$$SF = \frac{\sum_{i=1}^{N} F^2_{\text{layer 2}} / F^2_{\text{layer 1}}}{N}$$

where N is the number of reflections being considered. It was not important to determine the scale factors accurately at this point since they were to be obtained by least squares later. Only approximate values were needed so that a Patterson function could be calculated.

Solution of Structure

The plan of attack in solving this structure was to use the "heavy atom" method. Because of the mechanism of scattering by X-rays, the scattering power of a heavy atom often dominates the intensities, hence controlling many or all of the phases. An atom is heavy in the sense that it has more electrons than the other atoms in the structure. In

this structure it was assumed that the Br and Mg atoms would control the phases. The actual mechanics of the "heavy atom" approach won't be discussed here since this approach is discussed in most crystallographic texts.

The 9 layers of data taken do not represent all of the data in the Mo sphere, (λ = 0.71069) but it is so close to being complete three-dimensional data that all of the analyses were done in three dimensions. The alternative was to solve the structure by projections, but this would have been more difficult.

The Br and Mg positions were obtained by an analysis of the Patterson function using the symmetry of the space group. Pairs of symmetry-equivalent atoms give rise to peaks in certain two-dimensional sections and one-dimensional lines in the three-dimensional Patterson; these are called Harker sections (38). For example, the c glide plane in this structure will relate the point x, y, z and x, 1/2-y, 1/2+z; the vector in the Patterson between these two points will occur at $\pm$(0, 1/2+2y, 1/2), i.e., on the line 0, v, 1/2. The 2_1 axis relates the points x, y, z and $\bar{x}$, 1/2+y, 1/2-z; the corresponding peak will occur on the Harker plane u, 1/2, w.

The Br and Mg positions were obtained by analyzing the Harker sections making use of expected single peak heights and multiplicities (39). On the Harker line 0, v, 1/2 there was a large peak at v = 1/2; the height corresponded to an expected Br-Br interaction of multiplicity 4. This fixes the y coordinate for the Br atom at y = 0 since this v = 1/2

must be equal to 1/2 + 2y in electron density space. The x and z coordinates were obtained from the Harker plane u,1/2,w where there was a peak at u = 0.284 and w = 0.925; the peak height corresponded to a Br-Br interaction of multiplicity 2. The equations 2x = 0.284 and 1/2 + 2z = 0.925 gave the x and z coordinates immediately. The Mg positions were obtained from an analysis of Br-Mg vectors. A comparison of the positions calculated from the Patterson map and those obtained on refinement is made in Table 3.

Table 3. Bromine and magnesium positions

Atom	Coordinate	Calculated from Patterson	Refined by least-squares
Br	x	0.142	0.141
	y	0.000	-0.021
	z	0.213	0.211
Mg	x	0.280	0.276
	y	0.000	0.018
	z	0.087	0.096

At this point a three-dimensional Fourier synthesis of the electron density was calculated where the Fourier coefficients were the observed structure factors with the phases (signs) calculated from the Br and Mg positions. All of the O and C positions were obtained from electron density maps using either F_o or (F_o-F_c) as the Fourier coefficients;

F_o and F_c are the observed and calculated structure factors, respectively.

The variables in the initial refinement were 9 scale factors (1 for each layer), 3 positional parameters for each atom, and one isotropic temperature factor, B, for each atom. The isotropic temperature factor is used in multiplying the scattering factors by $\exp(-B \sin^2\theta/\lambda^2)$; it is related to the mean square displacement $\bar{u}^2$ of the atoms from their mean positions by $B = 8\pi^2\bar{u}^2$. The R factor at this point, where $R = \Sigma||F_o| - |F_c||/\Sigma|F_o|$, was 0.10. The layers were then scaled together and several cycles of anisotropic least squares were run reducing R to about 0.08. The pertinent details of the refinement will be discussed in the next section.

Refinement of Structure

A separate section has been reserved for the structure refinement since the final model can be quite dependent on certain aspects of the refinement. Five aspects of the refinement will be discussed in some detail; namely, the scaling of the 9 layers of data, the appropriateness of the weighting scheme, the anomalous dispersion correction for the bromine atom, the hydrogen atom contributions, and the analysis of the final fit as evidenced by the discrepency index R. Good positional parameters and thermal parameters were obtained from the first set of judged intensities. The refinement discussed here proceeds from these parameters and the second set of judged intensities reduced to their corresponding structure factors.

In this investigation the 9 scale factors correlating the intensity data were obtained by fitting the layers of data to the structure by least squares. The advantage of this method is that scale factors can be refined along with the positional and thermal parameters in the regular least squares program. More general methods of correlating data without making any assumptions about the model have been discussed by Rollett and Sparks (40) and more recently by Hamilton et al. (41).

The object of a least squares refinement is to minimize some function of the observed and calculated intensities with respect to the structure parameters. The function most commonly used and the one used in this investigation is

$$R' = \Sigma w(hkl)(|F_o(hkl)| - |F_c(hkl)|)^2$$

where the weight w(hkl) of a particular term is taken inversely proportional to the square of the probable error in F_o (42).

$$w(hkl) = 1/\sigma^2(hkl)$$

The real problem involves getting a good estimate of the probable error in F_o. Three approaches have been used in this regard. The first involves determining the probable error in F_o by repeated measurements. The second approach involves calculating the probable error in F_o on the basis of theoretical considerations (43). These two approaches are complicated by systematic errors. The third method involves using some arbitrary weighting scheme and then using $F_o - F_c$ as a measure of the

error in F_o. DeVries (44) has proposed that it might be better to regard σ not as a function of F or a function of F and θ, but rather as a function of I and θ.

The weighting scheme approach used in this investigation was essentially the third method described. The initial sigmas were chosen according to

$$\sigma = 4F_{min}/F_o \qquad F_o < 4F_{min}$$

$$\sigma = F_o/4F_{min} \qquad F_o > 4F_{min}$$

where F_{min} is the absolute value of the minimum observable F_o. This is a modified Hughes scheme used with some success in this laboratory (45). This differs from the regular Hughes method (42) in that it places less weight on those reflections for which $I_o < 16I_{min}$. The assumption made here was that the planes of medium $\sin\theta$ are the most accurate. A small number of reflections considered unobserveds were used in the refinement. These were either low order reflections conspicuously weak or high order reflections that could not be classified as observed or unobserved on the films. The intensities for these were set equal to $I_{min}/2$ and they were left in all least squares runs with 1/2 their calculated weights.

In the final refinement stage the appropriateness of the weighting scheme was checked by plotting the average values of $w\Delta^2$, where $\Delta = ||F_o| - |F_c||$, in ranges of $|F_o|$ and $\sin\theta/\lambda$. The criterion for a good weighting scheme is that the average values of $w\Delta^2$ must be constant when the $w\Delta^2$ values for a given structure are analyzed in any systematic

fashion (46). Accordingly the weighting scheme was modified slightly since the $w\Delta^2$ averages in the low $\sin\theta/\lambda$ regions were systematically too high. The experience of this investigation has been that much caution must be used in correcting a weighting scheme on the basis of a $w\Delta^2$ plot. This plot can be very model dependent even when as many as 100 reflections are considered for each average. Failure to account for anisotropic vibrations and hydrogen atom contributions and any incorrect parameter values can significantly affect the $w\Delta^2$ plot. An excellent weighting scheme would probably fit the constant $w\Delta^2$ criterion in sinesoidal fashion.

It was apparent from the method in which the data were taken that all the layers should not be scaled according to the same scheme. For example, the second layers would not be expected to be as reliable as the zero layers. To account for this the sigmas for all of the layers were multiplied by constant values; the constants were determined by analyzing the average $w\Delta^2$ values for all the layers.

Another factor which was considered in the refinement was the anomalous dispersion effect experienced by waves scattered by the bromine atom. Since the wavelength of the radiation used was just less than the bromine absorption edge, the radiation scattered by the bromine atom experienced an anomalous phase shift. The atomic scattering factor f for the bromine atom can be expressed as

$$f = f_o + \Delta f' + \Delta f''$$

where f_o is a real function of $\sin\theta/\lambda$ and f' and f" are the real and imaginary dispersion corrections, respectively. The f_o scattering factor tables used were those calculated by Hansen, et al. (47) from Hartree-Fock-Slater wave functions. The values used to correct for the anomalous dispersion were those listed by Dauben and Templeton in International Tables, Vol. III (48). The real part of the anomalous dispersion correction for Br is a constant and is simply added to the f_o table. The imaginary part is more difficult to correct for and in this investigation it was included in the least squares refinement after the method of Ibers and Hamilton (49).

The 25 hydrogen atoms per molecule represent a considerable amount of electron density even though their thermal motion would be expected to be quite large. The plan of attack in locating some of these was to first of all calculate their expected positions on the basis of tetrahedral geometry and then look for them on a Fourier difference map. All of the methylene hydrogens and 6 terminal methyl hydrogens in the asymmetric unit were located since they were the most prominent peaks remaining in the difference map. These 16 hydrogens were included in the refinement; however, none of the hydrogen positional or thermal parameters were varied. The isotropic B for the hydrogens was set equal to 4.5.

The refinement proceeded from a R factor of 9.66% for all reflections (895, including redundant data on different layers) with the old parameters and new data to 9.39% after one cycle of isotropic least squares. The sigmas for the layers were adjusted so that all layers were

weighted equally in the $w\Delta^2$ sense. The redundant data were then averaged together and all of the data was scaled together; 670 independent reflections remained with 637 of these being considered as observed reflections. The discrepency index went to 8.70% for all reflections after two cycles of anisotropic refinement. Sixteen hydrogen atoms were located and the weighting scheme was corrected on the basis of a $w\Delta^2$ vs. $\sin\theta/\lambda$ plot. The refinement was stopped after two more cycles of anisotropic refinement. An electron density map using (F_o-F_c) as Fourier coefficients indicated that all of the electron density had been accounted for. The final R factors were

	all refl.	observeds only
$R = \Sigma\Delta/\Sigma\lvert F_o\rvert$ =	.077	.073
$wR = \Sigma w'\Delta/\Sigma w'\lvert F_o\rvert$ =	.065	.064

The "standard error" of the fit for all reflections was

$$[\Sigma w\Delta^2/(m-n)]^{1/2} = 1.12.$$

The w' here represents $1/\sigma(F_o)$ opposed to the w used as a weight in least squares. A listing of the observed and calculated structure factors is given in Figure 3.

A more detailed analysis of the fit is given in Table 4; all of the data (including unobserveds) has been included in this summary. A complete analysis such as this is important since the data represent intensities taken from 2 different crystals and 9 different sets of photographs. In

Figure 3. Comparison of observed and calculated structure factors for $EtMgBr \cdot 2Et_2O$ (An asterisk following the first index denotes an unobserved reflection.)

H	K	L	FO	FC
2	0	0	127.6	-123.5
3	0	0	114.9	-111.5
4	0	0	91.3	-85.3
5	0	0	111.0	-109.2
7	0	0	96.4	100.4
8	0	0	52.4	54.0
10	0	0	44.3	-45.7
11	0	0	35.0	-37.9
14	0	0	22.7	20.2
15	0	0	13.6	12.2
4	1	0	19.2	-18.9
5	1	0	31.8	-29.0
6	1	0	16.0	-14.0
7	1	0	12.0	13.6
8	1	0	15.2	19.7
9	1	0	17.0	20.0
0	2	0	80.3	82.9
1	2	0	33.4	34.8
2	2	0	25.9	20.0
3	2	0	131.1	-131.7
4	2	0	35.6	-35.7
5	2	0	13.4	-14.0
6	2	0	17.6	17.9
7	2	0	93.2	95.0
8	2	0	45.1	42.7
9	2	0	35.6	-34.8
10	2	0	43.2	-44.5
14	2	0	26.4	24.1
1	3	0	81.9	82.3
2	3	0	74.6	76.1
3	3	0	21.7	23.1
4	3	0	12.9	-16.9
5	3	0	34.2	-35.5
6	3	0	34.5	-27.1
9	3	0	35.9	31.0
12	3	0	21.3	-15.6
0	4	0	107.6	107.5
2	4	0	27.5	-21.1
3	4	0	36.9	-34.3
4	4	0	55.1	-55.5
5	4	0	47.0	-44.7
6	4	0	38.8	36.0
7	4	0	68.0	66.6
10	4	0	14.6	-15.6
11	4	0	21.1	-10.9
14	4	0	14.9	14.5
1•	5	0	7.5	5.0
2	5	0	57.1	60.3
3	5	0	33.1	31.0
4	5	0	32.8	-26.5
5	5	0	38.8	-34.5
12	5	0	18.7	-17.8
0	6	0	73.4	76.4
1	6	0	22.1	27.0
2	6	0	27.7	-26.3
3	6	0	37.4	-36.0
7	6	0	37.4	31.6
10	6	0	21.1	-17.9
14	6	0	14.3	11.7
2	7	0	31.7	32.7
3	7	0	39.3	35.2
5	7	0	60.1	-59.1
6	7	0	18.6	-23.0
8	7	0	20.9	16.8
9	7	0	16.0	19.9
12	7	0	21.2	-15.5
0	8	0	24.8	26.3
1	8	0	13.5	12.3
2	8	0	16.9	-14.3
3	8	0	13.8	-12.9
7	8	0	27.4	27.2
1	9	0	18.6	18.5
2	9	0	42.7	40.8
3	9	0	16.4	13.6
4	9	0	18.2	-19.5
5	9	0	32.0	-27.1
9	9	0	21.6	16.7
12	9	0	15.8	-15.9
0	10	0	16.9	10.7
2	11	0	23.5	21.2
5	11	0	21.9	-17.6
0	1	1	119.6	111.7
1	1	1	92.0	-78.1
2	1	1	130.1	-121.1
3	1	1	74.7	-69.2
4	1	1	67.7	63.4
-4	1	1	43.9	-39.2
5	1	1	27.0	29.5
-5	1	1	50.7	-55.5
6	1	1	63.8	63.8
-6	1	1	98.0	-96.4
7	1	1	33.8	29.8
-7	1	1	39.6	40.6
8	1	1	22.9	-21.6
-8	1	1	68.7	70.6
9	1	1	50.4	-51.2
-9	1	1	38.7	40.4
10	1	1	23.9	-25.3
-10	1	1	16.0	-10.6
11	1	1	16.4	6.4
-11•	1	1	21.1	-15.9
-12	1	1	21.6	-21.6
13	1	1	19.8	21.2
-13	1	1	23.2	-23.3
-15	1	1	20.1	14.9
2	2	1	54.9	49.4
-3	2	1	27.2	-28.3
-6	2	1	27.1	29.7
0	3	1	26.9	18.3
1	3	1	126.1	-119.1
-1	3	1	136.5	123.1
2	3	1	68.6	-71.2
-2	3	1	94.1	90.0

H	K	L	FO	FC
3	3	1	29.7	-29.1
-3	3	1	50.6	51.7
-4	3	1	40.3	-42.3
5	3	1	20.4	21.4
-5	3	1	94.5	-96.1
6	3	1	79.6	76.5
-6	3	1	74.1	-72.6
7	3	1	34.1	36.1
-7	3	1	39.0	33.0
8	3	1	40.3	-40.6
-8	3	1	38.0	36.6
9	3	1	62.1	-61.2
-9	3	1	19.5	23.7
10	3	1	18.4	-16.2
11	3	1	21.4	22.1
-12	3	1	26.8	-24.4
-13	3	1	30.5	-25.5
0	4	1	32.0	33.8
1	4	1	27.9	30.0
2	4	1	18.4	17.0
-2	4	1	17.3	-15.3
3	4	1	51.0	-53.7
-3	4	1	23.6	-32.5
4	4	1	40.4	-43.7
-4	4	1	13.1	-9.6
6	4	1	38.8	42.5
-6	4	1	15.0	14.7
-7	4	1	24.7	23.8
-8	4	1	20.8	27.7
-9	4	1	17.6	-15.8
-10	4	1	30.2	-27.6
11•	4	1	13.6	-16.2
-11	4	1	18.9	-17.1
0	5	1	36.4	39.1
1	5	1	58.7	-60.0
-1	5	1	59.1	60.1
2	5	1	78.1	-80.3
-2	5	1	42.9	41.9
3	5	1	30.5	-27.4
4	5	1	27.2	22.5
-4	5	1	26.7	-27.7
5	5	1	21.2	20.4
-5	5	1	39.8	-39.3
6	5	1	47.8	49.6
-6	5	1	37.4	-40.0
7	5	1	27.9	23.7
8	5	1	24.5	-27.6
-8	5	1	36.6	37.0
9	5	1	30.2	-28.5
-9	5	1	36.1	36.4
-12	5	1	19.5	-18.8
-13	5	1	22.3	-20.6
0	6	1	47.8	49.6
-1	6	1	53.1	54.8
3	6	1	26.7	-25.7
-3	6	1	74.1	-70.1
4	6	1	31.7	-35.7
-4	6	1	45.7	-45.6
5	6	1	32.0	-32.5
6	6	1	24.4	24.1
-6	6	1	22.7	29.5
7	6	1	32.7	33.7
8	6	1	26.3	25.8
-8	6	1	17.7	18.2
-10	6	1	18.9	-18.5
11	6	1	19.5	-17.5
-11	6	1	23.9	-18.9
0	7	1	15.5	16.5
1	7	1	31.5	-30.2
-1	7	1	34.0	34.6
2	7	1	29.6	-32.2
5	7	1	16.8	16.9
-5	7	1	22.6	-24.5
6	7	1	19.6	17.5
-6	7	1	30.9	-31.0
7	7	1	18.0	16.5
-8	7	1	25.3	21.6
9	7	1	23.5	-23.6
10•	7	1	13.7	-14.7
0	8	1	27.3	28.4
1	8	1	17.4	18.1
-1	8	1	33.6	34.1
2	8	1	18.6	22.1
-2	8	1	25.8	-26.8
-3	8	1	57.7	-56.4
4	8	1	42.2	-41.2
-4	8	1	24.8	-20.1
5	8	1	24.1	-23.6
6	8	1	18.1	19.1
-7	8	1	18.3	20.2
-10	8	1	19.5	-16.6
11•	8	1	14.1	-13.2
-11	8	1	22.3	-16.4
0	9	1	19.5	16.2
2	9	1	17.6	-17.3
-5	9	1	20.6	-18.1
0	10	1	15.0	16.2
1	10	1	23.2	25.0
3	10	1	27.8	-25.4
-3	10	1	18.7	-16.0
4	10	1	34.3	-30.2
-4	10	1	21.2	-18.2
6	10	1	19.5	17.7
0•	10	1	14.1	8.8
-1	12	1	20.1	16.1
-3	12	1	22.7	-19.3
0•	0	2	5.0	-13.0
1	0	2	56.2	-57.0
-1	0	2	22.4	-20.7
2	0	2	118.0	-107.3
-2	0	2	63.2	-66.7
3	0	2	129.9	127.4
4	0	2	117.0	119.2

H	K	L	FO	FC
-4	0	2	73.0	76.7
5•	0	2	7.3	-7.7
-5•	0	2	6.7	9.8
6	0	2	26.7	-25.9
-6	0	2	110.5	-109.5
7	0	2	58.7	-56.4
-7	0	2	81.2	-84.5
8	0	2	57.9	-57.9
-8•	0	2	8.3	14.0
9•	0	2	9.1	-2.1
-9	0	2	32.1	30.0
10	0	2	37.9	42.4
-10	0	2	28.0	28.7
11	0	2	27.1	24.6
-11	0	2	23.4	22.1
-12	0	2	13.7	15.6
-13	0	2	26.1	-28.0
-14	0	2	18.5	-21.0
15	0	2	18.6	-15.4
0•	1	2	5.8	-8.9
1	1	2	40.8	-33.4
-1	1	2	25.7	37.1
-2	1	2	72.5	67.8
-3	1	2	48.7	42.8
-4	1	2	28.1	-23.7
6	1	2	22.5	21.1
0	2	2	204.4	-189.5
1	2	2	162.3	-159.4
3	2	2	81.1	78.6
-3	2	2	103.7	104.2
4	2	2	76.7	72.4
-4	2	2	102.0	102.8
5	2	2	54.2	56.8
6	2	2	23.3	19.5
-6	2	2	109.2	-108.7
7	2	2	43.5	-44.5
-7	2	2	55.6	-54.0
8	2	2	49.4	-53.2
9	2	2	30.1	-31.2
-10	2	2	38.3	37.1
11	2	2	32.3	34.2
-11	2	2	31.1	33.3
0	3	2	39.6	-29.9
-1	3	2	37.0	30.0
2	3	2	27.3	-23.1
-2	3	2	40.1	37.4
3	3	2	41.2	-39.2
5	3	2	42.5	46.8
-5	3	2	43.4	-33.3
6	3	2	30.7	34.9
7	3	2	25.9	-12.7
0	4	2	74.1	-70.3
1	4	2	81.2	-86.0
-1	4	2	18.0	13.9
2•	4	2	20.6	-23.5
-2	4	2	45.1	47.7
3	4	2	55.7	64.9
-3	4	2	62.5	60.7
4	4	2	55.9	55.9
-4	4	2	27.9	17.7
-6	4	2	51.2	-51.4
-7	4	2	47.2	-44.5
8	4	2	56.7	-52.2
10	4	2	34.6	31.3
0	5	2	17.4	16.7
-1	5	2	79.0	78.1
2	5	2	31.8	-32.5
-2	5	2	27.1	29.3
3	5	2	34.6	-36.0
4	5	2	34.7	-27.8
-4	5	2	46.1	-46.6
5	5	2	41.0	31.1
-5	5	2	39.9	-37.9
6	5	2	45.5	48.4
-8	5	2	51.4	44.1
-9	5	2	28.7	31.3
0	6	2	16.1	-14.0
1	6	2	54.0	-55.6
3	6	2	39.6	30.2
-3	6	2	22.5	27.9
-4	6	2	46.0	39.8
-6	6	2	42.0	-48.1
-7	6	2	39.4	-36.0
1•	7	2	12.4	-22.6
-1	7	2	56.3	57.5
2	7	2	39.5	-41.0
-2	7	2	42.2	40.9
-4	7	2	35.0	-36.3
0	8	2	15.7	-17.2
1	8	2	18.5	-21.8
1•	9	2	13.7	-5.7
-1	9	2	26.8	30.0
-2	9	2	20.4	24.1
1•	10	2	14.0	-11.0
-1	11	2	19.7	19.0
0	1	3	98.0	-83.5
1•	1	3	5.9	6.5
-1	1	3	91.6	-90.8
2	1	3	76.1	76.7
-2	1	3	82.3	-76.4
3	1	3	112.6	102.5
-3•	1	3	6.1	-8.1
4	1	3	34.1	27.8
-4	1	3	131.0	128.9
5	1	3	38.2	-34.4
-5	1	3	100.0	101.1
6	1	3	53.2	-53.3
-6•	1	3	8.3	-4.0
7	1	3	48.4	-47.9
-7	1	3	70.4	-74.8
-8	1	3	13.7	-24.6
9	1	3	40.2	35.6
-9	1	3	38.1	-36.5

H	K	L	FO	FC
10	1	3	44.2	43.5
-11	1	3	29.3	31.7
-12	1	3	40.3	43.3
-14	1	3	17.2	-21.3
0	2	3	50.9	-49.7
-1	2	3	26.0	18.9
-2	2	3	69.5	65.1
5	2	3	30.5	37.2
0	3	3	67.9	-76.0
1	3	3	32.1	-39.3
2	3	3	90.8	88.6
-2	3	3	31.2	-28.2
0	4	3	35.3	-37.9
1	4	3	21.8	-21.8
2	4	3	24.9	-23.2
-2	4	3	24.7	29.1
0	5	3	47.2	-47.9
-1	5	3	34.1	-32.9
2	5	3	50.8	49.9
-2	5	3	44.2	-43.7
0	6	3	37.2	-39.7
1	6	3	22.7	-28.7
2	6	3	26.3	-26.6
-2	6	3	56.4	54.5
0	7	3	22.4	-25.5
-1	7	3	23.0	-20.4
2	7	3	25.2	29.2
-2	7	3	33.5	-35.4
0	8	3	33.8	-37.9
1	8	3	34.8	-35.9
-2	8	3	28.2	28.1
0	10	3	23.5	-20.5
1	10	3	19.9	-11.4
-2	10	3	31.9	34.6
0	0	4	97.3	92.7
1	0	4	127.0	118.7
-1	0	4	27.3	-31.6
2	0	4	50.1	59.8
-2	0	4	99.2	-102.2
3	0	4	18.7	-14.0
-3	0	4	119.2	-119.1
4	0	4	67.5	-69.5
-4	0	4	12.2	8.1
5	0	4	55.2	-53.8
-5	0	4	57.8	58.0
6	0	4	20.8	-21.6
-6	0	4	61.6	62.4
-7•	0	4	7.9	11.6
8	0	4	35.1	36.6
-8•	0	4	8.4	2.6
9	0	4	38.0	40.9
-9	0	4	30.1	-28.1
10	0	4	19.3	16.0
-10	0	4	48.9	-52.0
11	0	4	30.2	-32.9
-11	0	4	13.3	-14.0
12	0	4	19.7	-18.1
-12	0	4	21.7	21.5
-13	0	4	30.5	32.2
0	1	4	17.1	-15.8
-1	1	4	18.2	-8.4
-2	1	4	42.2	44.6
0	2	4	17.0	14.2
1	2	4	61.1	59.4
2	2	4	83.0	82.5
-2	2	4	43.5	-43.7
-3	2	4	112.0	-107.9
4	2	4	106.1	-97.7
5	2	4	44.9	-44.7
-5	2	4	46.8	48.0
-6	2	4	66.5	69.2
8	2	4	23.8	30.6
-10	2	4	41.8	-46.8
11	2	4	26.9	-31.2
0	3	4	31.1	-33.6
-1	3	4	81.6	-76.8
2	3	4	47.8	47.6
1	4	4	49.3	52.5
2	4	4	54.7	59.1
-2	4	4	39.2	-36.7
0	5	4	20.2	-20.3
-1	5	4	47.7	-49.1
2	5	4	41.6	42.0
0	6	4	16.1	17.3
1	6	4	22.5	21.0
2	6	4	25.7	27.3
-2	6	4	34.9	-31.8
0	7	4	28.6	-32.6
-1	7	4	37.4	-42.5
1	8	4	19.0	19.4
0	9	4	21.4	-23.6
-1	9	4	29.1	-33.8
-1	11	4	21.7	-21.6
0	1	5	49.7	50.7
1	1	5	51.6	50.0
-1	1	5	53.6	55.0
2	1	5	16.8	-21.0
-2	1	5	14.1	17.9
3	1	5	74.8	-74.1
-3	1	5	73.0	-76.9
4	1	5	59.2	-58.0
-4	1	5	80.7	-86.3
5	1	5	31.4	31.5
-5	1	5	14.4	-18.2
6	1	5	33.1	36.5
7	1	5	22.7	24.7
-7	1	5	45.7	47.7
-8	1	5	46.2	47.9
-9	1	5	32.3	30.5
10	1	5	16.7	-21.5
-10	1	5	30.0	-30.2
11	1	5	17.1	-25.2

H	K	L	FO	FC
-11	1	5	41.5	-38.3
2	2	5	37.9	41.3
0	3	5	41.0	42.6
-1	3	5	82.0	85.1
-2	3	5	56.2	52.0
1	4	5	20.9	28.9
-1	4	5	61.2	-63.3
2	4	5	25.1	24.8
-2	4	5	50.6	-46.0
0	5	5	20.3	26.0
-1	5	5	45.9	44.0
-2	5	5	22.7	22.8
0	6	5	15.6	15.9
1	6	5	35.9	36.0
2	6	5	30.2	29.6
-2	6	5	27.3	-26.0
0•	7	5	11.2	12.8
-2	7	5	20.1	20.6
0	8	5	19.8	19.2
1	8	5	25.4	24.5
-1	8	5	19.8	-23.0
-2	8	5	20.0	-26.3
1	10	5	22.5	25.6
0•	0	6	9.5	-16.7
1	0	6	41.5	-40.5
-1	0	6	18.6	16.3
2	0	6	50.4	-52.6
-2	0	6	85.2	84.3
3	0	6	43.6	-44.3
-3	0	6	64.8	63.9
4	0	6	30.1	33.2
-4	0	6	20.1	-22.8
5	0	6	78.5	79.2
-5	0	6	49.0	-51.9
6	0	6	18.0	16.7
-6	0	6	44.5	-44.0
7	0	6	24.0	-22.0
-7	0	6	16.6	-22.5
8	0	6	28.2	-29.0
-8	0	6	15.1	10.8
-9	0	6	59.0	60.1
-10	0	6	20.8	24.0
-11	0	6	22.5	-21.4
-12	0	6	21.8	-22.5
-13	0	6	19.6	-16.8
-1	1	6	31.2	32.8
-4	1	6	17.1	-23.8
-7	1	6	21.5	26.9
0	2	6	34.3	-32.2
1	2	6	49.2	-47.6
-1	2	6	38.9	35.7
2	2	6	31.8	-30.0
-2	2	6	97.2	98.2
3	2	6	35.4	-33.8
-3	2	6	34.0	35.0
-4	2	6	38.7	-42.0
5	2	6	58.9	58.2
-5	2	6	48.5	-48.2
6	2	6	36.7	33.7
-6	2	6	42.8	-42.8
-9	2	6	38.2	45.4
-10	2	6	24.0	26.6
1	3	6	16.2	21.9
0	4	6	16.9	-10.5
1	4	6	29.8	-30.1
-1	4	6	20.3	26.7
2	4	6	16.8	-23.2
-2	4	6	60.0	62.9
0	5	6	31.1	36.0
1	5	6	25.6	28.7
-1	5	6	18.7	19.0
1	6	6	25.0	-28.3
-1	6	6	26.4	27.5
2	6	6	18.5	-22.6
-2	6	6	39.6	40.8
0	7	6	28.2	30.3
1	7	6	19.1	16.4
-1•	7	6	14.0	16.0
0	8	6	15.8	-11.1
-2	8	6	21.1	22.1
0	9	6	21.6	28.4
1	9	6	20.0	19.6
-1•	9	6	14.1	8.0
0	1	7	59.3	-62.6
1	1	7	23.7	-25.3
-1	1	7	57.6	-58.4
-2	1	7	38.4	37.8
-3	1	7	70.1	74.5
4	1	7	57.7	57.3
-4	1	7	25.9	32.7
5	1	7	36.6	31.3
6	1	7	23.3	-16.9
7	1	7	40.1	-40.6
-7	1	7	47.7	-45.0
8	1	7	16.5	-15.8
-8	1	7	30.7	-31.2
-9	1	7	15.1	18.3
-10	1	7	43.5	41.4
-11	1	7	20.6	16.0
-1	2	7	38.1	36.6
-4	2	7	26.6	-30.1
0	3	7	50.6	-54.7
1	3	7	29.3	-29.7
-1	3	7	27.0	-31.0
2	3	7	17.4	19.2
-2	3	7	38.4	34.1
2	4	7	34.0	-30.6
0	5	7	32.7	-34.2
-1	5	7	25.4	-26.4
-1	6	7	26.9	29.3
2	6	7	27.2	-30.7
0	7	7	20.1	-20.8

H	K	L	FO	FC
-1•	7	7	14.1	-15.8
-1•	8	7	14.2	17.8
2	8	7	29.2	-30.6
0	0	8	21.5	-17.9
1	0	8	47.5	47.1
-1	0	8	63.7	-63.8
2	0	8	28.9	30.2
-2	0	8	43.9	-41.4
3	0	8	12.7	4.3
-3	0	8	20.6	20.3
4	0	8	13.0	14.9
-4	0	8	30.2	20.1
5	0	8	13.3	-11.0
-5	0	8	34.8	38.2
6	0	8	30.5	-31.4
-6	0	8	35.6	33.6
7	0	8	20.7	-22.1
-7	0	8	12.6	-7.3
8	0	8	20.3	19.9
-8	0	8	39.6	-38.7
9	0	8	13.9	12.9
-9	0	8	30.4	-30.7
-12	0	8	15.6	13.2
-13	0	8	13.9	11.9
0	2	8	16.4	-14.4
1	2	8	31.8	33.2
-1	2	8	40.4	-47.9
2	2	8	35.2	35.1
-2	2	8	40.3	-37.4
-6	2	8	21.3	26.3
-8	2	8	36.6	-38.0
-9	2	8	33.8	-29.7
0	4	8	16.9	-16.4
1	4	8	27.2	27.3
-1	4	8	46.9	-47.3
2	4	8	23.4	27.6
-2	4	8	31.9	-31.8
1	5	8	19.1	-16.8
-1•	6	8	14.1	-20.2
-2	6	8	21.0	-18.6
1	7	8	22.4	-22.3
-1•	8	8	14.0	-17.6
0	1	9	35.8	35.7
1	1	9	55.6	54.7
-2	1	9	41.9	-40.8
3	1	9	15.3	-17.9
-3	1	9	29.1	-28.4
4	1	9	17.7	-20.7
-4	1	9	24.9	-25.4
5	1	9	16.2	-16.7
-6	1	9	40.2	43.2
-7	1	9	43.3	42.4
8	1	9	19.3	20.6
-9	1	9	32.3	-27.8
-10	1	9	21.6	-21.6
-11	1	9	16.6	-14.4
0	3	9	29.6	26.7
1	3	9	29.1	33.5
-2	3	9	30.6	-28.0
-1	4	9	19.8	-21.3
0	5	9	20.9	22.4
1	5	9	19.7	22.4
0	7	9	17.0	15.9
0	0	10	25.4	25.3
1•	0	10	9.5	4.5
-1	0	10	21.7	20.6
2	0	10	26.5	-28.8
3	0	10	25.3	-24.1
-4	0	10	21.0	-13.2
5	0	10	14.0	14.7
-5	0	10	32.5	-26.8
-6•	0	10	9.5	4.6
7	0	10	14.0	12.0
-7	0	10	28.4	25.2
-8	0	10	25.4	22.0
-12	0	10	14.0	-15.0
0	2	10	32.9	34.1
-1	2	10	19.7	24.1
2	2	10	24.7	-29.4
-5	2	10	43.5	-44.0
0	4	10	21.5	18.4
-1•	4	10	14.1	18.7
2	4	10	20.6	-25.6
0	6	10	20.0	17.8
-1•	6	10	13.9	16.3
2	6	10	21.2	-10.7
1	1	11	24.5	-26.3
-2	1	11	21.7	19.9
-3	1	11	25.1	19.0
-4	1	11	15.8	11.9
-5	1	11	22.5	-21.4
-6	1	11	26.9	-27.4
1	3	11	27.3	-24.6
-2	3	11	21.2	18.7
0	0	12	21.4	-18.7
1	0	12	20.1	-16.3
-1	0	12	14.2	-11.5
3	0	12	16.0	14.0
-3	0	12	15.9	15.2
4	0	12	14.1	10.5
-4	0	12	33.1	29.3
-6	0	12	22.6	-15.0
-7	0	12	20.1	-17.4
-8	0	12	21.4	-19.3
-11	0	12	20.3	16.6
-5	1	13	17.2	10.6
-3	0	14	17.9	11.7

TABLE 4. R FACTOR SUMMARY FOR ETHYL GRIGNARD REAGENT

CLASS OF REFL.	R	(NO.REF)
ALL ORDERS	0.07695	(670)
H EVEN	0.07592	(349)
H ODD	0.07808	(321)
K EVEN	0.07382	(372)
K ODD	0.08086	(298)
L EVEN	0.07900	(376)
L ODD	0.07426	(294)
H + K EVEN	0.08044	(345)
H + K ODD	0.07327	(325)
H + L EVEN	0.07793	(329)
H + L ODD	0.07601	(341)
K + L EVEN	0.06863	(470)
K + L ODD	0.10301	(200)
H + K + L EVEN	0.08045	(341)
H + K + L ODD	0.07326	(329)

R FACTORS FOR CONSTANT PLANES

CLASS			R	(NO.REF)	WR
0	K	L	0.08576	(68)	0.07434
1	K	L	0.08091	(60)	0.06461
-1	K	L	0.08465	(56)	0.05853
2	K	L	0.06728	(54)	0.05954
-2	K	L	0.05617	(47)	0.05240
H	0	L	0.07195	(129)	0.05793
H	1	L	0.08118	(122)	0.06265
H	2	L	0.05135	(76)	0.04942
H	K	0	0.07013	(81)	0.06591
H	K	1	0.07296	(138)	0.06327
H	K	2	0.08108	(102)	0.06855

general this table is quite consoling in that everything seems to be consistent with a good refinement.

The least squares and Fourier programs used in this structure analysis were the Fitzwater-Benson-Jackobs programs.[1]

Discussion

The refined structure as well as the numbering system to be used throughout this discussion is shown in Figure 4a. Figure 4b illustrates the same structural features in better perspective.

The final refined parameters are given in Table 5. The positional parameters are fractional atomic coordinates and the temperature factor is of the form

$$\exp(-\beta_{11}h^2-\beta_{22}k^2-\beta_{33}l^2-2\beta_{12}hk-2\beta_{13}hl-2\beta_{23}kl).$$

The temperature factor in terms of the β_{ij}'s cannot be interpreted very easily as far as the physical reality of anisotropic vibrations is concerned. The six components of the symmetric tensor U which describes the vibrations of an atom in an anisotropic harmonic potential field are much more physically meaningful quantities. The symmetric tensor U is defined (50) such that the mean square amplitude of vibration in the direction of a unit vector $\vec{l}$, with components l_i, is

$$\bar{u}^2 = U_{11}l_1^2+U_{22}l_2^2+U_{33}l_3^2+2U_{12}l_1l_2+2U_{13}l_1l_3+2U_{23}l_2l_3.$$

---

[1]Fitzwater, D. R., Benson, J. E., both of Ames Laboratory, Atomic Energy Commission, Ames, Iowa. Jackobs, J. J., (present address) Arizona State University, Tempe, Arizona. Least Squares Package. Private Communication. 1964.

Figure 4. The molecular configuration of $EtMgBr \cdot 2Et_2O$ (See Table 7 for refined bond distances and angles.)

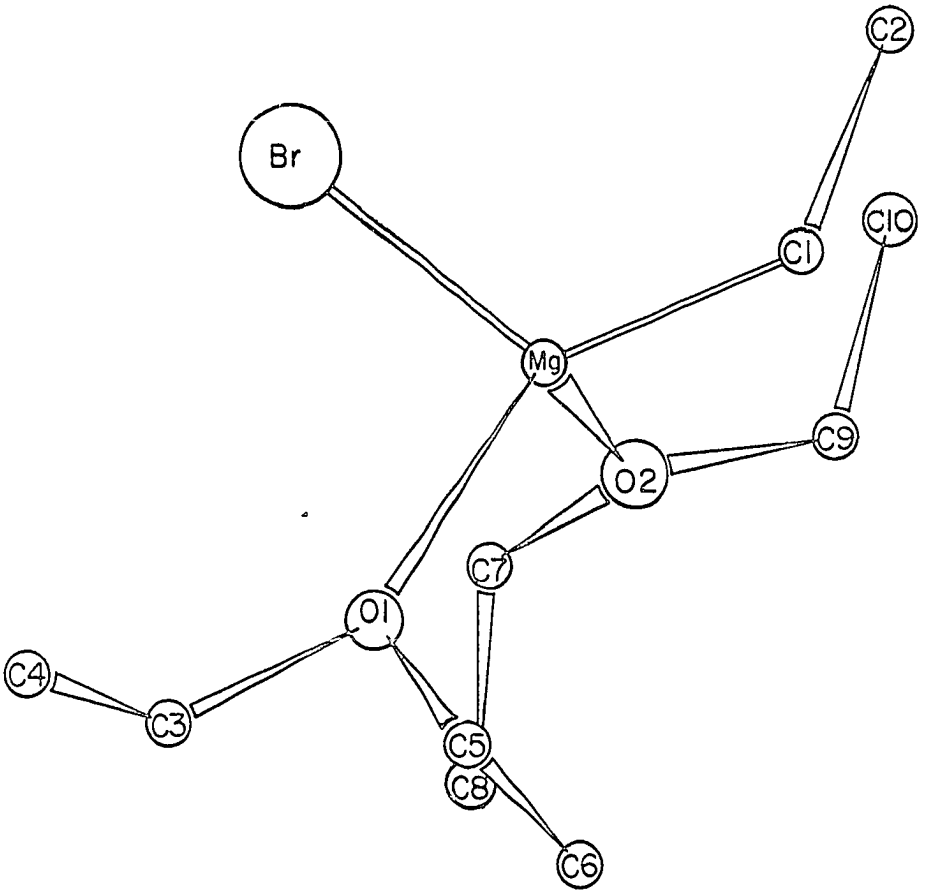
C2
Br
C10
C1
Mg
C9
O2
C7
O1
C4
C3
C5
C8
C6

(a)

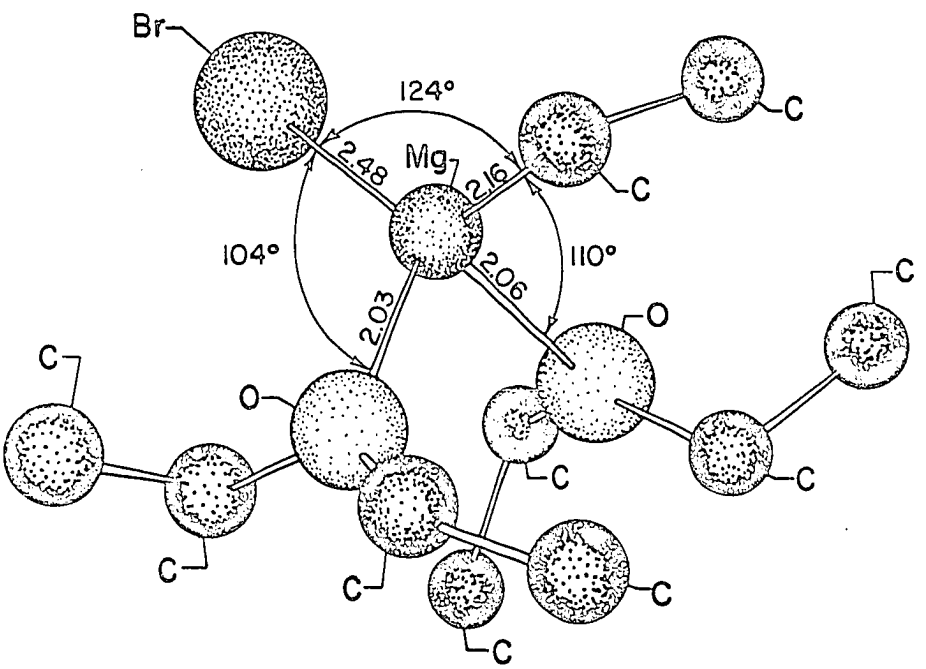
Br
124°
C
2.48
Mg
2.16
C
104°
110°
2.06
2.03
O
C
O
C
C
C
C
C
C
C

(b)

Table 5. Final positional and thermal parameters and their standard errors obtained from least squares refinement of $EtMgBr \cdot 2Et_2O$ (B's and errors are $\times 10^5$)

Atom	x	y	z	B_{11}	B_{22}	B_{33}	B_{12}	B_{13}	B_{23}
Br	0.14135	-.02134	0.21127	665	1060	939	-49	189	88
	(00017)	(00025)	(00019)	(13)	(27)	(18)	(31)	(12)	(39)
Mg	0.27620	0.01854	0.09622	609	819	810	53	89	92
	(00041)	(00080)	(00047)	(39)	(74)	(51)	(74)	(40)	(88)
O1	0.22467	0.18241	0.00229	712	665	1255	-225	378	213
	(00137)	(00135)	(00151)	(122)	(153)	(198)	(130)	(143)	(184)
O2	0.24528	-.11951	-.03735	578	844	1018	81	60	-160
	(00121)	(00142)	(00143)	(114)	(153)	(157)	(127)	(124)	(169)
C1	0.44099	0.02610	0.17259	339	981	796	-247	45	-43
	(00117)	(00239)	(00154)	(87)	(213)	(145)	(208)	(105)	(274)
C2	0.47593	-.05289	0.27967	1102	1460	1507	146	181	-748
	(00193)	(00265)	(00230)	(197)	(367)	(276)	(278)	(204)	(319)
C3	0.11473	0.22577	-.04802	279	1748	621	320	315	211
	(00134)	(00264)	(00180)	(125)	(341)	(160)	(215)	(145)	(315)
C4	0.09302	0.32843	0.03126	1151	918	1630	344	870	-331
	(00207)	(00236)	(00241)	(228)	(264)	(286)	(249)	(251)	(288)
C5	0.29893	0.26648	-.03356	854	1428	1098	29	-187	63
	(00281)	(00292)	(00308)	(261)	(353)	(375)	(305)	(310)	(334)
C6	0.33418	0.21628	-.13876	871	1649	2618	334	1004	-317
	(00207)	(00307)	(00356)	(212)	(373)	(456)	(270)	(299)	(414)

Table 5 (Continued)

Atom	x	y	z	B_{11}	B_{22}	B_{33}	B_{12}	B_{13}	B_{23}
C7	0.14137 (00141)	-.14725 (00223)	-.10709 (00214)	361 (128)	1132 (275)	1272 (250)	94 (184)	565 (167)	-432 (278)
C8	0.13034 (00200)	-.08856 (00281)	-.23353 (00220)	991 (194)	1732 (368)	1437 (271)	-43 (290)	534 (193)	-313 (321)
C9	0.32242 (00221)	-.21114 (00265)	-.05497 (00303)	607 (189)	1038 (289)	1464 (389)	109 (238)	223 (281)	455 (340)
C10	0.32389 (00245)	-.32859 (00273)	0.03122 (00264)	1330 (292)	1542 (356)	1380 (323)	245 (295)	-485 (291)	164 (341)
H1C1	0.46149	0.12783	0.19835	647	1067	861	0	172	0
H2C1	0.48179	-.00403	0.10510						
H3C2	0.56084	-.04158	0.31029						
H4C2	0.45842	-.15430	0.25501						
H5C2	0.43811	-.02245	0.34826						
H6C3	0.06000	0.14420	-.05119						
H7C3	0.10449	0.26192	-.14234						
H8C5	0.36920	0.27606	0.04396						
H9C5	0.26694	0.36606	-.05086						
H10C7	0.08201	-.10391	-.06656						

Table 5 (Continued)

Atom	x	y	z	B_{11}	B_{22}	B_{33}	B_{12}	B_{13}	B_{23}
H11C7	0.12641	-.25418	-.11452						
H12C8	0.05514	-.10974	-.29025						
H13C8	0.19097	-.13735	-.27411						
H14C8	0.14657	0.01292	-.22616						
H15C9	0.40020	-.16538	-.03789						
H16C9	0.30467	-.24816	-.14849						

The Debye B in the direction of $\vec{l}$ would be given by

$$B = 8\pi^2 \bar{u}^2.$$

Since Cruickshank (51) strongly recommends reporting the U_{ij}'s, they are listed for this structure in Table 6.

Table 6. Atomic vibrational parameters in $\mathring{A}^2$ (relative to orthogonal axes a, b, c*)

Atom	U_{11}	U_{22}	U_{33}	U_{12}	U_{13}	U_{23}
Br	0.0552	0.0566	0.0588	-.0046	0.0001	0.0051
Mg	0.0533	0.0437	0.0507	0.0024	-.0054	0.0053
O1	0.0538	0.0355	0.0786	-.0183	0.0094	0.0123
O2	0.0524	0.0451	0.0637	0.0077	-.0107	-.0093
C1	0.0311	0.0524	0.0498	-.0163	-.0085	-.0025
C2	0.0959	0.0780	0.0944	0.0203	-.0089	-.0433
C3	0.0157	0.0933	0.0389	0.0190	0.0142	0.0122
C4	0.0764	0.0490	0.1021	0.0281	0.0404	-.0191
C5	0.0856	0.0763	0.0687	0.0011	-.0302	0.0036
C6	0.0506	0.0881	0.1639	0.0272	0.0357	-.0183
C7	0.0164	0.0605	0.0796	0.0124	0.0231	-.0250
C8	0.0735	0.0925	0.0900	0.0013	0.0183	-.0181
C9	0.0507	0.0554	0.0917	0.0012	-.0052	0.0263
C10	0.1390	0.0823	0.0864	0.0146	-.0565	0.0095

The interatomic bond distances and bond angles are given in Table 7. All errors have been calculated using the complete variance-covariance matrix and the program of Busing and Levy (52). It is evident from a consideration of Figure 4 and the bond angles that the ethyl group, a bromine atom, and 2 ether molecules form a somewhat distorted tetrahedron about a single magnesium atom. The distortion is undoubtedly due to the steric requirements of the large bromine atom. The steric requirements of the ether molecules would be expected to be more stringent than the ethyl group; yet, the Br-Mg-Cl bond is the most distorted. The answer probably lies in the fact that the force on the ethers may be greater, but the resistance is also greater. Thus, the Br-Mg-Cl angle is large simply because the ethyl group is relatively free to move.

The bond distances (uncorrected for thermal motion) to the Mg atom compare favorably with those calculated on the basis of Pauling's (53) tetrahedral covalent radii. This comparison is shown in Table 8. Although the calculated Mg-O bond on the basis of tetrahedral covalent radii is 2.06Å, most Mg-O bonds are around 2.10Å or larger. The short Mg-O bond also occurs in the phenyl Grignard reagent and is discussed there by Stucky and Rundle (30). To check this bond distance further a rigid body thermal analysis was made on the ethyl Grignard reagent after the method of Cruickshank (54) using the program UCLATO1.[1] The assumption, which

---

[1]Gantzel, P., Coulter, C., and Trueblood, K. California Institute of Technology, Pasadena, California. IBM 709 or 7090 program UCLATO1. Private Communication. 1965.

Table 7. Bond distances and angles for $EtMgBr \cdot 2Et_2O$ (<Dist.> is the distance averaged over the thermal motion where the second atom is assumed to ride on the first. RMS(1) and RMS(2) are the root mean square amplitudes in the bond direction for the defining atoms, respectively)

Atoms	Dist. (Å)	Error (Å)	<Dist.> (Å)	RMS(1)	RMS(2)
Br-Mg	2.476	0.01	2.471	0.23	
Mg-O1	2.027	0.02	2.030	0.20	0.21
Mg-O2	2.054	0.02	2.059	0.23	0.21
Mg-C1	2.147	0.02	2.149	0.22	0.16
O1-C3	1.498	0.02	1.507	0.26	0.15
O1-C5	1.434	0.04	1.432	0.16	0.31
O2-C7	1.445	0.02	1.441	0.22	0.24
O2-C9	1.433	0.03	1.441	0.21	0.24
C1-C2	1.451	0.03	1.473	0.23	0.35
C3-C4	1.460	0.03	1.500	0.25	0.16
C5-C6	1.478	0.04	1.509	0.32	0.28
C7-C8	1.541	0.03	1.570	0.30	0.32
C9-C10	1.554	0.04	1.576	0.21	0.30

Atoms defining angle	Angle (°)	Error (°)
Br-Mg-O1	103.0	0.5
Br-Mg-O2	103.7	0.5
Br-Mg-C1	125.0	0.5
O1-Mg-O2	101.2	0.6
O1-Mg-C1	111.7	0.8
O2-Mg-C1	109.6	0.7
Mg-C1-C2	114.6	1.4
Mg-O1-C3	128.8	1.3
Mg-O1-C5	118.9	1.5
Mg-O2-C7	123.1	1.1
Mg-O2-C9	122.1	1.4
O1-C3-C4	106.7	1.7
O1-C5-C6	112.7	2.4
O2-C7-C8	108.2	1.7
O2-C9-C10	109.0	2.5
C3-O1-C5	112.0	1.6
C7-O2-C9	114.0	1.6

Table 8. Comparison of observed distances and sum of tetrahedral covalent radii

Bond	Observed distance (Å)	Sum of radii (Å)
Br-Mg	2.48±0.01	2.51
Mg-Cl	2.15±0.02	2.17
Mg-O1	2.03±0.02	2.06
Mg-O2	2.05±0.02	2.06

may be very tenuous, is that the tetrahedron about the Mg behaves as a rigid body. Cruickshank (55) has shown how rotational oscillations of rigid bodies can cause positional errors which in this case might show up as shortened Mg-O bonds. The details of this analysis won't be repeated here except to note that the librational correction to the Mg-O bond was only 0.006Å. There is no reason whatever to suppose that this short Mg-O bond is not real.

There are no solid state etherates characterized well enough for a comparison of ether distances and angles. The only diethyl ether distances and angles available are electron diffraction values (56). A comparison between the average uncorrected distances in this structure and the electron diffraction values is given in Table 9.

The planes defined by the methylene carbons and the oxygen atoms come within 0.17Å (C3-O1-C5) and 0.30Å (C7-O2-C9) of passing through the Mg atom. Thus the Mg atom is nearly in the ether planes; this along with the Mg-O-C bond angles indicates trigonal bonding about the two oxygen

Table 9. X-ray vs. electron diffraction distances and angles for ether molecules

Distance or angle	X-ray (Å,°)	Electron Diff. (Å,°)
C-C	1.51±0.02	1.50±0.02
C-O	1.45±0.02	1.43±0.02
<C-O-C	113.0±2	108±3
<C-C-O	109.2±2	110±3

atoms. The Br-C3 and Br-C7 distances are 3.85 and 3.86A, respectively; these are not exceptionally short in view of the expected 3.95Å Van der Waals's distance (53). However, there seems to be some Br-C3 and Br-C7 interaction since an examination of the anisotropic thermal vibrations shows that the two sets of methylene carbons are experiencing very different thermal motions. The magnitudes and orientation of the principal axes of thermal vibration for all the non-hydrogen atoms are given in Table 10; the corresponding errors in these quantities have been omitted in the interest of saving space. The two methylene carbons away from the bromine are not very anisotropic, but the two methylene carbons near the bromine are very markedly anisotropic.

The configuration of the ethyl group in diethyl ether has been discussed by Stuart (57, 58). From Kerr constants he concludes that the preferred configuration is

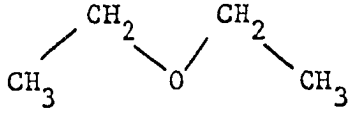

Table 10. Amplitudes and direction cosines of the principal thermal axes R

Atom	R	R.m.s. ampl.	cosθ(a)	cosθ(b)	cosθ(c*)	Atom	R	R.m.s. ampl.	cosθ(a)	cosθ(b)	cosθ(c*)
Br	1	0.223	0.5954	0.6968	-.4000	C4	1	0.118	0.5836	-.6958	-.4186
	2	0.239	0.7265	-.2543	0.6384		2	0.286	0.5515	0.7180	-.4246
	3	0.253	0.3431	-.6707	-.6576		3	0.363	0.5961	0.0169	0.8028
Mg	1	0.198	-.3319	0.7868	-.5203	C5	1	0.213	-.5985	0.1155	-.7927
	2	0.225	-.5863	-.6042	-.5397		2	0.277	-.1022	-.9925	-.0675
	3	0.240	-.7390	0.1259	0.6618		3	0.330	-.7946	0.0406	0.6058
O1	1	0.142	-.5163	-.8174	0.2554	C6	1	0.157	0.8512	-.4459	-.2769
	2	0.255	-.8314	0.5500	0.0793		2	0.320	0.4629	0.8864	-.0044
	3	0.288	-.2053	-.1714	-.9636		3	0.419	0.2474	-.1244	0.9609
O2	1	0.200	-.4162	0.8950	0.1607	C7	1	0.043	0.8670	-.3386	-.3657
	2	0.216	-.7609	-.2460	-.6004		2	0.236	0.4710	0.7963	0.3795
	3	0.274	-.4978	-.3722	0.7834		3	0.314	0.1627	-.5013	0.8499
C1	1	0.140	-.8509	-.4469	-.2762	C8	1	0.240	0.7236	-.3400	-.6007
	2	0.228	-.1510	-.2957	0.9433		2	0.292	0.6148	0.7131	0.3369
	3	0.248	-.5032	0.8443	0.1841		3	0.337	0.3138	-.6131	0.7250
C2	1	0.201	-.1893	0.7821	0.5937	C9	1	0.201	-.3274	0.8268	-.4573
	2	0.298	-.8865	0.1238	-.4458		2	0.227	-.9421	-.3229	0.0906
	3	0.373	-.4222	-.6107	0.6699		3	0.325	-.0727	0.4605	0.8847
C3	1	0.084	-.9232	0.1540	0.3522	C10	1	0.209	-.5141	0.3832	-.7674
	2	0.198	-.2938	0.3080	-.9049		2	0.297	-.1420	-.9203	-.3644
	3	0.319	-.2479	-.9388	-.2391		3	0.419	-.8459	-.0784	0.5275

with the methyl groups near the open positions of the oxygen atom; he attributes the stability of the configuration to attractive forces between the dipoles of the carbon-hydrogen bonds of the terminal methyl groups and the dipole of the carbon-oxygen bonds. The ether configuration found in this structure is different from that proposed by Stuart. Here one methyl group is forward and the other is back in the opposite direction; for example, the dihedral angle between the planes C3-O1-C5 and C4-C3-O1 is 82.2° while the same angle is 83.0° between the C3-O1-C5 and C6-C5-O1 planes. The rotations of the ethyl groups probably represent a compromise between the dipole-dipole interaction energy, the steric requirements of the ether group, and the steric requirements of the rest of the molecule.

A portion of the packing in the unit cell is shown in Figure 5. A sinistral coordinate system was used to be consistent with the output from the Fourier program. All the unique intermolecular non-hydrogen distances less than 4.0Å are given in Table 11. Those distances less than 4.0Å in Figure 5 are shown as dotted lines. There is nothing really unusual in the packing of this compound.

An interesting intermolecular distance in Figure 5 is the shortest Mg-Br distance between molecules; this distance is 5.81Å.

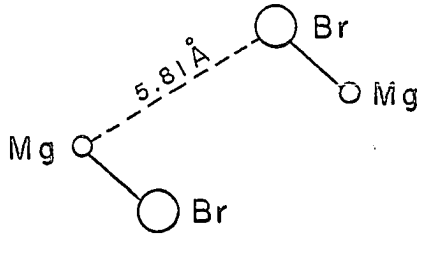

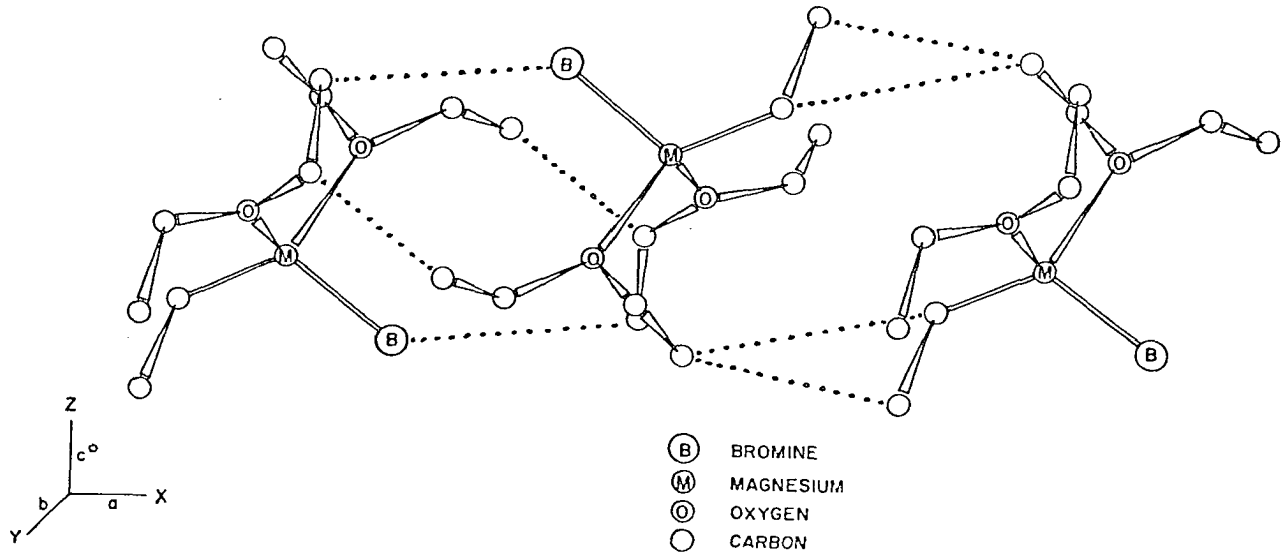

Figure 5. Packing of $EtMgBr \cdot 2Et_2O$ (The dotted lines represent the shortest intermolecular contacts.)

Table 11. Shortest intermolecular non-hydrogen distances

Atom 1	Atom 2	Symmetry transformation[a]	Dist. (A°)	Error (Å)
Br	C8	I	3.82	0.03
C7	C4	I	3.87	0.03
C1	C6	I,TX	3.96	0.03
C2	C6	I,TX	3.68	0.04
C2	C10	2_1,TX	3.78	0.04
C1	C6	c_b	3.88	0.04
C4	C8	c_b	3.74	0.04
Br	C7	c_b,-TY	3.99	0.02
C2	C9	c_b,-TY	3.91	0.04

[a]The I, 2_1, and c_b represent an inversion center, a twofold screw axis, and a c glide plane, respectively; TX and TY represent cell translations in the x and y directions, respectively. Atom 2 is transformed by the symmetry operation.

This distance is too long to correspond to any sort of chemical bond and rules out all dimeric structures involving bridging bromine atoms. There are no other bond distances which are consistent with anything but a monomeric structure.

The crystal structures of the ethyl and phenyl Grignard reagents present unambiguous evidence for monomeric solid state etherates. Also, in this study diffraction photographs were taken of many preparations which were purified to various degrees, and in no case was a species obtained

different from the monomeric species described. The evidence for the existence of a species of definite chemical composition, namely, the monomeric species, is therefore strong. Although the evidence presented here does not apply directly to the liquid state, the observations discussed by Stucky and Rundle (30) in this regard apply equally well here.

The results of this investigation as well as the "monomeric" (20) molecular weight evidence for dilute ethereal solutions and the "monomeric" (19) molecular weight evidence over a wide range of concentrations in THF strongly suggest that the RMgX species is an important part of the Grignard reagent and should be included in any equilibrium describing this reagent. In fact, more research may show that the RMgX is the prominent species even in ethereal solutions.

STRUCTURE OF TROPONOID PHOTO-OXIDATION PRODUCT

Literature Review

In a study on some photochemical dimerizations (59) Stoner carried out the following reaction (2).

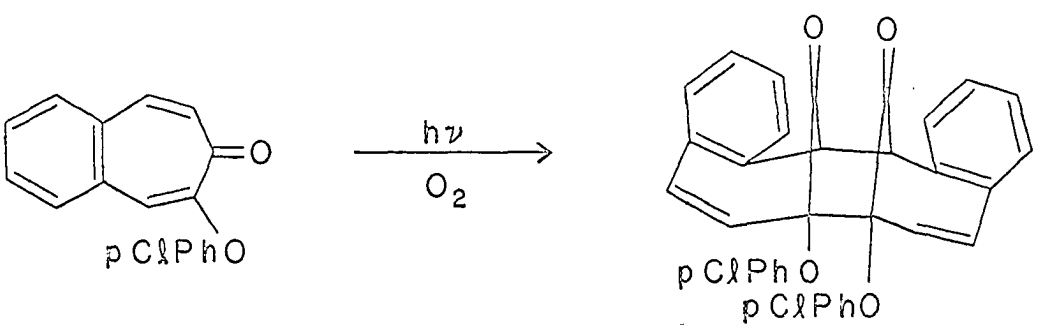

(Dimer I)

+ $C_{16}H_{11}O_3Cl$

(Dimer IV)

The irradiation of 2-(p-chlorophenoxy)-4,5-benztropone was done in tetrahydrofuran solution using a mercury arc lamp in a Pyrex immersion well. The structure of Dimer I was deduced by chemical methods as well as spectra analysis.

The irradiation product "Dimer IV" was obtained in low yield. Elemental analysis indicated a formula of $C_{16}H_{11}O_3Cl$ so that one carbon has been lost and one oxygen gained in the reaction. An osmometric molecular weight determination in benzene gave a molecular weight somewhere midway between the monomeric and dimeric values. Chemical methods,

mass, infrared, ultraviolet, and nuclear magnetic resonance spectra methods were employed in an attempt to find the structure of $C_{16}H_{11}O_3C\ell$. Putting together all the information obtained it was not possible to identify the structure. The number and scale of chemical reactions were limited by the small amount of material available.

An interesting piece of structural evidence observed by Stoner (2) in the n.m.r. spectrum was an AMX pattern at 7.22, 8.08, and 8.96τ. These high field peaks indicate that there are saturated carbon atoms in the structure. This was hard to rationalize in view of the starting material.

Purpose

The molecular configuration of this compound was of interest since available evidence indicated that there was a very unusual photochemical rearrangement involved. Since the organic chemists had given up on solving this structure it appeared that the only way of establishing the molecular configuration was by X-ray diffraction.

The primary reason for doing the structure, however, was that it looked like a good structure on which to do research on some crystallographic methods. Image-seeking methods were used exclusively in the solution of this structure. These methods will be discussed in some detail in the next section.

Image-Seeking Methods

When the so-called heavy atom approach is not applicable, crystal structures are generally solved either by an analysis of the Patterson

synthesis or by direct methods. In the $C_{16}H_{11}O_3C\ell$ structure it appeared that the heavy atom approach would not be immediately applicable for several reasons. First of all, the chlorine atom is not very heavy with its 17 electrons when the remainder of the structure contains 131 electrons. Secondly, this compound crystallizes in a non-centrosymmetric space group. Such structures are usually somewhat more sensitive to the "heaviness factor" since there is a phase factor, in addition to the sign, to be determined for each structure factor. Thirdly, the chlorine atoms are in general positions so that their phase contribution to the general reflections would probably not be a maximum. Also, all the other atoms are in general positions so that their would be no simplification due to special positions.

Some comment should be made on the heaviness of the chlorine atom in this structure. The heaviness index, $\Sigma Z_H^2/\Sigma Z_L^2$, is 0.37. The Z_H and Z_L represent the atomic numbers of the heavy (Cℓ) and light (O, C, H) atoms, respectively. This value would probably be in the "in between" range in the sense that the heavy atom approach might be useful in some structures with such a heaviness index. In these cases it is usually very difficult to predict when the heavy atom approach will be useful; this must be determined in light of the peculiarities of each structure. In this case it probably would have been possible to eventually solve the structure by finding the chlorine atom and several other atoms from the Patterson map and then calculating electron density maps and reiterating the process. This probably would have involved a great deal of trial and error and a large expenditure of effort.

Direct methods were not applicable in this case since they are presently restricted to centrosymmetric structures or projections. It was decided to solve this structure exclusively by image-seeking methods. These methods involve finding one image or picture of the structure in the Patterson map, thus the name image-seeking. Wrinch (60) was the first to suggest a method for the systematic analysis of vector distributions. The idea was rediscovered in 1950 by a number of investigators and only in recent years, with the advent of high speed computers, has the method become popular. See Fridrichsons and McL. Mathieson (61) and Buerger (39) for a list of references to the method. For the adaption of computers to these methods see Simpson et al. (62) and Mighell and Jacobson (63).

An appreciation of the problem can be obtained by considering some aspects of the Patterson function. A Patterson map is a vector map containing vectors between all the atoms in the unit cell; the vectors are all shifted to a common origin. The translational components of any symmetry elements in the unit cell are lost. As far as the number of peaks are concerned the Patterson function for non-centric structures with n atoms in the unit cell has $n^2 - n$ non-origin peaks; for centric structures the Patterson function has n non-origin single peaks and $(n^2 - 2n)/2$ non-origin double peaks. A double peak corresponds to two peaks falling on top of each other. Peaks of still higher multiplicity are obtained when there are symmetry elements present. Single peak heights are proportional to $Z_i Z_j$ where Z_i and Z_j are the atomic numbers of the atoms involved.

In the $C_{16}H_{11}O_3C\ell$ structure there 6320 peaks in the unit cell since there are 20 non-hydrogen atoms per molecule and four molecules per unit cell. This corresponds to 4.73 peaks per $\mathring{A}^3$. It is evident that there are probably no single peaks present. The problem is to sort out the peaks and identify the interaction causing them, and ultimately to isolate one out of the eighty images present.

The image-seeking method used in this investigation involves using the Patterson superposition technique in conjunction with the minimum function. This method is the only practical image-seeking method for a problem of this complexity. Specifically, the first order minimum function, $M_1(\vec{u})$, is given by

$$M_1(\vec{u}) = \text{Min } [P(\vec{u}), P(\vec{u} - \vec{s}_1)]$$

where $P(\vec{u})$ is the three-dimensional Patterson function and $P(\vec{u} - \vec{s}_1)$ is the Patterson function shifted by the vector $\vec{s}_1$, which for a rational superposition is an interatomic vector.

Consider an acentric structure of n atoms with atom i at $\vec{r}_i$ having scattering power f_i. The corresponding Patterson function will consist of $n^2 - n$ peaks at $\vec{r}_i - \vec{r}_j$ with strengths $f_i f_j$. If some single vector $\vec{s}_1$ is chosen as the shift vector and the minimum taken of the Patterson values at $P(\vec{u})$ and $P(\vec{u} - \vec{s}_1)$, the resulting minimum function ideally has $2n - 2$ peaks describing the structure and its inverse related by the center of symmetry at the midpoint of $\vec{s}_1$.

As a practical example consider the structure in Figure 6a which represents a structure in the plane group pg where the atoms 1,···, 5 are

Figure 6. A point atom structure and its corresponding Patterson

a) Point set in plane group pg

b) The vector set (The size of the circles indicate the number of overlapping interactions which go from one to four.)

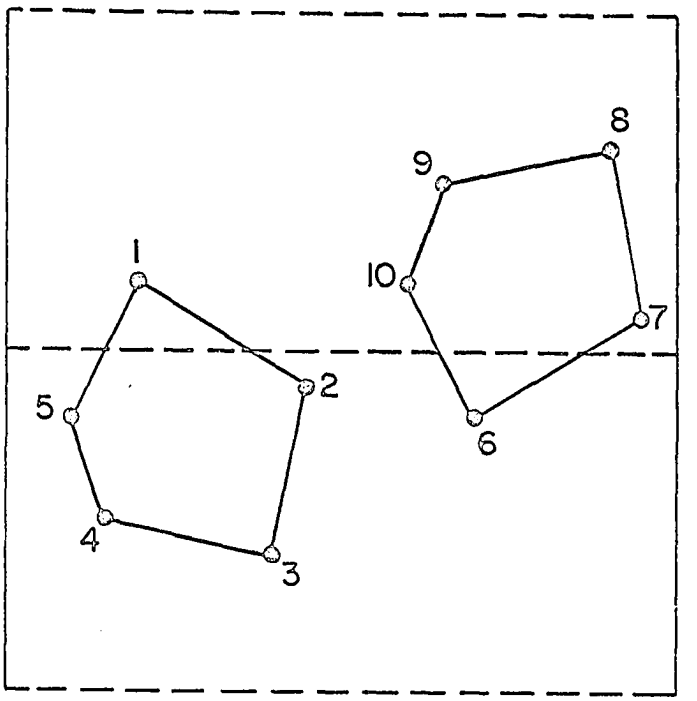
1
2
3
4
5
6
7
8
9
10

(a)

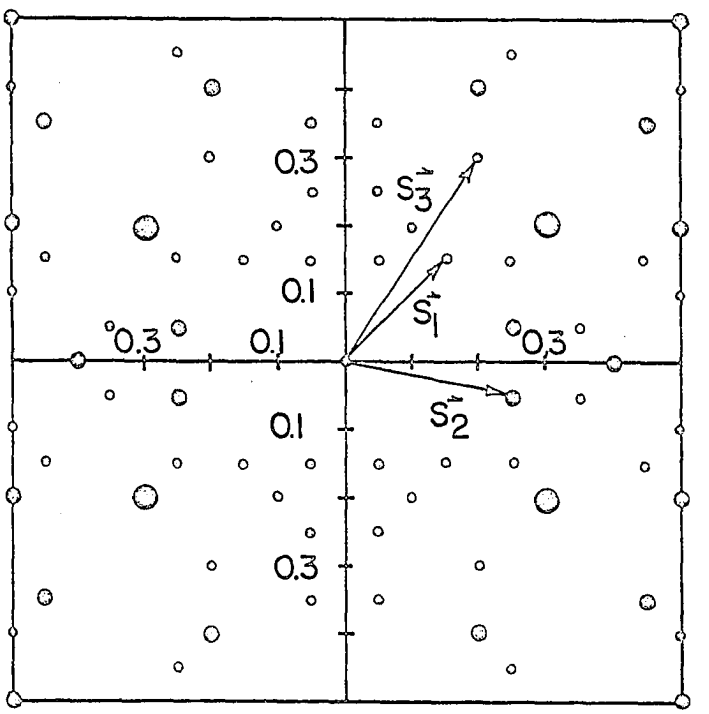
0.3
0.1
0.3
0.1
0.1
0.3
$S_3^{\rightarrow}$
$S_1^{\rightarrow}$
$S_2^{\rightarrow}$

(b)

related to the atoms 6,···, 10 by the glide plane. Suppose all the atoms have the same scattering power. The corresponding Patterson map is shown in Figure 6b where the origin has been reduced to a single interaction. If we choose $\vec{s}_1 = \vec{r}_{10} - \vec{r}_2$ the $M_1(\vec{u})$ function is shown in Figure 7a where the structure image is mapped out in the solid lines and the inverse image in the dashed lines. They are related by the center of symmetry marked by a plus sign.

The two points not belonging to the structure image or its inverse image represent the $\vec{r}_1 - \vec{r}_4$ and $\vec{r}_6 - \vec{r}_{10}$ vectors; these are accidental coincidences. That these should remain in $M_1(\vec{u})$ can be easily explained. The $M_1(\vec{u})$ function will consist of a subset of vectors, $r_k - r_\ell$, which satisfy the condition that

$$(\vec{r}_i - \vec{r}_j) + (\vec{r}_{10} - \vec{r}_2) \; \varepsilon \; (\vec{r}_i - \vec{r}_j).$$

The $\vec{r}_i - \vec{r}_j$ (i = 1,··, n; j = 1,··, n) is the set of all vectors in the Patterson and $\vec{r}_{10} - \vec{r}_2$ is the shift vector. But,

$$(\vec{r}_{10} - \vec{r}_6) + (\vec{r}_{10} - \vec{r}_2) = (\vec{r}_1 - \vec{r}_4)$$

$$(\vec{r}_4 - \vec{r}_1) + (\vec{r}_{10} - \vec{r}_2) = (\vec{r}_6 - \vec{r}_{10})$$

and since $(\vec{r}_1 - \vec{r}_4)$ and $(\vec{r}_6 - \vec{r}_{10}) \; \varepsilon \; (\vec{r}_i - \vec{r}_j)$ they also are members of the subset $(\vec{r}_k - \vec{r}_\ell)$ and consequently must appear in the $M_1(\vec{u})$ function.

The Patterson function can be further reduced by computing higher order minimum functions. The $M_2(\vec{u})$ function with $\vec{s}_1 = \vec{r}_{10} - \vec{r}_2$ as before and $\vec{s}_2 = \vec{r}_6 - \vec{r}_2$ is shown in Figure 7b. The $(\vec{r}_1 - \vec{r}_4)$ and $(\vec{r}_6 - \vec{r}_{10})$ vectors still remain because they were accidental coincidences using $\vec{s}_1$

Figure 7. The $M_1(\vec{u})$ and $M_2(\vec{u})$ functions

a) $M_1(\vec{u})$ with $\vec{s}_1 = \vec{r}_{10} - \vec{r}_2$

b) $M_2(\vec{u})$ with $\vec{s}_1 = \vec{r}_{10} - \vec{r}_2$ and $\vec{s}_2 = \vec{r}_6 - \vec{r}_2$

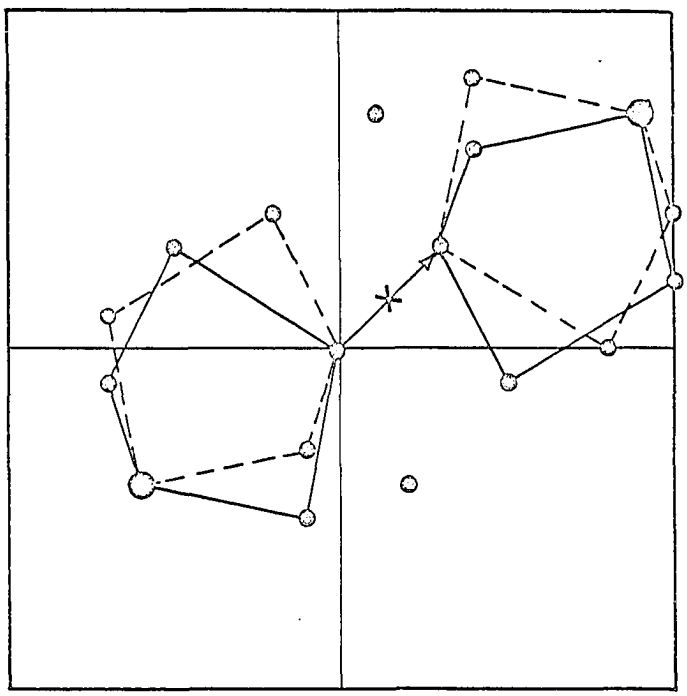

(a)

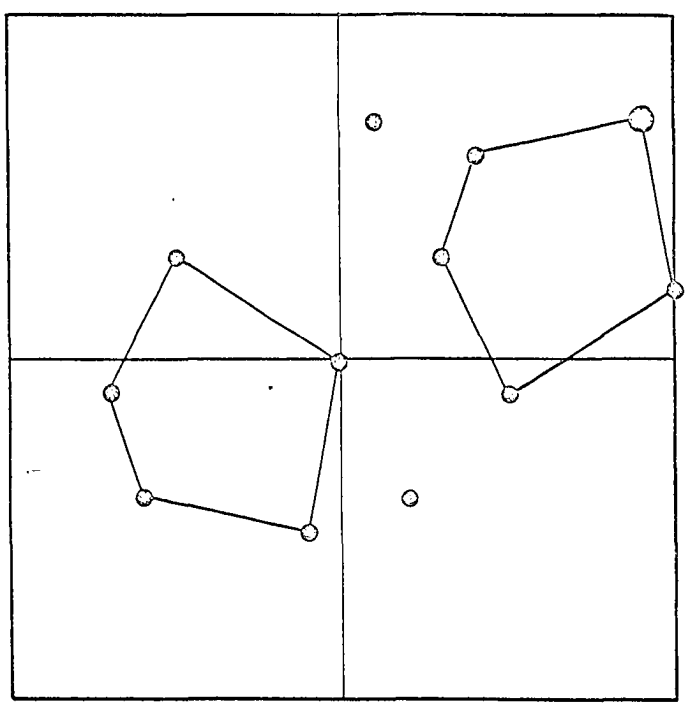

(b)

and belong to the inverse image using $\vec{s}_2$. These peaks do not appear in the $M_3(\vec{u})$ function with $\vec{s}_3 = \vec{r}_9 - \vec{r}_2$.

It was demonstrated in this investigation that the superposition technique in conjunction with the minimum function could be further exploited by appropriately weighting the shifted Patterson maps (64). With weighting factors included the general procedure can be expressed as

$$M_n(\vec{u}) = \text{Min } [P(\vec{u}), w_1P(\vec{u} - \vec{s}_1),\ldots w_nP(\vec{u} - \vec{s}_n)].$$

Since weighting factors played an important role in the solution of $C_{16}H_{11}O_3C\ell$, the effect of including them will be discussed in some detail. The nature of the weighting factor effect has apparently not been realized by other investigators.

The structure in Figure 8 will be used as an example in the following discussion. First of all, if the weighting factor is not included in the superposition function and one minimization is done with $\vec{s}_1 = \vec{r}_b - \vec{r}_a$, and if $M(f_a,f_b)$ means take the minimum of the individual atom scattering powers f_a and f_b, then each point in the structure image is weighted as $f_iM(f_a,f_b)$ where $i = 0,\ldots, n$ except when $i = a$ or b in which case the weight is f_af_b. In the inverse image for $i \neq a$ or b, each point is weighted as $f_iM(f_b,f_a)$. Clearly the structure and its inverse are now weighted equally, and in a structure of any complexity there would be no way of distinguishing between the two images.

Suppose the scattering power of atom a is somewhat greater than atoms b, c,...,n; now the structure contains one heavy atom (H) and many light

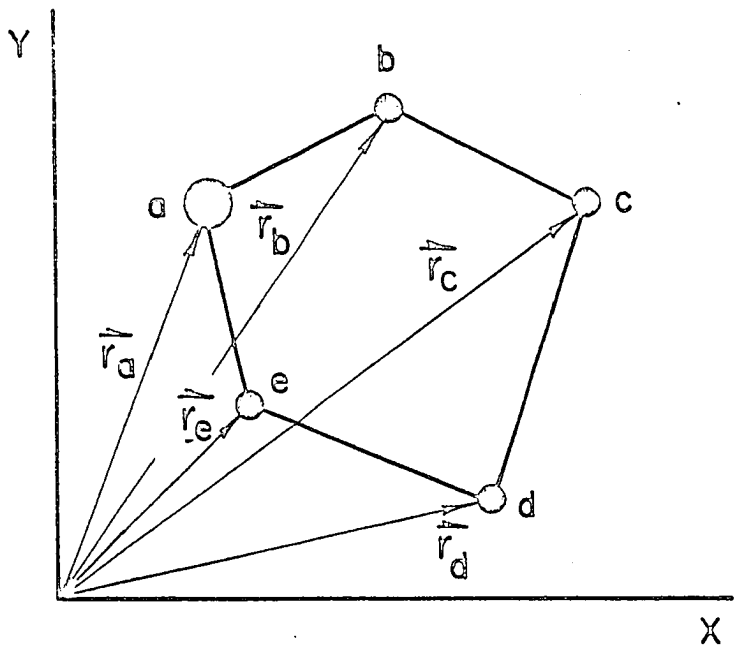

Figure 8. A structure with atoms at the ends of the position vectors

atoms (L) such that $f_a = f_H$ and $f_b, f_c, \ldots, f_n = f_L$ (Figure 8). In this case the structure image and its inverse would be weighted according to the smallest scattering power giving, in the general case, $f_i f_L$ as illustrated in Figure 9a; also, a poor peak to background ratio would result.

Now if the weighting factor is included in the superposition function the structure image would be weighted as $f_i M(f_H, w_1 f_L)$ for all i. The inverse image is weighted as $f_i M(f_L, w_1 f_H)$ for $i = 0, \ldots, n$ except for i = a or b which are part of the structure image and are weighted accordingly. Since the scattering power of atom a is greater than atom b, the weighting factor can be set equal to f_a/f_b (f_H/f_L) so that the structure image is weighted by the largest weight giving $f_i f_H$, and its inverse by the smallest weight giving $f_i f_L$. The result of including such a weighting factor in the superposition function is shown in Figure 9b. It is evident that the center of symmetry along the shift vector has now been destroyed since the peak heights of the structure image are higher than those of the related inverse image. Also in general the peak to background contrast has been improved.

Because of overlap and multiple vectors in complex problems, it is usually necessary to do several superpositions. In particular, if there is one heavy atom in a structure in a symmetry group of order p, initially p - 1 superpositions would be done with the shift vectors being the p - 1 HH vectors. Any further superpositions, p at a time, would most logically involve shift vectors of the HL type where the weighting factors should be included. The contrast between the structure image and its inverse

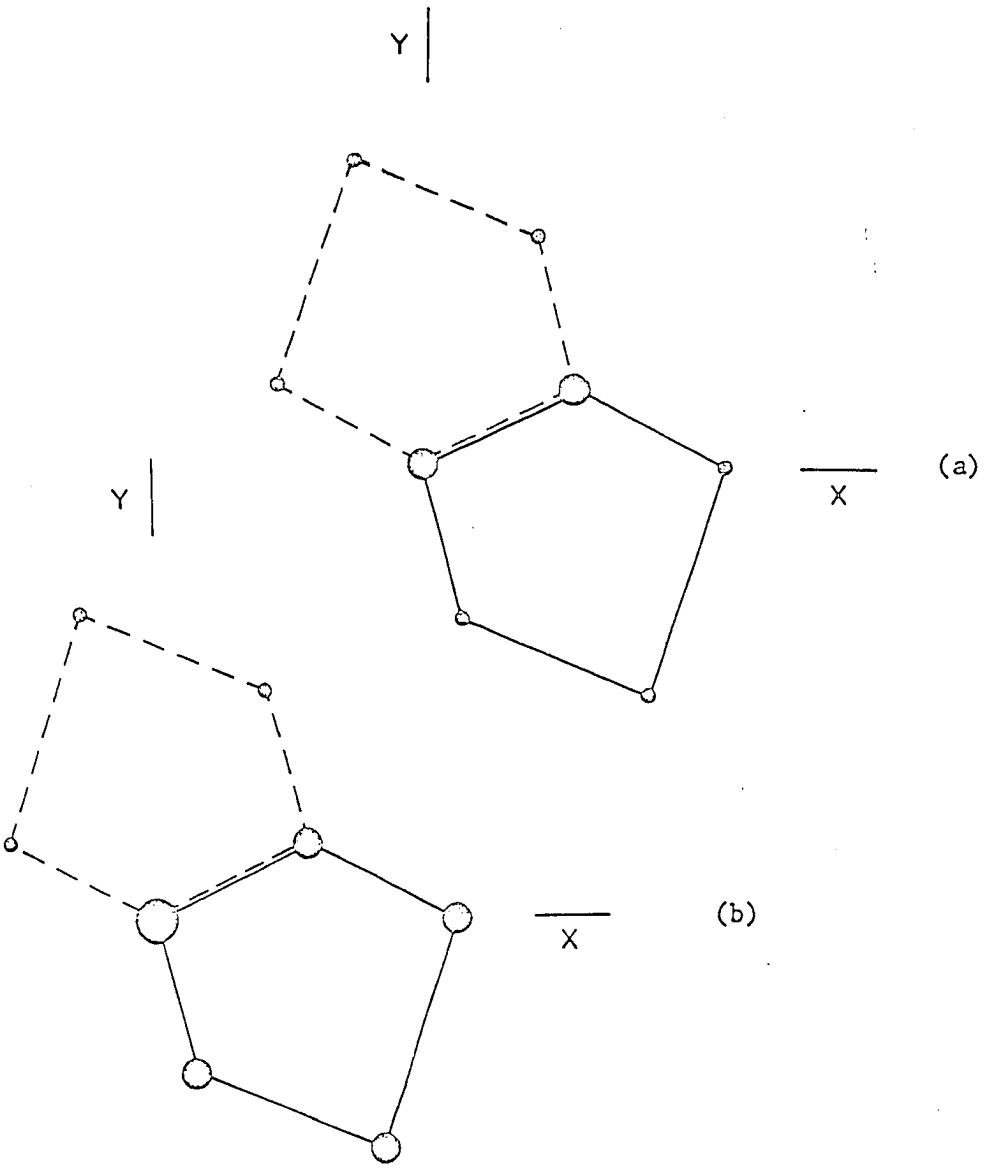

Figure 9. The $M_1(\vec{u})$ function with $\vec{s}_1 = \vec{r}_b - \vec{r}_a$ (The structure image and its inverse are indicated by the solid and dotted images. The circles represent the LL, HL, and HH interactions by their increasing size.)

a) Weighting factor not included

b) Weighting factor included

obtained by using a suitable weighting factor will be more distinct as the number of overlapping peaks is decreased and as the H to L ratio is increased providing the ratio of f_L to background is sufficiently large. With small H to L differences the weights may be taken as the ratios of the atomic numbers, but for larger H to L differences ratios of the appropriate observed single peak heights will work better, especially when "sharpened" data are used. The weighting factors can also be used to advantage in working with centrosymmetric crystals when superpositions are done using unsymmetrical shift vectors. Of course with symmetrical shift vectors the weighting factors are set equal to unity as they are in the equal atom case.

The effect, then, of including weighting factors in superposition methods using the minimum function is to (i) partially eliminate the center of symmetry resulting from the first superposition and (ii) keep the peak height of the structure image at the HH and HL level. This affords a convenient aid in sorting out a single image of the structure and is simple to apply in practice since computer programs can be easily adapted to allow for the scaling of successive shifted Pattersons. If the product function is used instead of the minimum function, weighting factors would have no effect other than on the scaling of the resultant map. If the sum function is used and one superposition done with $\vec{s}_1 = \vec{r}_b - \vec{r}_a$ (Figure 8) the two most prominent images would be weighted as $f_a f_i + w_1 f_b f_i$ and $f_b f_i + w_1 f_a f_i$. In this case some effect would be expected from weighting, but the results would not be as clear cut as with the minimum function, especially in view of the high backgrounds produced in the sum function.

Image-seeking methods usually don't work out as well in practice as might be expected from the theory since the Patterson map usually does not consist of discrete peaks. In fact, the volume of a three dimensional Patterson peak is about eight times the volume of an electron-density peak (39). This, along with the great number of peaks present, insures that there are no nicely resolved peaks. Modification functions are almost always used to improve the resolution of the Patterson map. The particular modification function used in this investigation will be discussed in the section on the collection and correction of data.

Lattice Constants and Space Group

The lattice constants were obtained by taking a weighted average of the lattice parameters measured from zero level precession photographs and those calculated from the 2θ values observed on the General Electric XRD-5 diffractometer. The lattice constants and their estimated standard deviations are

$a = 13.21 \pm 0.02$ Å $\quad \alpha = 90.0°$

$b = 13.80 \pm 0.02$ Å $\quad \beta = 90.0°$

$c = 7.33 \pm 0.02$ Å $\quad \gamma = 90.0°$

The Laue symmetry observed was Pmmm so that the crystal system is orthorhombic. The following extinctions were observed:

{h00}	h = 2n+1
{0k0}	k = 2n+1
{00ℓ}	ℓ = 2n+1

The space group was uniquely determined to be $P2_12_12_1$ on the basis of the preceding extinctions and the fact that there are 4 molecules per unit cell. The origin in electron density space was chosen halfway between the three pairs of non-intersecting screw axes. The fourfold equivalent positions for the space group $P2_12_12_1$ are given in Table 12.

Table 12. Equivalent positions of $P2_12_12_1$

No. of positions	Point symmetry	Equivalent positions
4	1	$x,y,z;$
		$1/2-x,\bar{y},1/2+z;$
		$1/2+x,1/2-y,\bar{z};$
		$\bar{x},1/2+y,1/2-z;$

The calculated density on the basis of 4 molecules per unit cell is 1.38 g./cm.^{3}. This density was not checked in the laboratory since the total supply of this compound available was 5 crystals. The linear absorption coefficient with Mo radiation is 2.8 cm.$^{-1}$.

Collection and Correction of Data

Complete three-dimensional intensity data were taken on a General Electric XRD-5 diffractometer using Zr-filtered Mo radiation. A total of 1377 reflections were measured in the Mo sphere out to $2\theta = 50°$; the stationary crystal-stationary counter technique was used with a peak count time of 40 seconds and a background count time of 20 seconds.

Background measurements were taken in various regions of the reciprocal lattice in anticipation of getting individual backgrounds from an average background curve.

Some difficulty was experienced in finding a suitable crystal for intensity data since there was a pronounced tendency toward preferential cleavage in the a-b plane. The data were collected over a period of about 2 1/2 days on a crystal fragment of dimensions 0.30 x 0.25 x 0.20 mm. A 8° take-off angle and a 2.6° diffracted beam aperture were used with the largest available beam collimator (about 0.85 mm.). The (600), (080), and (221) reflections were measured periodically to characterize crystal decomposition. Some 70 reflections were remeasured using the 2θ scan technique to check for a possible peak intensity to integrated intensity correction.

The (151), (322), (621), and (531) reflections were carefully measured along 2θ (out to 2x2θ) to characterize the streaking effect due to noncharacteristic radiation. The assumption was made that the streaking observed on these reflections would be representative of all the data. Accordingly an average streak curve was made so that the streaking from reflections $\vec{h}_i$, of order h_i, between the origin of the reciprocal lattice and some reflection $\vec{h}$, of order h, could be substracted from the intensity observed for reflection $\vec{h}$. This streak intensity, I_s, for a given reflection $\vec{h}$ was calculated by

$$I_s(\vec{h}) = \sum_{h_i} \frac{I(\vec{h}_i)L_p(\vec{h})\cos\theta(\vec{h})K(\lambda/\lambda_s)}{L_p(\vec{h}_i)\sin\theta(\vec{h})} .$$

where $h/2<h_i<h$ and I, L_p, and λ are the intensity, the Lorentz-polarization factor, and the wavelength, respectively. The values of K were obtained from the average streak curve which was conveniently plotted as a function of $\lambda/\lambda_s(h/h_i)$. This correction will not be discussed further since it has been used by other investigators in this laboratory and discussed by Williams (65).

A program was written to apply all the necessary corrections to the data. The backgrounds were found to vary with the instrument angles χ and ϕ in addition to the regular 2θ dependence; accordingly, 35 background curves were used in the program. No absorption correction was made because of the small linear absorption coefficient (2.8 $cm.^{-1}$). A decomposition correction (about 2%) was applied to a portion of the data. There was an observed power supply fluctuation (about 2% maximum), but this was too random to correct for.

It was not possible to determine the magnitude of the correction to be applied to convert the peak height data to integrated intensities from the 70 scanned reflections. This correction is necessary because of spectral dispersion and the separation of the Kα doublet components at larger Bragg angles. Since the correction curve couldn't be ascertained from the data taken, an expected curve was calculated using the apparent source width of 0.822°,[1] the 2θ separation of $K\alpha_1$-$K\alpha_2$ for Mo radiation listed by Furnas (66), and the correction curve given by Alexander and Smith (67). The calculated curve was used to correct all of the data.

[1]This corresponds to a rectangular X-ray focal spot of 15 mm. in length, a take-off angle of 8°, and a 14.55 cm. source to crystal distance.

The estimated errors in the intensities were calculated after the method of Williams (65) according to

$$(\Delta I)^2 = C_T+C_B+(0.03C_T)^2+(0.07C_B)^2+(0.15C_S)^2$$

where C_T, C_B, and C_S are the total, background, and streak counts, respectively. The 0.03, 0.07, and 0.15 are the corresponding systematic, but not statistical, errors in these quantities. The associated structure factor error was calculated according to

$$\Delta F = (L_p)^{-1/2}[-I^{1/2}+(I+\Delta I)^{1/2}].$$

A significance test was made so that all reflections with $F_o<1.5\sigma(F_o)$ were considered unobserved. About 700 out of the original 1377 reflections passed this test as observed reflections. The appropriateness of this test will be considered in the refinement section.

In order to get maximum resolution in the Patterson synthesis the structure factors were immediately modified, i.e., "sharpened." The effect of "sharpening" is to take out the $\sin\theta/\lambda$ decline of the scattering power, thus making the Patterson closer to a point atom Patterson. The modification function used in this investigation was that of Jacobson, Wunderlich, and Lipscomb (68) as programed by Barry Granoff.[1] The F(000) term was included in the Patterson function.

---

[1]Granoff, B. Department of Chemistry, Iowa State University, Ames, Iowa. Patterson Sharpening Program. Private Communication. 1965.

Solution and Refinement of Structure

A detailed analysis of the Patterson function gave possible coordinates for the four chlorine atoms which were consistent with the Patterson map. It should be noted that the assumption about a set of chlorine atom positions fixes the locations of the three 2_1 axes in Patterson space and consequently the correspondence between electron density space and vector space. The positions of the four Cℓ-Cℓ vectors in the Patterson synthesis are

	u	v	w
1)	0	0	0
2)	20.5/40	25.5/40	20/40
3)	0.5/40	19.5/40	20/40
4)	20.5/40	6/40	0

Although the Cℓ's are in general positions as far as space group symmetry requirements are concerned, it is evident that they are actually in rather special positions in the crystal. The fact that the Cℓ-Cℓ vectors were on mirror planes in the Patterson map made them easier to identify than was expected, but it also meant that they would not be of much help in the superposition approach since very little Patterson symmetry would be destroyed per Cℓ-Cℓ superposition. However, since the Cℓ atom positions were determined quite accurately, the Cℓ-Cℓ superpositions could do no harm and thus were always included in the high order superposition functions.

Initial superpositions were done using the 3 Cℓ-Cℓ shift vectors and one or more Cℓ-C shift vectors. The Cℓ-C peaks were chosen in the area of the expected Cℓ-C interactions for a given phenoxy group. No satisfactory model was obtained at this point. Part of the problem was that it was assumed that the phenoxy group would lie in the z=0 plane. It was assumed that the phenoxy group would lie in this plane because of the shorter c lattice parameter and the observed preferential cracking in the x-y plane, but later work showed this assumption to be wrong.

Maximum use was made of the symmetry elements in picking possible atom sites and shift vectors. For a given peak in vector space the three symmetry equivalent peaks were always examined and only if all four peaks were present at about the same height was a peak considered as a possible interaction vector for the image under consideration. The shapes of all four peaks were considered in determining the best coordinates to use for the four shift vectors.

The $M_7(\vec{u})$ function was calculated using the 3 Cℓ-Cℓ shift vectors and 4 possible Cℓ-O shift vectors. A systematic analysis of this function was very difficult since the peaks were for the most part indistinguishable from general background. At this point the Patterson superposition program was fixed to allow for the scaling of successive superpositions as discussed earlier. A systematic analysis of the weighted $M_7(\vec{u})$ function gave a model which made chemical sense. A comparison of the weighted and unweighted $M_7(\vec{u})$ functions is given in Table 13 where the peak heights of the 6 benzene carbons (not in the phenoxy group) are compared. The general

Table 13. Comparison of weighted and unweighted peak heights in $M_7(\vec{u})$ function

Atom	Weighted $M_7(\vec{u})$	Unweighted $M_7(\vec{u})$
C1	28	13
C2	25	13
C3	27	16
C4	24	14
C5	27	13
C6	25	15
Background peaks	12	12

backgrounds were lower than 12, but there were many spurious background peaks at 12 or even higher. The effect of including the weighting factor is clearly evident.

The coordinates of 19 out of the 20 non-hydrogen atoms were read directly from the weighted $M_7(\vec{u})$ function; after 1 cycle of least squares, without varying the isotropic temperature factors, the discrepency index was 30.4%. Another cycle of least squares took the R factor down to 30.0%; obviously this wasn't refining as rapidly as it should indicating that something was wrong with the model. An electron density map was calculated excluding 6 carbons and 1 oxygen of the phenoxy group. It was apparent from the electron density map and further study of the weighted $M_7(\vec{u})$ function that 4 of the phenoxy carbons had been misplaced.

Correcting these positions, locating the remaining carbon on an electron density difference map, and doing 2 cycles of least squares brought the R factor down to 17.0%. At this point 2 cycles of least squares were run varying the isotropic temperature factors; the R factor was now 13.5%.

The model determined was

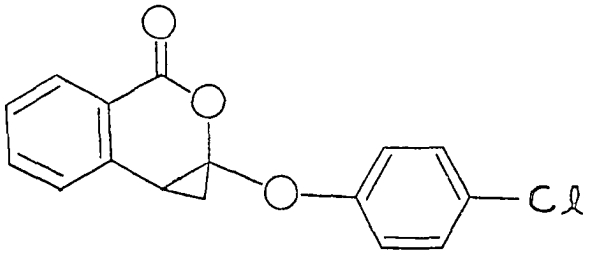

Since the identification of the lactone oxygen was important in view of the starting material, it was replaced by a carbon and a cycle of least squares run. The temperature factor of this atom went to -1.5 indicating that the oxygen assignment was correct. At this point 9 reflections were excluded in the refinement since there was some question about their angle settings. A cycle of anisotropic least squares was run, the hydrogen atom contributions included (but not refined), and the weighting scheme corrected according to the $w\Delta^2$ criterion discussed in the refinement of the ethyl Grignard reagent. The discrepency factor after another cycle of anistropic least squares was 8.15%. Only 682 observed reflections were considered in this refinement. No significance test was used in the least squares process. The scattering factor tables for all atoms were those calculated by Hansen, et al. (47).

The 70 scanned reflections were planimetered and reduced to their corresponding structure factors since they represented an independent

check on many of the low order strong reflections. The agreement between the structure factors from the original data and the properly scaled planimetered data was excellent. The planimetered F_o's and original F_o's were averaged together for 8 reflections. The weighting scheme was corrected once more and the refinement stopped after another cycle of anistropic least squares.

An electron density difference map was calculated; the maximum peak observed corresponded to about 1/2 of an electron. The final R factors were

	Observeds	All refl.
$R = \Sigma\Delta/\Sigma\|F_o\| =$	.069	.171
$wR = \Sigma w'\Delta/\Sigma w'\|F_c\| =$	.053	.091

where $w' = 1/\sigma(F_o)$. The "standard error" of the fit for the observed reflections was

$$[\Sigma w\Delta^2/(m-n)]^{1/2} = 1.12$$

A detailed R factor summary is given in Table 14.

A listing of the observed structure factors is given in Figure 10. Half of the data were considered unobserved; to show that this was justified, a listing of the unobserved structure factors is given in Figure 11. It should be noted that F_c's are, for the most part, very small. The effect of including these data in the refinement would most likely be negligible.

TABLE 14. R FACTOR SUMMARY FOR TROPONOID PHOTO-OXIDATION PRODUCT

	OBSERVEDS		ALL REFL.	
CLASS OF REFL.	R	(NO.REF)	R	(NO.REF)
ALL ORDERS	0.06871	(682)	0.17082	(1367)
H EVEN	0.06844	(355)	0.16577	(709)
H ODD	0.06900	(327)	0.17643	(658)
K EVEN	0.06393	(352)	0.16285	(710)
K ODD	0.07466	(330)	0.18054	(657)
L EVEN	0.07651	(364)	0.17205	(731)
L ODD	0.05893	(318)	0.16928	(636)
H + K EVEN	0.06142	(339)	0.16223	(692)
H + K ODD	0.07629	(343)	0.17981	(675)
H + L EVEN	0.07164	(339)	0.17125	(687)
H + L ODD	0.06575	(343)	0.17037	(680)
K + L EVEN	0.06392	(404)	0.13671	(688)
K + L ODD	0.07691	(278)	0.22171	(679)
H + K + L EVEN	0.06803	(353)	0.16298	(692)
H + K + L ODD	0.06942	(329)	0.17907	(675)

R FACTORS FOR CONSTANT PLANES

CLASS	R	(NO.REF)	WR	R	WR
0 K L	0.03981	(48)	0.02808	0.13117	0.06265
H 0 L	0.05402	(59)	0.03919	0.12147	0.06173
H K 0	0.06931	(108)	0.05073	0.15496	0.08423
H K 1	0.04786	(127)	0.03848	0.12506	0.06415
H K 2	0.08151	(142)	0.06513	0.12017	0.08143
H K 3	0.05797	(107)	0.04691	0.17307	0.08611
H K 4	0.06067	(73)	0.04514	0.20164	0.09896
H K 5	0.09328	(73)	0.07670	0.18085	0.12290
H K 6	0.09037	(33)	0.06815	0.28972	0.16361
H K 7	0.06263	(11)	0.05358	0.49500	0.30345

H	K	L	FOBS	FCAL	ACAL	BCAL
2	0	0	46.8	46.9	46.9	0.0
4	0	0	92.0	91.6	91.6	0.0
6	0	0	114.3	114.3	114.3	0.0
8	0	0	16.0	13.6	13.6	0.0
10	0	0	15.1	16.6	16.6	0.0
12	0	0	18.4	18.6	18.6	0.0
14	0	0	15.8	16.3	16.3	0.0
4	1	0	12.8	11.8	-11.8	-0.0
5	1	0	27.1	29.2	0.1	-29.2
6	1	0	30.1	29.0	-29.0	0.2
7	1	0	28.7	28.2	0.1	-28.2
8	1	0	19.5	18.1	18.1	0.0
9	1	0	12.4	9.5	-0.0	-9.5
11	1	0	10.7	12.7	0.1	-12.7
12	1	0	20.5	22.1	22.1	0.1
14	1	0	9.7	8.8	8.8	0.1
1	2	0	45.0	41.9	0.2	41.9
2	2	0	15.0	18.4	-18.4	0.1
3	2	0	44.6	44.9	-0.4	44.9
4	2	0	24.0	24.1	-24.1	-0.3
5	2	0	40.8	41.8	0.1	41.8
6	2	0	13.3	10.1	-10.1	0.4
7	2	0	35.5	37.6	-0.1	37.6
8	2	0	17.5	14.7	-14.7	-0.5
9	2	0	16.8	18.4	0.3	18.4
10	2	0	12.8	12.7	-12.7	0.5
1	3	0	48.2	47.3	0.1	47.3
3	3	0	11.5	10.8	-0.2	-10.8
4	3	0	21.3	13.8	13.8	-0.2
5	3	0	28.3	28.4	0.0	-28.4
6	3	0	9.4	11.3	-11.3	0.4
7	3	0	10.2	7.5	0.1	7.5
8	3	0	13.9	11.1	11.0	-0.8
10	3	0	13.8	12.6	12.5	0.9
11	3	0	13.0	11.7	-0.5	11.7
12	3	0	16.8	17.4	17.4	-0.5
0	4	0	57.0	56.3	-56.3	0.0
1	4	0	113.2	114.8	-0.1	-114.8
2	4	0	9.1	2.1	-2.0	-0.6
3	4	0	57.2	57.8	0.2	-57.8
4	4	0	25.1	26.0	26.0	0.3
5	4	0	30.6	32.1	-0.3	-32.1
6	4	0	11.3	11.9	-11.8	0.3
7	4	0	21.8	23.8	0.5	-23.8
9	4	0	27.1	26.7	0.4	-26.7
10	4	0	11.9	12.6	12.6	0.5
11	4	0	11.7	11.9	-0.2	-11.9
13	4	0	21.2	21.8	0.6	-21.7
14	4	0	8.8	4.4	-4.4	0.1
15	4	0	13.6	13.1	-0.0	-13.1
4	5	0	25.5	16.3	16.3	0.5
5	5	0	15.8	14.9	-0.3	14.9
6	5	0	8.1	6.3	-6.3	0.2
7	5	0	10.3	10.5	0.5	10.5
13	5	0	8.2	5.9	0.1	-5.9
2	6	0	25.2	23.8	-23.8	0.4
3	6	0	13.6	14.4	-0.8	14.3
4	6	0	28.8	28.2	28.2	0.0
5	6	0	32.0	33.6	0.1	33.6
6	6	0	17.2	18.0	18.0	0.2
7	6	0	8.6	0.6	-0.3	-0.6
8	6	0	18.3	17.3	17.3	1.2
10	6	0	20.1	20.6	20.5	-1.2
14	6	0	7.9	6.2	6.2	-0.2
1	7	0	26.4	27.0	-0.2	27.0
2	7	0	35.1	32.0	32.0	0.7
4	7	0	14.7	14.6	14.6	-0.5
5	7	0	22.1	19.2	0.9	19.1
6	7	0	12.8	7.3	-7.3	0.4
7	7	0	22.9	23.9	-1.2	23.9
8	7	0	26.4	28.4	28.4	0.8
0	8	0	55.7	55.9	-55.9	0.0
2	8	0	32.1	30.7	-30.7	0.4
3	8	0	8.5	5.6	-0.6	5.6
4	8	0	38.4	38.6	-38.6	-0.2
5	8	0	16.7	15.1	1.2	-15.0
6	8	0	13.3	13.5	-13.4	0.5
8	8	0	11.4	14.0	-14.0	0.4
10	8	0	22.3	21.9	-21.9	0.7
1	9	0	17.3	16.0	-0.2	16.0
5	9	0	10.2	11.2	0.4	11.2
6	9	0	21.1	21.2	-21.2	0.2
7	9	0	16.7	17.0	-1.1	17.0
10	9	0	9.9	11.2	-11.1	1.2
11	9	0	12.4	12.0	-1.0	12.0
12	9	0	17.4	18.6	-18.6	-0.5
1	10	0	8.6	6.7	-0.2	-6.7
2	10	0	10.1	9.3	-9.3	-0.1
3	10	0	18.2	17.1	0.6	-17.1
5	10	0	20.4	20.3	-0.5	-20.3
6	10	0	11.4	10.1	10.1	-0.4
7	10	0	24.9	25.3	-0.4	-25.3
8	10	0	10.7	8.9	-8.9	0.7
9	10	0	8.3	11.9	0.1	-11.9
11	10	0	13.6	12.1	-0.4	-12.1
1	11	0	10.3	8.9	-0.1	-8.9
2	11	0	15.4	17.6	-17.6	-0.1
3	11	0	17.9	16.9	0.4	-16.8
5	11	0	10.6	11.8	-0.5	-11.8
7	11	0	20.4	19.8	0.2	-19.8
8	11	0	17.9	18.3	-18.3	0.5
0	12	0	24.3	24.1	24.1	0.0
3	12	0	11.7	12.6	0.1	-12.6
4	12	0	8.7	9.3	9.3	-0.1
5	12	0	11.4	11.4	0.1	11.4
9	12	0	9.4	10.5	0.0	10.5
2	13	0	10.4	10.7	-10.7	0.2
3	16	0	10.0	6.8	0.4	-6.7
1	0	1	28.9	27.9	0.0	-27.9
2	0	1	28.6	27.6	0.0	-27.6
3	0	1	45.2	45.4	0.1	-45.4
5	0	1	13.7	15.3	0.2	-15.3
6	0	1	15.4	16.6	0.2	16.6
7	0	1	11.4	13.2	0.0	-13.2
8	0	1	9.9	10.5	-0.0	-10.5
9	0	1	13.0	15.2	0.1	-15.2
12	0	1	12.3	12.5	-0.0	-12.5
0	1	1	44.8	44.4	0.1	44.4
1	1	1	70.4	67.8	-67.8	0.8
2	1	1	21.6	20.8	17.9	10.6
3	1	1	22.5	21.8	-21.8	-1.3
4	1	1	17.8	17.2	16.3	5.5
6	1	1	21.6	23.0	2.5	22.8
7	1	1	18.0	18.9	18.8	-1.7
8	1	1	16.3	16.2	4.7	15.5
9	1	1	16.8	16.3	13.5	9.2
10	1	1	24.9	24.8	-9.9	22.7
11	1	1	7.9	7.2	4.6	-5.5
12	1	1	13.5	13.1	3.3	12.7
14	1	1	12.8	13.9	-2.3	13.7
0	2	1	52.9	53.1	53.1	-0.1
1	2	1	110.0	110.0	109.6	-8.9
2	2	1	45.7	45.1	-34.7	28.9
3	2	1	24.0	23.6	11.3	-20.8
4	2	1	32.3	32.9	-18.7	27.1
5	2	1	12.2	11.9	-10.5	-5.7
6	2	1	46.8	46.4	6.4	46.0
7	2	1	39.2	38.6	37.1	-10.7
8	2	1	25.9	26.7	-17.4	20.2
9	2	1	15.0	13.4	12.5	-4.6
10	2	1	32.1	33.0	-13.0	30.3
11	2	1	16.2	14.6	-8.1	-12.2
14	2	1	10.7	9.9	0.7	9.9
0	3	1	57.5	57.2	-0.1	57.2
1	3	1	61.4	60.6	-56.7	21.2
2	3	1	14.5	14.7	-0.5	-14.6
3	3	1	34.3	35.3	-29.6	-19.1
5	3	1	48.8	49.4	-37.5	-32.2
6	3	1	21.2	20.7	-13.0	-16.1
7	3	1	42.5	44.0	-43.8	4.7
8	3	1	16.6	15.6	10.1	-11.9
9	3	1	19.4	17.7	-17.7	0.6
10	3	1	16.9	16.7	-16.3	3.9
11	3	1	29.5	29.5	-29.2	-4.3
12	3	1	11.9	10.0	9.5	1.9
13	3	1	8.6	7.4	-7.3	0.7
15	3	1	8.8	8.9	-8.8	-1.0
0	4	1	67.0	65.4	-65.4	-0.1
1	4	1	13.0	11.2	-7.1	-8.6
2	4	1	32.7	31.3	30.2	8.4
3	4	1	18.2	18.6	-11.3	14.7
4	4	1	28.1	27.7	-27.3	5.2
5	4	1	34.9	32.2	-28.9	-14.2
6	4	1	15.4	13.7	-8.5	-10.7
7	4	1	9.2	10.3	-9.7	3.4
9	4	1	19.4	18.3	-16.3	8.4
10	4	1	24.4	24.6	-19.5	15.1
11	4	1	28.4	29.7	-27.9	-10.2
12	4	1	8.8	5.7	0.0	-5.7
13	4	1	14.4	12.8	-12.2	3.7
0	5	1	11.1	12.5	-0.0	-12.5
1	5	1	50.5	51.7	50.9	8.8
2	5	1	41.0	41.3	-23.4	-34.1
3	5	1	22.4	24.5	17.6	-17.0
4	5	1	12.4	13.1	1.0	-13.1
5	5	1	16.3	18.4	7.2	-16.9
6	5	1	38.6	39.7	-2.8	-39.7
7	5	1	10.6	10.4	10.4	-0.1
8	5	1	23.8	24.6	-3.8	-24.4
10	5	1	8.8	8.9	4.2	-7.8
13	5	1	10.2	12.2	11.1	-5.2
0	6	1	8.9	11.4	-11.4	0.1
2	6	1	20.6	22.5	-5.4	-21.9
3	6	1	16.1	16.3	-14.4	7.7
4	6	1	14.6	17.6	-4.3	-17.1
5	6	1	13.1	13.6	11.4	7.5
6	6	1	18.1	19.8	1.4	-19.8
8	6	1	19.0	18.4	-4.6	-17.8
9	6	1	15.6	15.1	0.8	15.0
10	6	1	10.3	9.1	-0.9	-9.1
11	6	1	10.6	10.3	10.3	0.7
0	7	1	37.4	38.1	-0.1	38.1

Figure 10. Comparison of the magnitudes of the observed and calculated structure factors for $C_{16}H_{11}O_3C\ell$

H	K	L	FOBS	FCAL	ACAL	BCAL
1	7	1	39.7	40.6	39.6	-8.6
2	7	1	36.5	37.1	-5.6	36.7
3	7	1	20.1	20.4	19.4	6.3
4	7	1	36.3	37.3	-10.2	35.8
6	7	1	23.1	24.3	-0.1	24.3
8	7	1	25.4	27.4	-1.2	27.4
9	7	1	10.6	10.6	8.2	6.7
10	7	1	18.9	20.0	0.6	20.0
2	8	1	17.3	17.8	-14.2	-10.8
5	8	1	8.6	8.9	2.6	8.5
0	9	1	20.9	20.7	0.0	-20.7
1	9	1	25.3	23.9	-23.7	3.2
2	9	1	9.0	9.4	7.2	-6.1
3	9	1	12.4	11.4	-2.0	11.2
5	9	1	13.4	14.1	-13.8	2.9
7	9	1	31.3	31.3	-30.1	8.6
8	9	1	19.2	18.7	9.6	16.0
10	9	1	8.2	6.3	-6.1	1.4
11	9	1	8.2	8.6	-8.1	-2.8
3	10	1	18.6	19.4	15.1	12.2
4	10	1	12.6	15.5	-5.7	14.4
6	10	1	11.1	10.6	6.4	-8.5
0	11	1	9.7	10.4	0.4	-10.4
1	11	1	18.5	17.4	17.4	0.4
2	11	1	10.3	8.0	7.3	3.3
3	11	1	29.9	30.1	29.2	7.6
4	11	1	12.0	11.6	-5.8	10.1
5	11	1	19.1	17.2	17.1	2.3
7	11	1	9.1	6.9	6.4	2.7
8	11	1	8.2	3.7	3.6	-0.8
9	11	1	15.6	13.0	13.0	0.6
11	11	1	9.3	9.4	8.7	3.6
4	12	1	9.0	10.3	-2.6	9.9
7	12	1	10.4	9.7	7.9	-5.7
0	13	1	20.1	21.4	0.1	21.4
1	13	1	11.8	10.0	-9.7	-2.6
2	13	1	21.8	21.2	3.7	20.9
3	13	1	13.6	14.6	-14.3	3.1
4	13	1	16.7	17.3	-0.5	17.3
6	13	1	16.5	14.5	5.3	13.5
2	15	1	8.8	9.6	-1.9	-9.4
4	15	1	11.6	13.8	5.3	-12.7
6	15	1	9.0	4.8	-1.4	-4.6
0	0	2	143.5	142.6	142.6	0.0
1	0	2	121.1	120.3	-120.3	-0.1
2	0	2	102.2	101.8	101.8	0.2
3	0	2	19.9	15.1	-15.1	-0.1
4	0	2	48.5	47.8	47.7	-0.5
5	0	2	15.3	10.8	10.8	-0.2
6	0	2	43.0	42.9	42.9	0.5
7	0	2	18.6	16.5	-16.5	0.2
8	0	2	28.2	26.9	26.9	-0.1
9	0	2	11.6	8.4	8.4	0.0
10	0	2	9.0	4.2	4.2	0.0
11	0	2	14.5	13.9	13.9	-0.1
12	0	2	14.8	12.0	12.0	0.3
13	0	2	11.8	7.2	7.2	0.1
14	0	2	9.6	8.4	8.4	-0.1
0	1	2	110.1	111.0	-0.1	111.0
1	1	2	25.5	27.6	-22.2	-16.4
2	1	2	38.4	37.6	-9.2	-36.5
3	1	2	22.0	19.7	-12.8	-14.9
4	1	2	8.7	4.9	-0.9	4.8
5	1	2	21.1	19.2	-14.4	-12.6
6	1	2	28.9	26.3	-9.2	24.6
7	1	2	22.4	23.1	9.7	-20.9
8	1	2	14.3	8.7	-0.2	8.7
9	1	2	21.3	20.9	0.5	-20.9
10	1	2	16.0	13.9	12.9	5.3
11	1	2	13.7	11.8	9.4	-7.1
12	1	2	14.2	11.6	9.0	7.4
13	1	2	14.1	9.3	-2.5	-9.0
14	1	2	11.0	6.1	5.6	-2.3
15	1	2	12.7	9.3	-0.9	-9.3
0	2	2	13.2	10.4	-10.4	0.2
1	2	2	79.0	80.0	-3.6	79.9
2	2	2	51.6	49.6	-40.3	28.9
3	2	2	59.2	58.8	-23.3	54.0
4	2	2	26.8	27.2	-25.9	8.3
5	2	2	49.4	49.1	11.7	47.7
6	2	2	18.4	16.3	-16.3	0.5
7	2	2	39.4	38.7	6.1	38.2
8	2	2	26.3	24.9	-23.7	7.8
9	2	2	21.4	19.6	2.9	19.4
10	2	2	19.9	17.3	-7.2	-15.7
11	2	2	15.8	12.5	11.3	5.1
12	2	2	14.5	8.0	-6.6	4.4
13	2	2	12.9	6.3	1.5	6.1
14	2	2	11.2	6.6	-6.6	-0.6
15	2	2	11.6	6.3	0.2	6.3
0	3	2	36.2	36.9	-0.2	36.9
1	3	2	19.0	17.8	-13.9	-11.1
2	3	2	25.4	26.8	-6.9	-25.9
3	3	2	10.7	12.4	10.9	5.9
4	3	2	8.1	8.1	8.0	-1.4
5	3	2	22.1	21.8	-4.9	-21.2
6	3	2	9.8	8.1	0.8	8.0
7	3	2	10.1	8.5	6.4	-5.5
8	3	2	8.5	5.8	-0.5	-5.7
9	3	2	24.8	23.8	22.9	6.7
10	3	2	14.1	13.3	7.4	11.0
12	3	2	11.4	8.2	8.0	-2.0
13	3	2	11.8	7.0	2.4	6.6
0	4	2	23.8	26.2	-26.2	0.3
1	4	2	46.4	49.0	6.9	-48.5
2	4	2	34.0	34.1	0.5	34.1
3	4	2	27.4	26.8	17.7	-20.1
4	4	2	28.7	29.7	21.0	21.0
5	4	2	18.8	19.9	-0.2	-19.9
7	4	2	13.8	12.6	4.1	-11.9
8	4	2	10.2	8.2	-1.1	8.1
9	4	2	19.3	18.7	7.0	-17.4
10	4	2	15.1	12.7	11.0	-6.5
11	4	2	9.0	11.2	-6.3	-9.3
13	4	2	14.0	12.2	-2.7	-11.9
1	5	2	20.7	20.5	6.0	19.6
2	5	2	13.6	13.9	-11.6	7.8
4	5	2	13.8	13.5	5.4	12.4
7	5	2	14.1	12.7	-0.3	12.7
9	5	2	15.9	15.2	14.3	-5.2
10	5	2	11.0	11.1	-10.5	-3.8
1	6	2	38.4	38.2	-35.0	15.2
2	6	2	27.6	28.7	28.1	5.7
3	6	2	47.0	46.8	39.6	25.0
4	6	2	28.2	29.2	17.8	23.1
5	6	2	15.9	17.0	2.9	16.8
6	6	2	25.7	26.5	19.0	-18.5
7	6	2	14.5	15.6	-8.7	13.0
8	6	2	28.2	28.3	27.0	8.4
9	6	2	9.7	8.7	7.4	4.5
10	6	2	10.2	12.8	12.8	-0.3
11	6	2	9.8	10.6	-8.1	6.9
12	6	2	11.8	10.3	9.4	-4.1
1	7	2	23.0	24.6	24.2	4.4
2	7	2	15.4	13.3	13.3	-0.6
3	7	2	11.4	15.0	-14.8	2.3
5	7	2	18.6	19.1	-0.9	19.1
7	7	2	17.6	17.4	11.4	13.2
8	7	2	17.2	16.8	10.5	-13.1
9	7	2	12.2	12.6	-12.5	-0.6
10	7	2	8.8	10.5	4.8	-9.4
0	8	2	16.2	15.4	-15.4	0.1
1	8	2	9.3	7.1	-3.7	6.1
2	8	2	24.8	24.5	-23.7	-6.1
3	8	2	16.2	17.3	6.4	-16.0
4	8	2	25.0	24.6	-23.0	-8.7
6	8	2	11.6	11.8	-7.3	-9.2
7	8	2	10.2	8.2	-7.5	-3.3
8	8	2	11.8	12.0	-12.0	-0.0
10	8	2	11.8	10.8	-10.8	0.3
12	8	2	8.1	6.7	-6.1	2.6
1	9	2	12.6	12.3	11.7	3.9
2	9	2	8.7	6.6	3.1	-5.8
3	9	2	12.6	11.1	1.1	11.1
4	9	2	11.9	13.2	-13.2	-0.4
5	9	2	11.1	9.8	0.1	9.8
6	9	2	14.5	12.8	-10.2	7.7
7	9	2	13.7	14.1	7.3	12.0
9	9	2	15.0	17.8	-7.0	16.4
1	10	2	18.0	17.5	-4.7	-16.9
2	10	2	15.2	13.9	-2.0	-13.7
3	10	2	21.3	21.1	5.1	-20.5
4	10	2	12.0	9.6	0.8	-9.6
5	10	2	23.9	23.5	1.2	-23.5
6	10	2	10.2	10.1	6.2	-7.9
7	10	2	19.7	20.5	-3.9	-20.1
9	10	2	17.0	16.0	-0.2	-16.0
11	10	2	9.6	10.5	2.7	-10.2
0	11	2	11.3	8.9	-0.4	-8.9
2	11	2	16.4	16.1	-12.4	-10.3
3	11	2	17.3	16.7	12.9	-10.5
5	11	2	13.2	12.6	1.9	-12.5
7	11	2	12.9	9.1	-2.9	-8.6
1	12	2	11.1	13.1	-5.2	-12.0
2	12	2	10.2	9.5	5.3	-7.9
4	12	2	8.8	4.9	-0.1	4.9
5	12	2	8.8	6.5	-5.7	-3.2
6	12	2	9.2	4.6	3.9	-2.3
3	13	2	15.5	15.0	14.8	-2.5
2	14	2	9.1	3.9	-2.5	3.0
3	14	2	8.7	8.5	-7.5	-4.1
4	14	2	9.6	7.0	-5.8	-3.9
6	14	2	12.3	9.3	-7.9	4.9
1	15	2	8.2	5.5	-5.5	0.2
4	15	2	10.0	8.1	-8.1	-0.2
1	0	3	11.7	15.3	0.0	-15.3
2	0	3	22.3	21.7	0.3	-21.7
9	0	3	10.2	13.7	0.3	-13.7
10	0	3	13.5	13.8	0.2	-13.8
0	1	3	10.9	13.8	0.0	13.8
1	1	3	29.3	28.9	-17.8	22.8
2	1	3	36.4	36.1	33.8	12.7

Figure 10 (Continued)

H	K	L	FOBS	FCAL	ACAL	BCAL
3	1	3	19.1	18.7	9.0	-16.4
6	1	3	21.5	21.5	-4.0	21.1
8	1	3	24.9	26.1	4.7	25.7
9	1	3	8.8	12.2	10.7	6.0
10	1	3	21.9	22.6	-22.2	4.3
12	1	3	15.1	15.9	-5.1	15.1
0	2	3	49.3	49.9	49.9	0.0
1	2	3	24.0	24.8	-24.7	1.7
2	2	3	24.7	24.0	22.4	8.7
3	2	3	23.4	21.9	21.3	4.9
4	2	3	20.9	20.8	-0.7	20.8
6	2	3	17.9	17.2	12.5	11.8
7	2	3	10.3	7.6	-4.3	-6.2
8	2	3	20.4	20.9	-4.0	20.5
9	2	3	12.9	14.2	13.8	-3.3
10	2	3	21.0	20.6	-19.5	6.6
12	2	3	14.1	15.1	0.7	15.1
1	3	3	31.6	30.2	-30.0	3.0
2	3	3	12.5	13.4	-3.2	-13.0
3	3	3	38.8	38.6	-28.2	-26.5
4	3	3	23.4	24.0	-9.0	-22.3
5	3	3	29.9	30.3	-24.3	-18.1
6	3	3	15.6	16.9	-15.1	7.5
7	3	3	21.1	20.4	-20.3	2.7
9	3	3	31.7	31.2	-30.9	4.3
10	3	3	16.9	16.2	-15.0	-6.3
13	3	3	13.8	14.1	-13.7	3.2
1	4	3	17.8	17.8	11.6	-13.5
2	4	3	29.1	28.9	27.6	8.5
3	4	3	31.7	31.1	-30.9	-2.9
5	4	3	15.9	16.2	-7.7	-14.3
6	4	3	12.1	11.4	11.3	-1.0
7	4	3	13.4	12.3	-12.0	-2.5
9	4	3	25.6	26.1	-25.4	6.0
10	4	3	10.7	10.0	-9.7	-2.5
11	4	3	13.2	14.7	-6.2	-13.3
0	5	3	32.3	32.2	0.5	-32.2
1	5	3	17.0	16.4	16.1	-2.9
2	5	3	33.5	34.5	-21.6	-26.9
3	5	3	16.7	18.3	9.4	-15.8
4	5	3	18.2	19.6	-3.4	-19.3
5	5	3	19.7	19.4	12.7	-14.6
6	5	3	15.6	17.6	4.5	-17.0
7	5	3	11.5	12.2	12.1	1.4
8	5	3	18.0	19.7	-4.3	-19.2
10	5	3	8.8	9.3	8.2	-4.4
12	5	3	8.5	11.4	8.1	-8.0
0	6	3	19.9	20.0	-20.0	-0.4
1	6	3	17.1	17.8	-8.2	-15.9
2	6	3	16.8	16.5	4.3	-16.0
5	6	3	13.8	11.9	9.9	-6.8
8	6	3	9.3	9.1	-2.3	-8.8
9	6	3	11.7	11.9	0.1	11.9
10	6	3	8.5	10.2	2.2	-10.0
11	6	3	8.8	5.9	5.8	-1.3
0	7	3	21.5	22.1	-0.2	22.1
1	7	3	18.9	17.8	16.8	5.9
2	7	3	34.6	34.7	-9.6	33.4
4	7	3	21.9	20.9	-4.5	20.5
5	7	3	11.2	12.7	10.1	7.7
6	7	3	19.8	19.7	5.7	18.9
7	7	3	11.4	12.0	11.5	3.5
8	7	3	19.4	20.4	4.3	20.0
10	7	3	11.2	8.8	6.3	6.2
12	7	3	9.6	10.9	3.3	10.4
0	8	3	14.6	14.9	-14.8	-1.0
1	8	3	12.1	9.9	-3.4	-9.3
2	8	3	15.1	15.8	-15.0	-4.8
4	8	3	8.8	8.2	-7.5	-3.2
6	8	3	8.6	9.0	-5.0	-7.4
7	8	3	11.5	9.6	-2.9	-9.2
9	8	3	12.6	12.3	6.6	10.4
1	9	3	17.8	16.5	-16.5	-0.2
2	9	3	11.3	13.3	12.6	-4.5
3	9	3	20.0	19.5	-11.6	15.6
4	9	3	13.2	13.6	-12.2	-6.0
5	9	3	15.9	16.5	-12.2	11.1
6	9	3	9.0	8.8	3.0	8.3
8	9	3	13.2	12.9	12.7	-1.7
9	9	3	14.1	12.8	-12.8	0.2
1	10	3	14.6	16.1	12.3	10.4
2	10	3	18.0	18.4	-9.6	15.7
4	10	3	17.5	18.0	-10.1	-14.9
5	10	3	8.5	8.1	7.8	-1.9
7	10	3	8.2	7.7	4.9	-5.9
1	11	3	16.8	15.9	15.9	-0.3
2	11	3	11.2	11.4	10.9	3.4
3	11	3	22.7	23.1	19.1	12.9
4	11	3	12.1	10.5	-9.7	4.1
5	11	3	14.7	11.5	11.5	-0.2
7	11	3	9.4	8.3	8.2	1.2
1	12	3	10.5	10.9	-3.7	10.3
2	12	3	15.7	15.5	-15.5	0.2
3	12	3	8.8	5.6	-1.7	5.4
4	12	3	11.6	10.9	-10.8	2.0
0	13	3	13.4	10.6	-0.0	10.6
2	13	3	19.1	18.3	1.7	18.2
3	13	3	11.3	12.6	-12.6	1.0
4	13	3	11.6	11.5	5.2	10.3
2	15	3	8.9	7.0	-1.2	-6.9
0	0	4	14.1	10.9	-10.9	0.0
2	0	4	89.2	89.5	89.5	-0.2
3	0	4	32.0	31.9	-31.9	-0.2
4	0	4	39.2	39.6	39.6	-0.0
6	0	4	26.2	26.7	26.7	-0.0
8	0	4	36.9	37.2	37.2	0.3
10	0	4	12.3	14.0	14.0	-0.1
11	0	4	15.5	16.3	16.3	0.4
12	0	4	9.3	6.1	6.1	0.8
0	1	4	22.0	22.8	0.1	22.8
1	1	4	37.4	38.9	-27.9	-27.1
4	1	4	17.3	16.9	5.3	16.1
5	1	4	16.8	17.6	-11.5	13.4
9	1	4	15.0	14.5	11.2	-9.2
10	1	4	18.3	19.1	16.1	10.3
0	2	4	38.9	39.4	-39.4	-0.1
1	2	4	34.9	36.6	-3.9	36.4
3	2	4	24.5	25.6	-2.6	25.5
4	2	4	11.5	11.3	-2.5	11.0
5	2	4	10.2	11.8	9.5	6.9
6	2	4	8.9	10.9	-10.9	-0.6
7	2	4	11.4	11.8	-0.2	11.8
9	2	4	12.6	13.4	12.6	4.5
12	2	4	7.5	6.8	-5.7	3.7
0	3	4	8.7	11.3	-0.2	-11.3
1	3	4	16.1	16.1	-15.5	-4.5
4	3	4	13.0	14.1	10.8	-9.1
6	3	4	11.2	13.2	12.5	4.3
9	3	4	22.9	22.7	18.6	13.0
1	4	4	22.2	20.7	7.1	-19.4
2	4	4	14.5	14.0	-0.7	14.0
3	4	4	23.4	24.1	13.7	-19.8
4	4	4	15.4	14.7	-1.5	14.6
5	4	4	25.7	25.6	-0.1	-25.6
7	4	4	25.9	26.4	-0.1	-26.3
9	4	4	12.5	14.4	8.3	-11.8
11	4	4	16.4	16.4	-7.0	-14.8
0	5	4	18.3	20.1	-0.5	20.1
1	5	4	11.3	14.3	-1.7	-14.2
6	5	4	15.2	15.1	12.5	8.5
1	6	4	16.5	18.4	9.9	15.5
2	6	4	20.3	19.9	18.8	6.3
3	6	4	12.4	11.6	5.2	10.3
7	6	4	8.8	10.2	2.1	10.0
8	6	4	9.1	8.7	8.7	0.4
1	7	4	19.9	20.5	12.7	-16.1
6	7	4	12.0	12.0	11.6	-3.1
8	7	4	8.2	7.5	0.3	-7.5
10	7	4	11.9	9.9	9.1	-3.9
1	8	4	14.9	15.8	-14.2	6.9
2	8	4	24.6	23.9	-19.0	-14.6
3	8	4	10.5	11.6	3.7	-11.0
4	8	4	16.8	17.4	-17.4	0.5
6	8	4	21.4	21.6	-20.4	-7.1
7	8	4	18.9	16.6	-12.0	11.4
8	8	4	12.1	12.1	-11.7	-2.9
11	8	4	8.2	5.3	-2.7	4.6
1	9	4	13.3	13.4	13.4	-0.6
3	9	4	9.7	10.1	0.6	10.0
4	9	4	14.1	14.0	-12.7	-5.9
5	9	4	12.2	12.4	10.0	7.3
8	9	4	9.3	5.9	-5.5	2.2
10	9	4	8.0	6.4	-4.1	-4.9
1	10	4	16.1	15.4	-8.6	-12.8
2	10	4	10.4	11.6	2.8	-11.2
3	10	4	10.9	9.2	4.4	-8.0
4	10	4	11.9	10.3	2.2	-10.1
2	11	4	10.8	12.1	-2.4	-11.8
3	11	4	13.6	14.8	14.7	2.0
4	11	4	8.8	7.5	-4.8	-5.7
1	12	4	10.8	8.2	0.4	-8.2
2	12	4	12.0	10.3	9.5	3.9
3	12	4	15.2	14.6	-2.4	14.4
1	0	5	29.0	27.7	0.1	-27.7
3	0	5	10.6	8.6	-0.0	-8.6
4	0	5	19.0	17.7	-0.0	-17.7
5	0	5	12.7	13.8	-0.1	-13.8
9	0	5	9.3	7.5	-0.1	-7.5
10	0	5	10.1	8.3	0.0	-8.3
0	1	5	19.6	19.4	-0.1	19.4
1	1	5	15.5	16.2	15.9	-3.2
2	1	5	17.5	15.1	15.0	-1.9
5	1	5	11.2	10.5	-1.0	10.4
6	1	5	14.9	15.7	-0.8	15.7
8	1	5	13.9	14.1	3.9	13.6
10	1	5	12.7	9.1	-4.1	8.1
11	1	5	8.4	5.1	0.9	5.1
12	1	5	9.8	7.3	-5.9	4.3
1	2	5	12.8	13.6	-11.3	-7.6
2	2	5	15.1	15.0	11.5	9.6
8	2	5	13.9	13.6	-3.2	13.2
9	2	5	9.2	9.9	-0.7	-9.8

Figure 10 (Continued)

H	K	L	FOBS	FCAL	ACAL	BCAL
10	2	5	12.7	12.9	-12.7	-2.4
11	2	5	10.0	9.5	9.5	0.5
12	2	5	12.1	11.3	-2.4	11.1
0	3	5	15.8	18.0	-0.2	-18.0
1	3	5	18.3	17.3	-14.C	-10.0
3	3	5	17.3	19.6	-16.1	-11.2
5	3	5	12.0	11.7	-11.3	3.1
6	3	5	10.1	11.4	-6.9	9.1
7	3	5	17.7	18.3	-15.1	-10.3
8	3	5	13.6	13.4	-10.9	7.7
9	3	5	15.3	14.3	-13.4	-5.0
10	3	5	9.1	5.8	5.2	-2.4
12	3	5	9.0	7.2	-7.1	1.1
1	4	5	12.5	13.5	-13.5	0.3
2	4	5	9.7	11.6	-11.1	3.4
7	4	5	18.9	17.8	-17.7	-1.8
8	4	5	12.0	10.9	-10.7	1.9
9	4	5	10.2	8.4	-7.1	-4.4
0	5	5	38.0	38.2	-0.0	-38.2
2	5	5	9.6	8.6	-5.9	-6.3
3	5	5	10.5	11.4	6.9	-9.1
4	5	5	13.0	12.0	-1.7	-11.9
5	5	5	18.7	18.7	17.9	-5.5
6	5	5	9.3	6.1	4.1	-4.5
7	5	5	12.7	11.7	9.9	-6.3
9	5	5	10.5	7.1	7.1	-0.9
10	5	5	9.7	5.5	3.8	-4.0
11	5	5	11.2	11.2	11.C	-1.9
0	6	5	15.5	15.6	-15.6	0.0
3	6	5	9.8	10.5	6.C	8.6
6	6	5	11.0	10.9	-8.1	7.2
7	6	5	9.7	6.0	0.9	6.0
8	6	5	8.9	8.0	-1.3	-7.9
9	6	5	8.2	5.9	0.8	5.8
0	7	5	18.8	18.5	0.8	18.5
1	7	5	8.7	9.3	4.6	8.1
2	7	5	8.8	8.8	-5.5	6.9
4	7	5	15.4	15.4	2.8	15.2
6	7	5	11.4	10.6	5.5	9.1
7	7	5	16.7	15.8	15.3	4.0
0	8	5	14.6	15.1	-15.1	-0.7
1	8	5	8.6	9.6	9.6	-0.4
6	8	5	11.3	10.8	-10.3	3.3
1	9	5	9.5	10.0	-9.9	1.5
3	9	5	11.5	12.2	-10.8	5.6
4	9	5	8.4	7.0	-0.1	-7.0
5	9	5	12.6	12.2	-2.7	11.9
9	9	5	10.2	9.8	-9.5	2.4
0	10	5	8.9	9.2	9.2	-0.3
1	10	5	13.6	12.2	3.1	11.8
4	10	5	8.9	9.6	2.0	-9.4
1	11	5	11.6	8.0	7.8	1.8
5	11	5	9.6	7.7	7.2	2.9
0	13	5	13.5	12.8	-0.6	12.8

H	K	L	FOBS	FCAL	ACAL	BCAL
1	0	6	12.3	11.3	11.3	-0.1
4	0	6	12.6	12.0	12.C	C.3
6	0	6	13.9	13.2	13.2	-0.3
8	0	6	11.6	9.9	9.9	0.4
10	0	6	9.7	9.9	9.9	0.1
0	1	6	8.8	10.5	-0.1	-10.5
1	1	6	9.5	9.2	-9.2	-0.0
2	1	6	28.2	28.3	10.8	26.1
4	1	6	13.1	13.6	-3.1	13.3
8	1	6	8.9	9.5	6.8	6.6
9	1	6	8.6	5.6	5.1	-2.3
0	2	6	25.0	25.8	-25.8	C.1
1	2	6	21.5	20.1	7.3	18.7
3	2	6	19.9	20.5	4.5	2C.0
6	2	6	8.6	11.3	-11.1	2.1
9	2	6	10.2	8.1	1.5	8.0
10	2	6	8.6	9.5	-8.6	4.0
1	3	6	10.7	10.8	0.C	10.8
8	3	6	9.3	7.4	5.6	4.8
1	4	6	10.5	11.6	11.6	-0.7
7	4	6	18.1	16.4	5.0	-15.6
6	5	6	9.2	6.3	3.8	5.0
7	5	6	9.4	6.9	-1.7	-6.7
0	6	6	26.7	26.5	26.5	0.1
1	6	6	14.5	16.3	10.4	12.5
3	6	6	10.5	9.3	-7.5	5.5
5	6	6	10.3	9.2	-2.9	8.7
6	6	6	10.1	8.5	6.6	5.3
2	8	6	8.6	7.1	-3.2	-6.3
6	8	6	13.4	12.5	-12.2	3.1
7	8	6	8.2	7.8	-1.5	7.7
1	10	6	12.0	11.8	-0.1	-11.8
4	10	6	8.4	8.6	6.8	-5.3
3	0	7	13.9	13.4	0.3	-13.4
1	1	7	19.6	19.3	15.5	-11.5
5	1	7	9.2	10.1	8.2	5.9
0	2	7	11.9	10.0	10.C	0.1
0	3	7	13.6	14.2	-0.2	-14.2
1	3	7	9.9	9.7	-8.2	-5.2
7	3	7	8.3	8.2	-7.7	-2.7
1	4	7	8.5	8.7	-8.6	1.5
0	5	7	16.7	16.5	0.0	-16.5
2	5	7	10.5	9.2	-1.2	-9.1
1	9	7	8.7	6.7	-5.5	3.9
0	0	8	9.4	8.3	8.3	C.0
3	0	8	9.2	5.0	5.0	-0.1
4	0	8	8.7	5.3	5.3	-0.1
0	1	8	10.6	5.2	-0.C	-5.2
1	1	8	10.9	9.6	-1.4	9.5
2	1	8	13.1	10.2	4.2	9.3
3	1	8	9.3	8.8	-8.3	-3.0
2	2	8	8.6	5.2	-5.C	1.5

Figure 10 (Continued)

H	K	L	FO	FC
2	1	0	0.0	9.9
3	1	0	4.2	6.6
10	1	0	5.9	1.8
13	1	0	7.0	1.0
11	2	0	5.5	1.0
12	2	0	2.4	1.0
13	2	0	7.6	1.9
14	2	0	3.1	3.4
15	2	0	7.2	3.4
9	3	0	5.7	6.2
14	3	0	5.3	5.7
15	3	0	5.9	8.8
8	4	0	6.3	5.6
12	4	0	0.0	2.1
2	5	0	7.5	2.3
3	5	0	0.0	4.7
8	5	0	7.0	2.6
9	5	0	7.0	6.4
10	5	0	0.0	1.3
11	5	0	7.9	11.4
12	5	0	5.3	2.2
14	5	0	0.0	1.7
0	6	0	7.7	12.7
9	6	0	0.0	4.8
11	6	0	5.9	8.7
12	6	0	0.0	3.4
13	6	0	5.1	2.3
3	7	0	4.5	5.6
9	7	0	6.9	5.6
10	7	0	0.0	3.8
11	7	0	5.0	11.2
12	7	0	6.8	2.7
13	7	0	0.0	1.0
14	7	0	0.0	4.8
7	8	0	8.3	5.9
9	8	0	3.2	1.2
11	8	0	0.0	7.2
12	8	0	0.0	5.8
13	8	0	5.5	5.7
3	9	0	2.7	1.3
4	9	0	7.4	5.1
8	9	0	3.5	5.6
9	9	0	4.7	10.2
13	9	0	0.0	1.2
0	10	0	6.2	3.3
4	10	0	0.0	1.5
10	10	0	0.0	1.9
12	10	0	5.4	6.7
4	11	0	2.9	1.1
6	11	0	3.5	4.8
9	11	0	3.2	0.4
10	11	0	0.0	8.4
11	11	0	0.0	3.0
1	12	0	8.4	2.2
2	12	0	7.3	1.1
6	12	0	6.0	7.1
7	12	0	4.4	7.9
8	12	0	7.7	3.4
10	12	0	4.2	4.6
1	13	0	6.5	5.8
3	13	0	5.1	4.7
4	13	0	5.7	5.6
5	13	0	0.0	3.4
6	13	0	0.0	5.4
7	13	0	0.0	1.8
8	13	0	0.0	1.0
9	13	0	2.2	2.4
0	14	0	0.0	5.4
1	14	0	0.8	0.4
2	14	0	5.7	6.3
3	14	0	0.0	4.2
4	14	0	4.1	4.3
5	14	0	0.0	1.4
6	14	0	6.6	8.3
7	14	0	0.0	5.2
8	14	0	7.9	6.3
1	15	0	5.5	2.2
2	15	0	2.0	0.7
3	15	0	0.0	3.0
4	15	0	0.0	8.5
5	15	0	0.0	0.1
6	15	0	7.6	13.2
0	16	0	0.0	1.2
1	16	0	5.0	0.7
2	16	0	3.5	1.4
4	0	1	7.1	2.8
10	0	1	0.0	6.1
11	0	1	0.0	6.5
13	0	1	0.0	1.0
14	0	1	0.0	3.6
15	0	1	0.0	1.1
5	1	1	0.0	6.4
13	1	1	4.4	5.1
15	1	1	5.0	5.0
12	2	1	6.4	4.0
13	2	1	7.5	2.9
15	2	1	3.1	5.3
4	3	1	0.0	2.8
14	3	1	0.0	4.4
8	4	1	7.8	1.2
14	4	1	2.1	1.8
15	4	1	6.8	8.5
9	5	1	1.7	5.8
11	5	1	0.0	3.2
12	5	1	0.0	2.2
14	5	1	0.0	4.4
1	6	1	7.3	8.8
7	6	1	6.7	4.6
12	6	1	0.9	2.7
13	6	1	0.0	6.1
14	6	1	0.0	3.0
5	7	1	2.8	6.3
7	7	1	3.5	6.0
11	7	1	0.0	7.5

H	K	L	FO	FC
12	7	1	0.0	7.8
13	7	1	0.0	4.5
14	7	1	6.4	11.3
0	8	1	4.8	4.9
1	8	1	3.0	1.6
3	8	1	7.4	5.0
4	8	1	6.2	8.0
6	8	1	2.4	8.4
7	8	1	5.8	6.1
8	8	1	5.8	9.2
9	8	1	8.0	14.9
10	8	1	0.0	3.5
11	8	1	6.8	11.2
12	8	1	6.2	8.5
13	8	1	0.0	4.3
4	9	1	8.6	10.2
6	9	1	2.3	1.7
9	9	1	5.1	3.4
12	9	1	0.0	6.2
13	9	1	5.1	6.9
0	10	1	1.8	3.9
1	10	1	7.4	8.4
2	10	1	6.9	7.7
5	10	1	3.6	6.1
7	10	1	0.0	5.2
8	10	1	6.6	5.3
9	10	1	8.0	9.2
10	10	1	3.6	0.4
11	10	1	0.0	3.3
12	10	1	4.3	8.7
6	11	1	0.0	2.0
10	11	1	2.2	3.0
0	12	1	4.4	4.2
1	12	1	5.9	4.5
2	12	1	6.5	4.8
3	12	1	6.6	2.7
5	12	1	5.8	3.0
6	12	1	4.6	6.4
8	12	1	2.9	1.4
9	12	1	0.0	0.6
10	12	1	0.0	2.6
5	13	1	5.4	6.7
7	13	1	0.0	8.5
8	13	1	0.0	1.2
9	13	1	0.0	2.6
0	14	1	6.7	2.6
1	14	1	7.7	6.3
2	14	1	5.4	5.2
3	14	1	5.2	7.1
4	14	1	0.0	0.3
5	14	1	0.0	1.0
6	14	1	0.0	7.4
7	14	1	0.0	5.2
1	15	1	5.5	6.7
3	15	1	7.7	8.5
5	15	1	0.0	1.8
0	16	1	5.9	1.9
1	16	1	3.9	3.2
2	16	1	7.4	4.5
15	0	2	0.0	0.3
11	3	2	6.3	4.1
14	3	2	6.6	3.7
15	3	2	5.3	3.9
6	4	2	5.9	2.4
12	4	2	6.4	3.9
14	4	2	7.4	3.7
0	5	2	2.7	10.9
3	5	2	3.4	1.7
5	5	2	3.3	3.5
6	5	2	7.7	5.1
8	5	2	7.0	6.4
11	5	2	7.2	4.6
12	5	2	7.5	3.7
13	5	2	6.9	6.1
14	5	2	0.0	5.0
0	6	2	5.7	0.2
13	6	2	0.0	2.2
14	6	2	4.9	9.0
0	7	2	3.2	1.4
4	7	2	6.6	5.1
6	7	2	1.8	5.1
11	7	2	5.7	5.3
12	7	2	5.5	2.9
13	7	2	0.0	2.7
5	8	2	3.6	6.5
9	8	2	8.0	8.4
11	8	2	6.1	3.7
13	8	2	0.0	3.3
0	9	2	7.1	0.8
8	9	2	7.0	9.7
10	9	2	4.8	7.0
11	9	2	5.3	7.4
12	9	2	6.8	9.5
0	10	2	3.6	1.7
8	10	2	5.9	6.5
10	10	2	2.7	1.9
1	11	2	4.4	2.6
4	11	2	8.2	0.8
6	11	2	4.5	3.3
8	11	2	5.1	9.7
9	11	2	6.5	5.2
10	11	2	0.0	6.4
11	11	2	0.0	1.3
0	12	2	4.0	6.3
3	12	2	6.2	2.4
7	12	2	4.5	2.5
8	12	2	3.8	2.5
9	12	2	4.5	6.6
10	12	2	0.0	0.1
0	13	2	3.0	1.6
1	13	2	7.7	5.9
2	13	2	6.1	5.3
4	13	2	7.2	4.9
5	13	2	4.5	4.4

H	K	L	FO	FC
6	13	2	7.9	7.1
7	13	2	2.8	3.2
8	13	2	1.8	3.2
0	14	2	8.1	4.8
1	14	2	7.4	4.0
5	14	2	3.2	5.4
7	14	2	4.9	2.0
0	15	2	4.4	4.0
2	15	2	4.9	3.8
3	15	2	5.2	3.0
5	15	2	5.0	3.2
3	0	3	5.1	3.5
4	0	3	3.8	5.8
5	0	3	0.0	6.0
6	0	3	0.0	4.5
7	0	3	0.0	0.3
8	0	3	0.0	5.7
11	0	3	0.0	4.3
12	0	3	0.0	3.2
13	0	3	0.0	3.1
14	0	3	0.0	2.8
4	1	3	7.6	5.6
5	1	3	6.1	6.4
7	1	3	7.5	8.9
11	1	3	0.0	8.2
13	1	3	0.0	3.7
14	1	3	4.5	8.7
5	2	3	6.2	8.0
11	2	3	3.9	9.3
13	2	3	0.0	3.3
14	2	3	0.0	6.3
0	3	3	4.5	0.9
8	3	3	7.3	2.4
11	3	3	3.0	2.8
12	3	3	2.2	4.7
14	3	3	0.0	4.4
0	4	3	2.6	3.6
4	4	3	7.7	4.2
8	4	3	0.0	4.3
12	4	3	5.2	3.4
13	4	3	6.6	7.3
14	4	3	0.0	3.1
9	5	3	4.9	6.2
11	5	3	3.4	8.6
13	5	3	4.7	5.0
3	6	3	8.0	5.1
4	6	3	8.0	6.5
6	6	3	8.0	10.4
7	6	3	0.0	1.6
12	6	3	6.1	5.5
13	6	3	7.4	6.8
3	7	3	8.2	4.2
9	7	3	0.0	2.0
11	7	3	2.1	0.7
13	7	3	0.0	2.8
3	8	3	1.5	8.6
5	8	3	6.2	4.6
8	8	3	6.4	4.6
10	8	3	4.0	0.9
11	8	3	0.0	4.3
12	8	3	0.0	4.3
0	9	3	3.1	8.1
7	9	3	6.1	8.5
10	9	3	0.0	1.7
11	9	3	0.0	4.5
0	10	3	2.1	0.6
3	10	3	5.2	4.6
6	10	3	7.3	1.6
8	10	3	7.5	4.7
9	10	3	0.0	1.4
10	10	3	0.0	4.2
11	10	3	0.0	4.2
0	11	3	4.3	0.8
6	11	3	5.8	1.2
8	11	3	0.0	5.6
9	11	3	6.0	5.0
10	11	3	0.0	3.9
0	12	3	0.4	1.5
5	12	3	5.7	3.6
6	12	3	0.0	3.2
7	12	3	0.0	1.9
8	12	3	0.0	4.8
9	12	3	0.0	4.0
1	13	3	5.4	2.1
5	13	3	0.0	4.4
6	13	3	0.0	7.1
7	13	3	0.0	1.5
0	14	3	3.9	4.5
1	14	3	6.1	2.6
2	14	3	3.4	6.7
3	14	3	0.0	2.4
4	14	3	4.5	4.3
5	14	3	0.0	2.5
6	14	3	5.6	3.6
0	15	3	4.9	4.4
1	15	3	4.0	5.0
3	15	3	0.0	4.6
1	0	4	5.8	0.7
5	0	4	0.0	2.6
7	0	4	0.0	2.6
9	0	4	0.0	3.2
13	0	4	5.4	4.4
2	1	4	1.9	2.3
3	1	4	3.9	5.8
6	1	4	4.4	8.5
7	1	4	0.0	7.9
8	1	4	0.0	2.1
11	1	4	2.7	1.9
12	1	4	0.0	3.3
13	1	4	1.7	6.7
2	2	4	4.7	5.9
8	2	4	0.0	3.7
10	2	4	7.0	8.4

H	K	L	FO	FC
11	2	4	6.7	5.2
13	2	4	0.0	4.0
2	3	4	5.6	5.1
3	3	4	4.5	3.6
5	3	4	0.0	1.0
7	3	4	0.0	5.6
8	3	4	2.4	6.8
10	3	4	7.6	8.8
11	3	4	4.8	4.6
12	3	4	3.9	5.2
13	3	4	0.0	4.7
0	4	4	8.2	8.3
6	4	4	4.8	8.0
8	4	4	3.2	4.9
10	4	4	0.0	4.4
12	4	4	0.0	2.2
13	4	4	5.3	6.8
2	5	4	6.5	6.4
3	5	4	8.4	6.0
4	5	4	8.4	9.5
5	5	4	8.2	9.0
7	5	4	2.6	5.2
8	5	4	0.0	5.5
9	5	4	0.0	4.6
10	5	4	5.3	6.3
11	5	4	6.0	3.6
12	5	4	0.3	2.5
13	5	4	0.0	2.7
0	6	4	6.3	4.7
4	6	4	5.2	5.3
5	6	4	0.0	0.8
6	6	4	7.1	2.8
9	6	4	4.3	5.9
10	6	4	5.0	1.6
11	6	4	3.6	2.7
12	6	4	0.0	4.1
0	7	4	0.0	2.2
2	7	4	1.6	5.2
3	7	4	0.0	6.0
4	7	4	0.0	1.5
5	7	4	7.4	4.3
7	7	4	2.8	7.7
9	7	4	0.0	1.1
11	7	4	3.5	2.8
12	7	4	0.0	4.2
0	8	4	7.6	9.8
5	8	4	5.2	3.2
9	8	4	5.5	4.2
10	8	4	5.7	8.2
0	9	4	5.6	9.1
2	9	4	6.6	5.7
6	9	4	6.5	8.7
7	9	4	6.9	5.6
9	9	4	7.7	7.1
0	10	4	6.3	8.3
5	10	4	8.0	8.3
6	10	4	7.0	6.7
7	10	4	5.9	6.6
8	10	4	5.7	8.8
9	10	4	0.0	5.8
10	10	4	0.0	3.0
0	11	4	0.0	4.5
1	11	4	0.0	3.0
5	11	4	7.8	6.6
6	11	4	4.8	6.9
7	11	4	0.0	3.8
8	11	4	4.1	5.4
9	11	4	0.0	4.9
0	12	4	7.9	1.9
4	12	4	5.6	4.7
5	12	4	0.0	0.8
6	12	4	6.6	6.2
7	12	4	2.0	4.4
0	13	4	5.9	1.1
1	13	4	4.4	0.6
2	13	4	1.8	4.1
3	13	4	6.4	9.6
4	13	4	0.0	2.8
5	13	4	0.0	4.3
6	13	4	0.0	2.7
0	14	4	0.0	2.4
1	14	4	3.7	1.2
2	14	4	0.0	0.8
3	14	4	6.8	5.1
2	0	5	7.2	4.3
6	0	5	7.0	6.0
7	0	5	7.8	7.3
8	0	5	3.1	3.3
11	0	5	6.0	4.2
12	0	5	3.3	2.3
3	1	5	5.2	9.0
4	1	5	7.5	11.0
7	1	5	0.0	2.4
9	1	5	5.2	3.1
0	2	5	0.0	1.0
3	2	5	0.0	3.2
4	2	5	0.0	4.7
5	2	5	8.1	10.8
6	2	5	6.0	5.4
7	2	5	7.6	4.9
2	3	5	3.6	6.5
4	3	5	8.1	9.4
11	3	5	6.2	0.5
0	4	5	3.9	6.6
3	4	5	4.3	7.3
4	4	5	3.9	3.6
5	4	5	5.3	6.2
6	4	5	3.5	1.7
10	4	5	3.7	5.2
11	4	5	6.4	5.2
12	4	5	0.0	2.1
1	5	5	6.3	7.9
8	5	5	7.9	6.3
1	6	5	3.3	1.7
2	6	5	4.4	1.7

H	K	L	FO	FC
4	6	5	6.6	3.6
5	6	5	6.5	4.9
10	6	5	4.4	5.3
11	6	5	2.1	4.0
3	7	5	7.2	5.6
5	7	5	7.3	8.8
8	7	5	4.0	3.2
9	7	5	0.3	3.7
10	7	5	6.1	7.6
2	8	5	5.7	3.7
3	8	5	4.2	5.6
4	8	5	7.1	6.1
5	8	5	3.6	1.6
7	8	5	7.1	7.1
8	8	5	3.0	6.1
9	8	5	3.5	2.8
10	8	5	0.0	1.5
0	9	5	5.8	4.9
2	9	5	0.0	3.7
6	9	5	4.8	4.7
7	9	5	1.9	2.4
8	9	5	6.4	6.2
2	10	5	8.0	6.4
3	10	5	7.3	4.9
5	10	5	5.8	9.0
6	10	5	7.1	3.9
7	10	5	3.2	3.1
8	10	5	0.0	4.6
0	11	5	1.6	4.7
2	11	5	0.8	2.9
3	11	5	8.0	6.5
4	11	5	5.8	5.1
6	11	5	0.0	2.8
7	11	5	1.4	2.2
0	12	5	5.4	3.1
1	12	5	4.1	5.4
2	12	5	8.1	8.9
3	12	5	0.0	4.1
4	12	5	5.2	7.2
5	12	5	6.6	6.5
1	13	5	0.0	2.6
2	13	5	5.8	3.8
3	13	5	6.2	3.2
0	0	6	0.0	1.5
2	0	6	7.2	9.0
3	0	6	8.6	5.7
5	0	6	4.4	0.3
7	0	6	0.8	3.3
9	0	6	5.0	0.5
11	0	6	0.0	2.7
3	1	6	6.3	6.1
5	1	6	0.0	4.7
6	1	6	4.3	3.6
7	1	6	6.9	4.2
10	1	6	5.2	4.4
11	1	6	6.6	7.7
2	2	6	8.4	6.8
4	2	6	8.2	0.3
5	2	6	3.6	7.3
7	2	6	4.6	7.5
8	2	6	1.3	2.7
11	2	6	0.0	5.6
0	3	6	0.0	1.7
2	3	6	7.5	9.8
3	3	6	5.4	6.0
4	3	6	0.0	0.1
5	3	6	0.0	5.8
6	3	6	3.0	3.0
7	3	6	6.1	3.0
9	3	6	4.0	7.5
10	3	6	0.0	0.2
11	3	6	5.5	6.3
0	4	6	0.0	0.5
2	4	6	4.3	3.5
3	4	6	0.0	1.3
4	4	6	0.0	3.7
5	4	6	0.0	6.2
6	4	6	2.7	4.3
8	4	6	3.0	5.0
9	4	6	4.1	1.5
10	4	6	3.9	7.1
0	5	6	1.1	1.9
1	5	6	8.2	8.7
2	5	6	4.6	3.9
3	5	6	4.3	4.5
4	5	6	5.0	4.0
5	5	6	8.1	6.8
8	5	6	4.7	4.5
9	5	6	0.0	6.0
10	5	6	0.0	2.3
2	6	6	6.0	4.0
4	6	6	7.2	4.7
7	6	6	5.6	4.0
8	6	6	0.0	2.3
9	6	6	0.0	5.4
0	7	6	8.2	9.7
1	7	6	7.0	8.1
2	7	6	4.0	0.3
3	7	6	4.0	1.3
4	7	6	3.9	4.0
5	7	6	3.6	3.7
6	7	6	7.0	8.7
7	7	6	4.9	3.7
8	7	6	4.0	3.8
9	7	6	0.0	1.8
0	8	6	4.5	3.9
1	8	6	5.9	1.2
3	8	6	0.0	5.8
4	8	6	5.4	3.3
5	8	6	5.4	4.7
8	8	6	6.2	5.5
0	9	6	6.1	2.5
1	9	6	4.1	1.4
2	9	6	2.5	1.4
3	9	6	0.0	3.4

H	K	L	FO	FC
4	9	6	0.0	0.7
5	9	6	5.4	6.7
6	9	6	8.1	8.5
7	9	6	0.0	4.0
0	10	6	0.0	3.9
2	10	6	3.2	5.5
3	10	6	5.7	6.0
5	10	6	4.9	4.5
6	10	6	5.6	6.1
0	11	6	6.0	7.1
1	11	6	4.8	5.8
2	11	6	0.0	3.6
3	11	6	0.0	4.2
4	11	6	6.6	5.1
1	0	7	0.0	2.4
2	0	7	0.0	1.2
4	0	7	0.0	3.9
5	0	7	0.0	4.6
6	0	7	6.2	5.9
7	0	7	0.0	0.5
8	0	7	0.0	0.1
9	0	7	0.0	3.0
0	1	7	2.4	2.2
2	1	7	8.3	10.6
3	1	7	8.2	9.9
4	1	7	2.4	5.0
6	1	7	6.0	5.1
7	1	7	0.0	3.5
8	1	7	7.8	7.6
9	1	7	6.2	2.8
1	2	7	0.0	3.0
2	2	7	1.1	2.9
3	2	7	4.9	7.1
4	2	7	0.0	2.6
5	2	7	0.0	3.7
6	2	7	0.0	3.3
7	2	7	0.0	1.8
8	2	7	0.6	3.2
9	2	7	0.0	4.1
2	3	7	4.2	5.4
3	3	7	0.0	4.9
4	3	7	0.0	3.2
5	3	7	5.3	7.5
6	3	7	4.9	5.9
8	3	7	4.0	4.8
0	4	7	2.5	3.7
2	4	7	0.0	1.1
3	4	7	0.0	2.3
4	4	7	3.8	4.8
5	4	7	0.0	4.6
6	4	7	3.8	0.5
7	4	7	7.0	7.2
8	4	7	2.7	5.5
1	5	7	5.1	4.4
3	5	7	4.7	5.2
4	5	7	7.6	8.9
5	5	7	6.0	5.9
6	5	7	2.3	6.6
7	5	7	4.6	3.0
8	5	7	6.5	5.3
0	6	7	6.2	0.7
1	6	7	6.5	1.5
2	6	7	4.7	1.4
3	6	7	0.0	4.2
4	6	7	0.0	1.0
5	6	7	0.0	5.8
6	6	7	0.0	3.8
7	6	7	3.0	3.7
0	7	7	7.3	4.6
1	7	7	6.6	2.4
2	7	7	7.7	5.9
3	7	7	0.0	4.7
4	7	7	5.6	8.9
5	7	7	4.5	5.2
6	7	7	6.2	5.6
0	8	7	2.9	1.0
1	8	7	7.6	4.5
2	8	7	4.3	1.0
3	8	7	5.3	5.7
4	8	7	0.0	4.4
5	8	7	8.0	5.2
0	9	7	0.0	3.6
2	9	7	0.0	1.6
3	9	7	5.7	4.4
1	0	8	6.9	3.8
2	0	8	7.2	1.2
5	0	8	2.3	2.3
6	0	8	7.6	6.4
4	1	8	4.4	2.9
5	1	8	0.0	2.1
6	1	8	5.2	4.3
0	2	8	0.0	0.2
1	2	8	0.0	5.1
3	2	8	0.0	4.4
4	2	8	3.1	7.9
5	2	8	0.0	5.5
0	3	8	2.5	1.2
1	3	8	2.3	1.0
2	3	8	2.8	6.2
3	3	8	0.0	4.9
4	3	8	0.0	0.9
5	3	8	4.2	2.4
0	4	8	0.0	4.4
1	4	8	0.0	4.3
2	4	8	5.0	3.4
3	4	8	3.0	5.4
4	4	8	0.0	4.5
0	5	8	0.0	0.3
1	5	8	0.0	5.5
2	5	8	0.0	2.7
3	5	8	0.0	3.8
0	6	8	3.3	7.5
1	6	8	3.5	2.1
2	6	8	4.0	1.4

Figure 11. Comparison of the magnitudes of the observed and calculated structure factors for those reflections called unobserved in the refinement of $C_{16}H_{11}O_3Cl$

The Fitzwater-Benson-Jackobs least squares and Fourier programs were used in this analysis.[1] All computer computations were done on the IBM 7074.

Discussion

The refined structure as well as the numbering system to be used throughout this discussion is shown in Figure 12. For identification purposes the molecular fragments will be called the phenoxy group (C$_\ell$,C1, C2,C3,C4,C5,C6,O1), the lactone ring (O2,C7,C9,C10,C15,C16,O3), the benzene ring (C10,C11,C12,C13,C14,C15), and the cyclopropane ring (C7, C8,C9).

The final refined parameters and their errors are given in Table 15. The positional parameters are listed in terms of fractional atomic coordinates and the temperature factor is of the form

$$\exp(-\beta_{11}h^2-\beta_{22}k^2-\beta_{33}l^2-2\beta_{12}hk-2\beta_{13}hl-2\beta_{23}kl).$$

The hydrogen atom parameters are given in Table 16. The notation used is such that H1C2 represents hydrogen one attached to atom C2, H2C3 represents hydrogen two attached to atom C3, etc. The hydrogen atoms were placed in their calculated positions which were generally locations of high electron density in the electron density difference map. The individual atom mean

---

[1] Fitzwater, D. R., Benson, J. E., both of Ames Laboratory, Atomic Energy Commission, Ames, Iowa. Jackobs, J. J., (present address) Arizona State University, Tempe, Arizona. Least Squares Package. Private Communication. 1965.

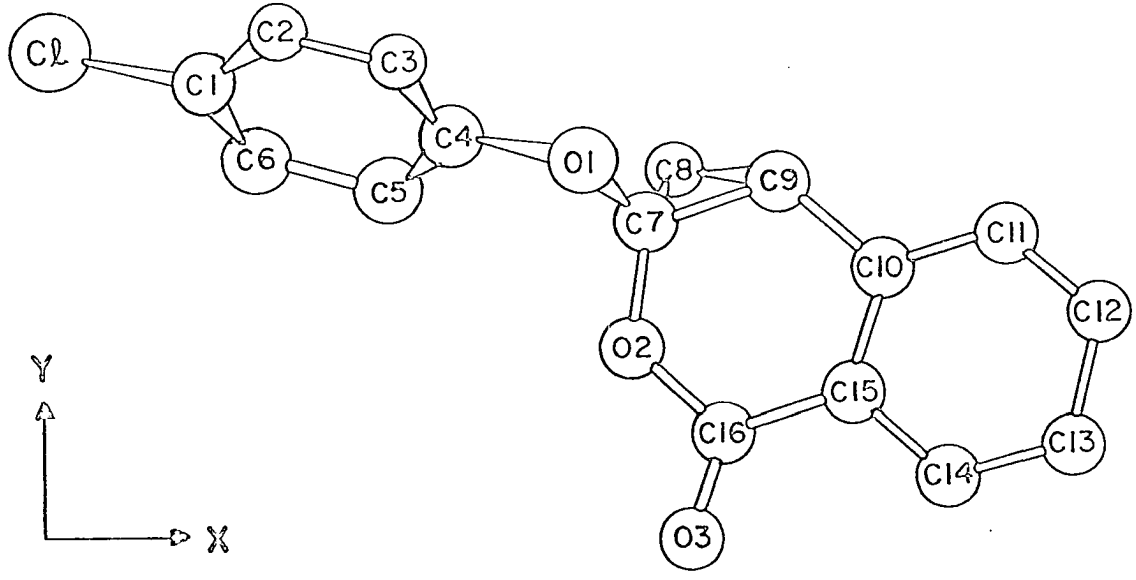

Figure 12. The molecular configuration of $C_{16}H_{11}O_3Cl$

Table 15. Final positional and thermal parameters and their standard errors from least squares refinement of $C_{16}H_{11}O_3Cl$ (errors and B's are x 10^5)

Atom	x	y	z	B_{11}	B_{22}	B_{33}	B_{12}	B_{13}	B_{23}
Cl	0.00847 (00022)	0.67725 (00027)	0.49523 (00069)	376 (16)	639 (18)	2613 (98)	22 (21)	-32 (44)	-62 (61)
O1	0.43914 (00054)	0.58170 (00060)	0.58511 (00117)	324 (45)	430 (52)	1921 (237)	-54 (43)	25 (88)	56 (94)
O2	0.47377 (00046)	0.43038 (00048)	0.47420 (00143)	430 (44)	318 (46)	2212 (253)	-87 (37)	176 (94)	-65 (102)
O3	0.52170 (00077)	0.27950 (00062)	0.47428 (00194)	969 (75)	515 (58)	2782 (342)	-152 (58)	-33 (158)	121 (134)
C1	0.13762 (00077)	0.64865 (00071)	0.52129 (00242	453 (67)	127 (68)	2527 (418)	-9 (53)	28 (182)	-103 (162)
C2	0.19111 (00098)	0.68642 (00108)	0.66432 (00209)	730 (95)	374 (85)	1559 (394)	-54 (90)	192 (155)	-99 (167)
C3	0.29410 (00087)	0.66315 (00107)	0.67417 (00199)	448 (77)	467 (96)	1906 (385)	-34 (74)	-120 (137)	97 (168)
C4	0.33823 (00093)	0.60085 (00089)	0.55312 (00187)	480 (80)	375 (80)	1546 (374)	87 (65)	101 (152)	-183 (150)
C5	0.28111 (00099)	0.56265 (00102)	0.41343 (00197)	796 (110)	481 (95)	1235 (393)	216 (95)	362 (167)	-467 (172)
C6	0.17786 (00105)	0.58735 (00107)	0.39475 (00242)	691 (96)	448 (91)	2778 (461)	236 (87)	-193 (195)	-609 (208)

Table 15 (Continued)

Atom	x	y	z	B_{11}	B_{22}	B_{33}	B_{12}	B_{13}	B_{23}
C7	0.48857 (00080)	0.53081 (00077)	0.44964 (00193)	223 (64)	304 (73)	2266 (437)	176 (63)	156 (150)	-170 (143)
C8	0.50975 (00103)	0.57105 (00113)	0.26659 (00200)	593 (76)	733 (87)	1775 (295)	-300 (89)	-551 (146)	563 (132)
C9	0.59544 (00089)	0.56214 (00098)	0.40852 (00201)	564 (87)	465 (88)	2388 (431)	24 (79)	255 (154)	587 (165)
C10	0.67781 (00087)	0.49300 (00099)	0.39195 (00182)	421 (78)	621 (91)	541 (286)	-87 (76)	87 (129)	30 (143)
C11	0.77852 (00091)	0.51720 (00111)	0.36485 (00225)	367 (85)	714 (112)	1899 (384)	169 (85)	435 (155)	-296 (195)
C12	0.85106 (00106)	0.45133 (00132)	0.35404 (00220)	587 (96)	946 (132)	1702 (385)	-75 (112)	107 (162)	-43 (213)
C13	0.82705 (00094)	0.35008 (00129)	0.35831 (00232)	389 (85)	973 (154)	1921 (441)	237 (97)	178 (166)	-213 (220)
C14	0.72729 (00091)	0.32281 (00128)	0.38752 (00205)	608 (92)	759 (106)	1239 (350)	542 (115)	235 (158)	-308 (217)
C15	0.65116 (00093)	0.39357 (00086)	0.40810 (00197)	504 (80)	357 (88)	1272 (319)	160 (74)	80 (134)	-63 (139)
C16	0.54949 (00088)	0.36066 (00085)	0.45286 (00192)	548 (84)	178 (67)	1713 (413)	44 (65)	265 (142)	95 (133)

Table 16. The hydrogen positional parameters and their isotropic temperature factor

Atom	x	y	z	B
H1C2	0.15736	0.72645	0.75887	4.0
H2C3	0.33707	0.69224	0.77181	4.0
H3C5	0.31275	0.51854	0.32143	4.0
H4C6	0.13543	0.56021	0.29392	4.0
H5C8	0.48244	0.64176	0.22801	4.0
H6C8	0.50867	0.52269	0.14724	4.0
H7C9	0.61613	0.62889	0.46989	4.0
H8C11	0.79720	0.58703	0.35463	4.0
H9C12	0.92498	0.47252	0.34191	4.0
H10C13	0.88056	0.29914	0.34006	4.0
H11C14	0.70891	0.25118	0.39377	4.0

square amplitude tensors will not be given here. The U_{ij}'s can be calculated from the β_{ij}'s; for example,

$$U_{12} = \beta_{12}/2\pi^2 a^* b^*.$$

The intramolecular bond distances and bond angles are given in Table 17. The bond distances in the third column have been corrected for rigid body librations, to be discussed later. Three decimal places are reported for the bond distances so that a comparison can be made between the corrected and uncorrected distances. All errors have been

Table 17. Bond distances and angles for $C_{16}H_{11}O_3Cl$ (The corrected distance has been corrected for librational motion. RMS (1) and RMS (2) are the root mean square amplitudes of vibration (Å) in the bond direction for the first and second defining atoms, respectively.)

Atoms	Dist. (Å)	Dist.(corr)	Error (Å)	RMS(1)	RMS(2)
Cl-C1	1.762	1.764	0.01	0.18	0.20
C1-C2	1.368	1.375	0.02	0.22	0.22
C1-C6	1.363	1.371	0.02	0.19	0.17
C2-C3	1.400	1.402	0.02	0.26	0.20
C3-C4	1.366	1.374	0.02	0.24	0.16
C4-C5	1.377	1.384	0.02	0.21	0.24
C5-C6	1.413	1.414	0.02	0.25	0.22
C4-01	1.379	1.381	0.01	0.20	0.18
01-C7	1.380	1.382	0.01	0.22	0.16
C7-C8	1.479	1.485	0.02	0.25	0.19
C7-C9	1.507	1.513	0.01	0.17	0.21
C8-C9	1.542	1.547	0.02	0.16	0.26
C7-02	1.411	1.419	0.01	0.19	0.17
02-C16	1.397	1.403	0.01	0.20	0.17
C16-03	1.189	1.193	0.01	0.14	0.21
C16-C15	1.456	1.461	0.01	0.20	0.22
C15-C10	1.422	1.430	0.01	0.21	0.23
C10-C9	1.452	1.459	0.01	0.23	0.22
C10-C11	1.386	1.390	0.01	0.18	0.19
C11-C12	1.323	1.328	0.02	0.18	0.28
C12-C13	1.433	1.439	0.02	0.29	0.32
C13-C14	1.387	1.391	0.02	0.22	0.28
C14-C15	1.409	1.414	0.01	0.10	0.15

Defining atoms	Angle (°)	Error (°)
Cl-C1-C2	119.9	0.9
Cl-C1-C6	116.3	1.0
C2-C1-C6	123.8	1.1
C1-C2-C3	117.0	1.1
C2-C3-C4	121.7	1.2
C3-C4-C5	119.3	1.0
C3-C4-01	115.0	1.0
C5-C4-01	125.7	1.0
C4-C5-C6	120.6	1.0
C5-C6-C1	117.4	1.2
C4-01-C7	115.6	0.8
01-C7-C8	123.4	0.9
01-C7-C9	116.2	0.9

Table 17 (Continued)

Defining atoms	Angle (°)	Error (°)
O1-C7-O2	110.0	0.9
C8-C7-C9	62.2	0.7
C8-C7-O2	120.7	1.0
C9-C7-O2	115.9	0.8
C7-C8-C9	59.8	0.7
C7-C9-C8	58.0	0.7
C7-C9-C10	122.0	0.9
C7-O2-C16	124.3	0.7
O2-C16-O3	114.4	0.9
C15-C16-O3	127.5	0.9
C16-C15-C10	123.3	0.9
C16-C15-C14	117.8	1.0
C15-C10-C9	116.2	0.9
C15-C10-C11	118.8	1.0
C10-C11-C12	122.6	1.2
C11-C12-C13	120.5	1.1
C12-C13-C14	118.6	1.2
C13-C14-C15	120.4	1.3

calculated using the variance-covariance matrix and the program of Busing and Levy (52). Because of size limitations on the Busing and Levy program, the structure was analyzed in two parts using overlapping portions of the complete variance-covariance matrix.

The bond distances and angles are quite normal in view of the known molecular geometry of other organic compounds. A comparison of the observed bond distances, corrected for librational motion, and the expected distances is given in Table 18; a straight average was used when more than one distance was involved. The first three expected distances are based on the average values observed in many compounds (69). The cyclopropane expected ring distance is based on the 1.52Å distance in cyclopropane (70),

Table 18. Comparison of observed and expected bond distances for $C_{16}H_{11}O_3Cl$

Bond type	Observed dist.(Å)	Expected dist.(Å)
C-C (aromatic)	1.39	1.39
C-Cl	1.76	1.77
C=O	1.19	1.21
C-C (cyclopropane ring)	1.52	1.52
C-C (C_6H_5-C=O)	1.46	1.46
C-C (C_6H_5-C)	1.46	<1.51
C-O	1.40	1.36-1.43

the 1.51Å distance in cyclopropyl chloride (71), and the 1.52Å distance in a recent crystal structure (72). The expected C-C (C_6H_5-C=O) distance of 1.46Å is based on the same distances observed in salicylic acid (73) and for the single bond length in 1,3,5,7-cyclooctatetraene (74). The expected C-C(C_6H_5-C) distance is based on the observed distance of 1.51Å in toluene (75); this is a poor approximation to the coordination in this molecule and probably represents the maximum distance possible. The known C-O distances vary considerably; they range from 1.36Å in the furans (65, 76) to 1.43Å in 1,5-dihydrofuran (77) and tetrahydrofuran (77).

An analysis of the four C-O bonds suggests that there might be two types of C-O bonds. The two bonds involving O1 are 1.38Å in length while the two bond distances involving O2 are 1.42Å and 1.40Å. The four bonds could be equivalent, however, in view of their estimated standard

deviations. The C11-C12 distance is very short, but not exceeding 3σ; evidence will be presented later to show that this could be a result of intermolecular contacts.

It is of interest to examine the planarity of several regions of this molecule; the equations of the least squares planes and the displacements of the atoms from these planes are given in Table 19. The X, Y, and Z are coordinates in Å referred to the coordinate system defined by the cell axes. This analysis was done using a program written by Williams.[1] Equations A and B are for the benzene rings, C for the lactone ring, D for the lactone-benzene ring, and E for the cyclopropane ring. It is evident that even the combined benzene-lactone ring (D) is quite planar. This plane (D) is tilted 10.7° out of the x-y plane. The angle between planes A and D is 118.6°; the angle between planes E and D is 69.8°. Note the relatively large displacement of C12 from planes B and D.

All the intermolecular distances less than 4.0Å were calculated; the shortest unique non-hydrogen contacts are listed in Table 20. The shortest contact involves C12 and may be partly responsible for the relatively large displacement of C12 from planes B and D and the short C11-C12 bond distance. The deviation of C12 from the molecular planes is such as to maximize the C9-C12 intermolecular contact. The contact between the hydrogen on C9 and the transformed C12 is 3.06Å. It is of interest to note that the interplanar spacing in graphite is 3.35Å (78).

---

[1]Williams, D. E. Department of Chemistry, Iowa State University, Ames, Iowa. Least squares plane. Private communication. 1965.

Table 19. Equations and deviations of atoms from least squares planes

Equations

A: C1,C2,C3,C4,C5,C6
0.2413X + 0.7815Y - 0.5753Z - 5.231 = 0

B: C10,C11,C12,C13,C14,C15
0.1439X + 0.0227Y + 0.9893Z - 4.299 = 0

C: C9,C7,02,C16,03,C15,C10
0.1976X + 0.0701Y + 0.9778Z - 5.030 = 0

D: C9,C7,02,C16,03,C15,C10,C11,C12,C13,C14
0.1768X + 0.0561Y + 0.9826Z - 4.809 = 0

E: C7,C8,C9
-0.2094X + 0.9181Y + 0.3364Z - 6.484 = 0

Deviations

Atom	ΔA	ΔB	ΔC	ΔD	ΔE
C1	0.01				
C2	-0.02				
C3	0.02				
C4	0.00				
C5	-0.01				
C6	0.01				
C7			-0.02	-0.02	0.00
C8					0.00
C9			0.00	-0.04	0.00
C10		-0.01	0.02	-0.02	
C11		-0.01		0.04	
C12		0.03		0.08	
C13		-0.02		-0.03	
C14		-0.01		-0.07	
C15		0.02	-0.02	-0.04	
C16			0.00	0.02	
02			0.02	0.05	
03			0.00	0.04	

Table 20. Shortest intermolecular non-hydrogen distances

Atom 1	Atom 2	Symmetry transformation on atom 2[a]	Dist. (Å)
C9	C12	$2_1(z)$,TX,TY	3.35
C13	O3	$2_1(x)$,TZ	3.36
C8	O3	$2_1(y)$,TX	3.40
O1	C12	$2_1(z)$,TX,TY	3.43
Cℓ	C16	$2_1(z)$,TY	3.48
C10	C12	$2_1(z)$,TX,TY	3.49
O1	Cℓ	$2_1(x)$,TY,TZ	3.50
C10	C11	$2_1(z)$,TX,TY	3.52
C2	O2	$2_1(z)$,TY	3.54
C12	C8	$2_1(z)$,TX,TY	3.55
Cℓ	O3	$2_1(z)$,TY	3.58
O1	C6	$2_1(z)$,TY	3.60

[a]The $2_1(x)$,$2_1(y)$, and $2_1(z)$ represent the three two-fold screw axes while TX, TY, and TZ represent cell translations in the x, y, and z directions.

An attempt was made to accurately characterize the thermal motion of this compound. The magnitudes and orientation of the principal axes of thermal vibration for all the non-hydrogen atoms are given in Table 21; the corresponding errors in these quantities have been omitted in the interest of saving space. The data in Table 21 is such that thermal

Table 21. Amplitudes and direction cosines of the principal thermal axes R

Atom	R	RMS amp.(Å)	Cosθ(X)	Cosθ(Y)	Atom	R	RMS amp.(Å)	Cosθ(X)	Cosθ(Y)
Cl	1	0.269	-.0540	-.2982	C7	1	0.253	.0949	-.1995
	2	.247	.0531	.9522		2	.203	.6218	.7769
	3	.182	.9971	-.0668		3	.073	-.7774	.5971
O1	1	.230	-.0008	.2426	C8	1	.338	-.5280	.6769
	2	.207	.3442	-.9108		2	.185	-.5964	-.7255
	3	.164	-.9389	-.3342		3	.152	.6046	-.1244
O2	1	.253	.3569	-.1768	C9	1	.300	.2775	.5427
	2	.198	-.7432	.5411		2	.219	-.9378	.3322
	3	.159	-.5659	-.8222		3	.148	-.2087	-.7714
O3	1	.302	-.9115	.3414	C10	1	.250	-.3027	.9531
	2	.275	.2720	.0816		2	.189	.9317	.2951
	3	.210	-.3086	-.9364		3	.117	-.2006	-.0674
C1	1	.263	.0493	-.0927	C11	1	.279	-.1055	-.8964
	2	.200	-.9985	.0202		2	.253	.6257	.2767
	3	.108	.0248	.9955		3	.104	-.7729	.3464
C2	1	.263	.9142	-.1921	C12	1	.304	.1755	-.9822
	2	.201	-.4051	-.4538		2	.232	.8274	.1838
	3	.182	-.0095	.8703		3	.208	-.5334	-.0381
C3	1	.239	-.3576	.4365	C13	1	.320	-.2848	-.9457
	2	.206	.0047	-.8832		2	.236	.4040	.0298
	3	.192	.9339	.1707		3	.150	-.8693	.3237
C4	1	.222	-.3102	-.6742	C14	1	.339	-.6258	-.7775
	2	.217	.8305	.1509		2	.211	.4296	-.2769
	3	.156	-.4626	.7230		3	.037	-.6510	.5647
C5	1	.287	.8989	.4209	C15	1	.235	.8178	.5717
	2	.252	.2302	-.6896		2	.191	.1581	-.3337
	3	.069	-.3727	.5894		3	.148	-.5534	.7495
C6	1	.322	-.4317	-.5305	C16	1	.248	.7216	.1407
	2	.239	.8327	.0764		2	.186	-.6884	.0419
	3	.139	-.3466	.8442		3	.128	.0735	-.9892

stereograms can be plotted immediately in the x-y plane. There was no pronounced tendency for maximum individual atom vibrations in the c direction as might be expected.

Because of the rigidity of the molecule as a whole, it appeared that the molecule could be divided into two groups so that thermal motion of the molecule could be expressed as rigid body translations and librations of these groups. Group I was comprised of the 8 atom phenoxy group; the remaining 12 atoms were included in group II. The individual atomic vibrations were expressed as rigid body translations and librations after the method of Cruickshank (54) using the program UCLAT01.[1] The center of libration of group I was allowed to move along the O1-Cℓ direction; the translational tensor T and the librational tensor ω were examined at 27 points along this direction. The T and ω tensors for group II were examined at 15 points between the midpoints of C10-C15 and C7-02. The energy minima were poorly defined; either the right rigid body combination wasn't found or else the data are not good enough to merit such a sophisticated treatment. The latter is most probably the case.

A reasonably good fit was found with the librational centers 0.92Å from C1 towards C4 and 0.63Å from the midpoint of C10-C15 for groups I and II, respectively. The root mean square difference between the U_{ij}'s derived from the refined β_{ij}'s and those calculated from rigid body parameters were 0.0107Å^2 and 0.0138Å^2 for groups I and II, respectively.

---

[1]Gantzel, P., Coulter, C., and Trueblood, K. California Institute of Technology, Pasadena, California. IBM 709 or 7090 program UCLAT01. Private Communication. 1965.

These values are larger than would be expected on the basis of the molecular geometry. The translational oscillations for both groups were not markedly anisotropic; neither were the librational oscillations of group II. There was a large angular oscillation of 7.3° about the C1-C4 direction in group I; a large rotation would be expected about this direction. Corrections to the bond lengths due to angular oscillations were calculated by the method of Cruickshank (55, 79). The corrected distances are listed in Table 17. The details of this thermal analysis will not be given since the rigid body approximation seems to be quite tenuous in this case.

The packing of the molecules in the unit cell is illustrated in Figure 13. All of the shaded molecules are very nearly in the same plane as are the unshaded molecules. The two planes are separated by half a lattice translation in the c direction. The size of the C4-O1-C7 angle is apparent in this figure. This angle at 115.6° is larger than expected. The angle strain, which is not excessive, is undoubtedly a result of steric factors.

The author regrets that X-ray diffraction alone gives no insight into the history of this compound. The very fundamental question as to how and why this compound forms at all is open to discussion.

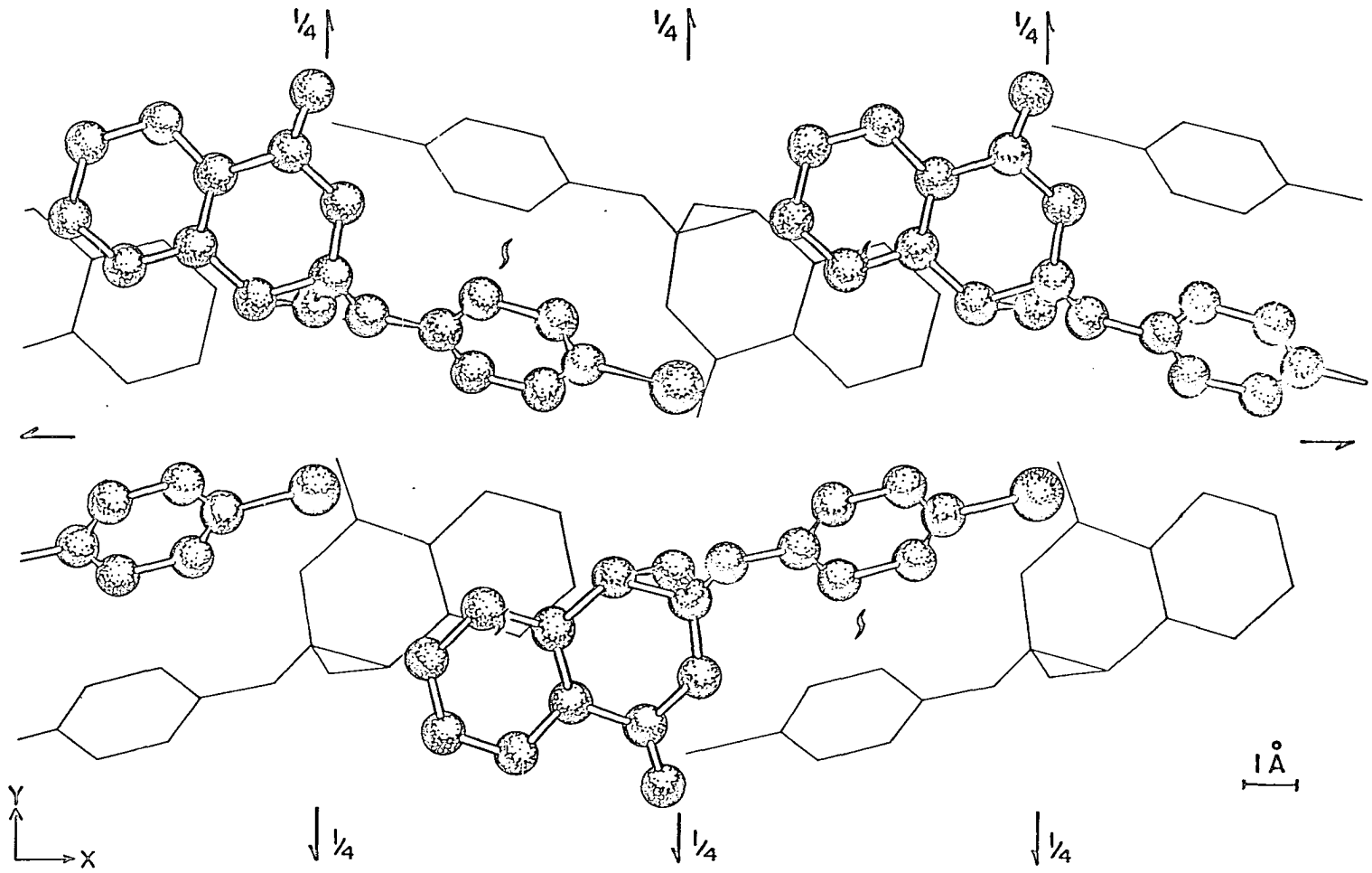

Figure 13. The structure of $C_{16}H_{11}O_3Cl$ looking down the c axis (The shaded layer is half a cell translation above the unshaded layer.)

SUMMARY

The structure of the ethyl Grignard reagent in diethyl ether, $EtMgBr \cdot 2Et_2O$, has been determined by X-ray diffraction techniques. This compound crystallizes in the monoclinic space group $P2_1/c$ with cell parameters a = 13.18±0.03, b = 10.27±0.03, c = 11.42±0.03Å, and β = 103.3±0.3°. A single crystal was grown from the liquid and the data recorded at about -75° C.

The structure consists of ethylmagnesium bromide monomers with the ethyl group, a bromine atom, and two ether molecules forming a somewhat distorted tetrahedron about a single magnesium atom. Pertinent structural features are short Mg-O bonds (2.04Å), trigonal bonding about the oxygen atoms, and the configuration of the ether methyl groups where the methyl groups are rotated out of the ether planes with one methyl carbon forward and the other back. There was nothing in this structure to indicate anything but a monomeric species; thus eliminating species such as $R_2Mg \cdot MgX_2$.

The troponoid photo-oxidation product $C_{16}H_{11}O_3Cl$, was prepared from 2-(p-chlorophenoxy)-4,5-benztropone ($C_{17}H_{11}O_2Cl$). This compound crystallizes in the orthorhombic space group $P2_12_12_1$ with cell parameters a = 13.21±0.02, b = 13.80±0.02, and c = 7.33±0.02Å.

The structure of $C_{16}H_{11}O_3Cl$ was solved using image-seeking methods; namely, using multiple Patterson superpositions in conjunction with the minimum function. Appropriate weighting of successive shifted Patterson maps resulted in a significant increase in the resolution of the minimum

function. The molecular configuration found in the refined crystal structure is

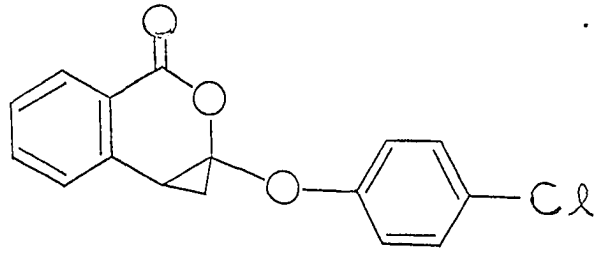

The bond distances and valency angles found are normal for this type of compound.

LITERATURE CITED

1. Grignard, V. Comptes Rendus des Travaux de Chimie 130: 1322. 1900.

2. Stoner, Marshall R. Studies on the photochemistry of 2-(p-halophenoxy)-4,5-benztropones. Unpublished Ph.D. thesis. Ames, Iowa, Library, Iowa State University of Science and Technology. 1964.

3. Kharasch, M. S. and Reinmuth, O. Grignard reactions of nonmetallic substances. New York, N.Y., Prentice-Hall. 1954.

4. Rochow, E. G., Hurd, D. T. and Lewis, R. N. The chemistry of organometallic compounds. New York, N.Y., John Wiley and Sons. 1957.

5. Salinger, R. M. Survey of Progress in Chemistry 1: 301. 1963.

6. Yoffe', S. T. and Nesmeyanov, A. N. Handbook of magnesium-organic compounds. 3 vols. London, England, Pergamon Press. 1957.

7. Grignard, V. Ann. Chim. 24: 433. 1901.

8. Meisenheimer, J. and Schlichenmaier, W. Berichte 61: 720. 1928.

9. Schlenk, W. and Schlenk, W., Jr. Berichte 62: 920. 1929.

10. Noller, C. R. and White, W. R. J. Am. Chem. Soc. 59: 1354. 1937.

11. Kullmann, R. Comptes Rendus des Travaux de Chimie 231: 866. 1950.

12. Wotiz, J. H., Hollingsworth, C. A. and Dessy, R. E. J. Org. Chem. 21: 1063. 1956.

13. Dessy, R. E., Handler, G. S., Wotiz, J. H. and Hollingsworth, C. A. J. Am. Chem. Soc. 79: 3476. 1957.

14. Dessy, R. E. and Handler, G. S. J. Am. Chem. Soc. 80: 5824. 1958.

15. Dessy, R. E. J. Org. Chem. 25: 2260. 1960.

16. Hayes, S. Ann. Chim. (Paris) 8: 545. 1963.

17. Hamelin, R. Bull. Soc. Chim. France 1961: 684. 1961.

18. Kirrmann, A., Hamelin, R. and Hayes, S. Bull. Soc. Chim. France 1963: 1395. 1963.

19. Ashby, E. C. and Becker, W. E. J. Am. Chem. Soc. 85: 118. 1963.

20. Vreugdenhil, A. D. and Blomberg, C. Rec. Trav. Chim. 82: 453. 1963.

21. Slough, W. and Ubbelohde, A. R. J. Chem. Soc. 1955: 108. 1955.

22. Vreugdenhil, A. D. and Blomberg, C. Rec. Trav. Chim. 82: 461. 1963.

23. Ashby, E. C. and Smith, M. B. J. Am. Chem. Soc. 86: 4363. 1964.

24. Dessy, R. E., Green, S. E. I. and Salinger, R. M. Tetrahedron Letters 21: 1369. 1964.

25. Cowan, D. O., Hsu, J. and Roberts, J. D. J. Org. Chem. 29: 3688. 1964.

26. Salinger, R. M. and Mosher, H. S. J. Am. Chem. Soc. 86: 1782. 1964.

27. Evans, D. F. and Maher, J. P. J. Chem. Soc. 1962: 5125. 1962.

28. Roos, H. and Zeil, W. Z. Elektrochem. 67: 28. 1963.

29. Guggenberger, L. J. and Rundle, R. E. J. Am. Chem. Soc. 86: 5344. 1964.

30. Stucky, G. D. and Rundle, R. E. J. Am. Chem. Soc. 85: 1002. 1963.

31. Schröder, Friedrich. Ein Beitrag zur Kenntnis der Struktur der "Grignard'schen Verbindungen." Unpublished Ph.D. thesis. Braunschweig, Germany, Library, Technischen Hochschule, Institut für Anorganische Chimie. 1965.

32. Evans, W. V. and Rowley, H. H. J. Am. Chem. Soc. 52: 3523. 1930.

33. Ashby, E. C. J. Am. Chem. Soc. 87: 2509. 1965.

34. Weiss, E. J. Organometal. Chem. 2: 314. 1964.

35. Dessy, R. E. and Jones, R. M. J. Org. Chem. 24: 1685. 1959.

36. Vreugdenhil, A. D. and Blomberg, C. Rec. Trav. Chim. 83: 1096. 1964.

37. Stucky, G. D. and Rundle, R. E. J. Am. Chem. Soc. 86: 4825. 1964.

38. Harker, D. J. Chem. Phys. 4: 381. 1936.

39. Buerger, M. J. Vector space. New York, N.Y., John Wiley and Sons. 1959.

40. Rollett, J. S. and Sparks, R. A. Acta Cryst. 13: 273. 1960.

41. Hamilton, W. C., Rollett, J. S. and Sparks, R. A. Acta Cryst. 18: 129. 1965.

42. International tables for X-ray crystallography. Vol. II. Birmingham, England, Kynoch Press. 1959.

43. Evans, H. T. Acta Cryst. 14: 689. 1961.

44. DeVries, A. Acta Cryst. 18: 1077. 1965.

45. Willett, R. D. The crystal structures and magnetic properties of some red cupric chloride complexes. Unpublished Ph.D. thesis. Ames, Iowa, Library, Iowa State University of Science and Technology. 1962.

46. Cruickshank, D. W. J. and Pilling, D. E. Crystallographic calculations on the Ferranti Pegasus and Mark I computers. In Pepinsky, R., Robertson, J. M. and Speakman, J. C., eds., Computing methods and the phase problem in X-ray crystal analysis. pp. 32-78. New York, N.Y., Pergamon Press. 1961.

47. Hansen, H. P., Herman, F., Lea, J. D. and Skillman, S. Acta Cryst. 17: 1040. 1964.

48. International tables for X-ray crystallography. Vol. III. Birmingham, England, Kynoch Press. 1962.

49. Ibers, J. A. and Hamilton, W. C. Acta Cryst. 17: 781. 1964.

50. Cruickshank, D. W. J. Acta Cryst. 9: 747. 1956.

51. Cruickshank, D. W. J. Acta. Cryst. 19: 153. 1965.

52. Busing, W. R. and Levy, H. A. U. S. Atomic Energy Commission Report ORNL 59-12-3 [Oak Ridge National Laboratory, Tenn.]. 1959.

53. Pauling, L. Nature of the chemical bond. 3rd ed. Ithaca, New York, Cornell University Press. 1960.

54. Cruickshank, D. W. J. Acta Cryst. 9: 754. 1956.

55. Cruickshank, D. W. J. Acta Cryst. 9: 757. 1956.

56. Allen, P. W. and Sutton, L. E. Acta Cryst. 3: 46. 1950.

57. Stuart, H. A. Die struktur des freien moleküls. Berlin, Julius Springer. 1934.

58. Stuart, H. A. Phy. Rev. 38: 1372. 1931.

59. Chapman, O. L., Smith, H. G., King, R. W., Pasto, D. J. and Stoner, M. R. J. Am. Chem. Soc. 85: 2031. 1963.

60. Wrinch, D. M. Phil. Mag. 27: 98. 1939.

61. Fridrichsons, J. and McL. Mathieson, A. Acta Cryst. 15: 1065. 1962.

62. Simpson, P. G., Dobrott, R. D. and Lipscomb, W. N. Acta Cryst. 18: 169. 1965.

63. Mighell, A. D. and Jacobson, R. A. Acta Cryst. 17: 1554. 1964.

64. Jacobson, R. A. and Guggenberger, L. J. Acta Cryst. [in press]. 1965.

65. Williams, D. E. and Rundle, R. E. J. Am. Chem. Soc. 86: 1660. 1964.

66. Furnas, T. C., Jr. Single crystal orienter instruction manual. Milwaukee, Wisconsin, General Electric Company. 1957.

67. Alexander, L. E. and Smith, G. S. Acta Cryst. 15: 983. 1962.

68. Jacobson, R. A., Wunderlich, J. A. and Lipscomb, W. N. Acta Cryst. 14: 598. 1961.

69. Sutton, L. E., ed., Chemical Society (London) Special Publication No. 18. 1965.

70. Günthard, H. H., Lord, R. C. and McCubbin, T. K., Jr. J. Chem. Phys. 25: 768. 1956.

71. Friend, J. P. and Dailey, B. P. J. Chem. Phys. 29: 577. 1958.

72. MacDonald, A. C. and Trotter, J. Acta Cryst. 18: 243. 1965.

73. Sundaralingam, M. and Jensen, L. H. Acta Cryst. 18: 1053. 1965.

74. Bastiansen, O., Hedberg, L. and Hedberg, K. J. Chem. Phys. 27: 1311. 1957.

75. Keidel, F. A. and Bauer, S. H. J. Chem. Phys. 25: 1218. 1956.

76. Bak, B., Christensen, D., Dixon, W., Hansen-Nygaard L., Andersen, J. and Schottländer, M. J. Mol. Spectry. 9: 124. 1962.

77. Beach, J. Y. J. Chem. Phys. 9: 54. 1941.

78. Nelson, J. B. and Riley, D. P. Proc. Phys. Soc. 57: 477. 1945.

79. Cruickshank, D. W. J. Acta Cryst. 14: 896. 1961.

ACKNOWLEDGMENTS

The author wishes to express his gratitude to Dr. R. A. Jacobson for his interest and guidance in the later stages of this research. The author is deeply grateful for the guidance and inspiration of the late Dr. R. E. Rundle in the earlier stages of this research.

The author would like to thank Dr. D. E. Williams for helpful discussions during the course of this research and Mr. J. E. Benson who very graciously helped out with some of the computing problems encountered. The day to day assistance of Mr. H. F. Hollenbeck is gratefully acknowledged. Thanks go to Dr. O. L. Chapman for suppling crystals of the troponoid compound.

The author is especially indebted to his wife, Mary, for her patience and understanding throughout the last four years; her assistance in assembling this thesis is appreciated.